The Dissertation Committee for Poonam Agarwal Certifies that this is the approved version of the following dissertation:

UNDERSTANDING CHROMATIN MECHANISMS INVOLVED IN DNA DAMAGE AND CHEMOTHERAPEUTIC RESPONSES

Committee:

Kyle M. Miller, Supervisor

Vishwanath R. Iyer

Tanya T. Paull

Karen M. Vasquez

Blerta Xhemalce

UNDERSTANDING CHROMATIN MECHANISMS INVOLVED IN DNA DAMAGE AND CHEMOTHERAPEUTIC RESPONSES

by

Poonam Agarwal

Dissertation

Presented to the Faculty of the Graduate School of

The University of Texas at Austin

in Partial Fulfillment

of the Requirements

for the Degree of

Doctor of Philosophy

The University of Texas at Austin

December 2017

Dedication

To my beloved family!

Acknowledgements

Firstly, I would like to thank my supervisor at the University of Texas at Austin, Dr. Kyle M Miller, Ph.D. for his guidance and continual support during my graduate study at the University of Texas at Austin. His wise insights towards science and suggestions are critical for the successful completion of my degree. I am privileged to be a PhD student mentored and graduated from the Miller lab.

I would like to express my sincere acknowledgement to my dissertation committee members: Dr. Vishwanath Iyer, Dr. Tanya Paull, Dr. Blerta Xhemalce, and Dr. Karen Vasquez for their valuable comments and suggestions on my projects.

I would like to thank all previous and present members of the Miller lab, including Dr. Justin Leung, Dr. Fade Gong, Wei-Ta Chen, Li-Ya Chiu and Mercedes Perez for their help and insightful comments on my graduate work, as well as creating a cohesive environment for me to enjoy the laboratory life during my entire graduate study.

I am extremely grateful to my collaborators Dr. Raphael Rodriguez (Curie Institute, France), Dr. Blerta Xhemalce and Dr. Illya Finkelstein and their groups (UT Austin) for providing important data for our Angewandte Chemie paper and PLoS Genetics paper respectively and their critical discussions. In addition, I would like to thank Dr. Jon Huibregtse for providing me an opportunity to join their interesting research projects that lead to great results and publication.

I am also happy to acknowledge Dr. Xhemalce lab, Dr. Paull lab, Dr. Dan Durocher lab (Samuel Lunenfeld Research Institute, Mount Sinai Hospital, Toronto, Canada) and Dr. Roger Greenberg lab (UPENN) for providing important reagents.

It would not have been possible without the continual support and encouragement that I received from my parents, Kartik, friends and family members throughout these years and I express my love and gratitude towards them.

UNDERSTANDING CHROMATIN MECHANISMS INVOLVED IN DNA DAMAGE AND CHEMOTHERAPEUTIC RESPONSES

Poonam Agarwal, Ph.D.

The University of Texas at Austin, 2017

Supervisor: Kyle M.Miller

One of the hallmarks of cancer is genomic instability driven by DNA damage. Cells respond to these genetic insults through chromatin-based mechanisms that repair the damage. Chromatin plays a pivotal role in protecting cells from genome and epigenome instability that drive cancer progression. Chromatin, a highly dynamic complex of DNA and proteins, undergoes structural and functional changes in response to cellular factors that are essential for replication, transcription, DNA damage responses (DDR) and repair. Chromatin structure and function are highly dependent on histone modifications. Histones are modified on distinct amino acids by post-translational modifications (PTMs). Delineating chromatin-regulated processes are fundamental for understanding the nuclear pathways that regulate access to, and protection of, our genetic and epigenetic information. The first part of my project focused on analyzing the contribution of a chromatin domain, the nucleosome acidic patch in regulating histone H2A/X ubiquitination and the DDR using *in vitro* and *in vivo* approaches. I established techniques to biochemically purify human recombinant histones and reconstituted nucleosome core particles (NCPs) containing WT or acidic patch mutant H2A/X for *in vitro* Ub assays with purified E3 ligases, RNF168 and RING1B/BMI1. Both E3s ubiquitinated H2A/X within WT NCPs but not mutant NCPs. Thus, this assay confirmed our hypothesis that the effect of the acidic patch mutation on H2AX/ H2Aub is direct and that it mediates site-specific ubiquitinations. I showed that the acidic patch interacting peptide LANA could compete with RNF168 and RING1B/BMI1 dependent H2AX/H2A

Ub. In the second project, I tested how chromatin alters targeting of an anticancer drug using a cisplatin derivative that acts on the genome. I identified that cotreatment of cisplatin and the clinically approved drug Vorinostat/SAHA generated clusters of lesions that co-localized with translesion synthesis factors. However, I found that activated translesion synthesis no longer acted as a bypass mechanism but instead promoted apoptosis. These results demonstrated that pharmacological alterations of chromatin reprograms genome targeting with platinum drugs and, concomitantly, drug response.

The third project for my thesis work involves functional analysis of the bromodomain containing TRIM proteins in DDR. These proteins belong to the bromodomain (BRD) family, which are the readers of PTM acetylation. I identified specific domains in TRIM24 required for its recruitment to damaged DNA and its dependency on other chromatin associated factors, namely, SUV39H1, KAT6B, TRIM28, TRIM33 that regulate TRIM24 dynamics in the context of DNA damage. I validated some interactors of TRIM24, TRIM28 and TRIM33 including the FACT and MCM complex. In summary, knowledge gained from these studies will help to understand how these BRD reader proteins promote the DDR within acetylated chromatin to preserve genome stability.

Table of Contents

List of Tables

List of Figures

CHAPTER 1: INTRODUCTION

THE DNA DAMAGE RESPONSE

Maintenance of genomic integrity through the preservation of genetic information is crucial for organismal survival and homeostasis. Genomic instability can be caused by high incidences of DNA damage that occur frequently in cells as a consequence of recurrent exposure to genotoxic cellular processes and agents including replication stress, reactions involving production of metabolic by-products, transcription-associated damage, and exposure to external factors including UV radiation, environmental agents, and clinical treatments like radiotherapy and chemotherapeutics (1, 2). DNA damage must be detected and repaired in a timely and efficient manner to avert genomic and cellular alterations that can cause diseases, including cancer (2). To combat the harmful effects posed by DNA damage, cells use a highly coordinated network of DNA damage response (DDR) pathways to detect the damaged DNA lesion, signal its presence to downstream effector proteins, which orchestrate the appropriate cellular responses and DDR pathways to repair the lesion by damage-specific repair pathway such as double strand break repair, nucleotide exchange repair, base excision repair or mismatch repair (1, 2). Nuclear eukaryotic DNA is bound by histone proteins and structurally organized

Portions of this chapter have been published as follows:

- *Poonam Agarwal and Kyle M. Miller (2016) The nucleosome: orchestrating DNA damage signaling and repair within chromatin. Biochemistry and Cell Biology 94: 1–15. (Contributions: P.A. and K.M.M. wrote the manuscript together).*
- *Poonam Agarwal and Kyle. M. Miller (2016) Book chapter: Chromatin Dynamics and DNA repair in Chromatin Regulation and Dynamics, Elsevier (Contributions: P.A. and K.M.M. wrote the manuscript together).*

into chromatin through the formation of nucleosomes, the basic unit of chromatin which consists of ~146 bp of nuclear DNA wrapped around the octameric histone core. Chromatin therefore constitutes the legitimate *in vivo* substrate in which all processes involving DNA occur, including DNA replication, transcription, and repair. Thus, the DNA damage response and repair machinery that operates at the sites of DNA damage must function within the context of chromatin (Figure 1.1). It is well established that a

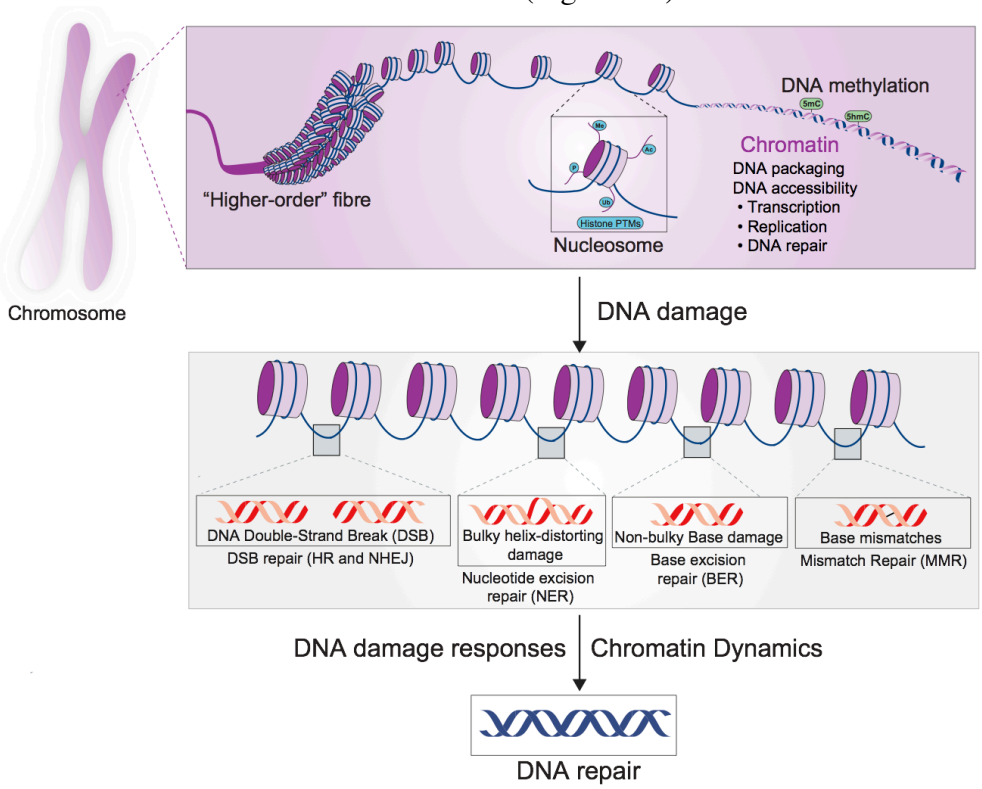

Figure 1.1 Chromatin and the DNA damage response

Nuclear DNA in eukaryotes is organized into nucleosomes and packaged in higher-order chromatin structure that regulates several DNA-based processes including DNA repair. DNA damage occurs within chromatin where specialized DNA repair pathways detect, signal and promote an appropriate DNA-damage repair pathway in order to maintain genome integrity. DNA damage response pathways (DDR) cooperate with various chromatin pathways to orchestrate DNA repair within the context of chromatin (3).

multitude of DNA repair factors are recruited to chromatin upon DNA damage and that chromatin features, including chromatin architecture, histone modifications, histone variants and chromatin remodeling complexes, shape the epigenetic landscape to

orchestrate DNA repair reactions within the chromatin environment (4-7). What is less clear however is how specificity for chromatin binding and modification of histones by DDR factors is achieved within chromatin to promote DNA damage signaling and repair.

CHROMATIN DYNAMICS AND DNA DOUBLE-STRAND BREAK REPAIR

DNA double-strand breaks (DSB) are considered a particularly dangerous DNA lesion, as failure to repair the broken ends accurately can promote genomic instability through chromosome loss, rearrangements and (or) mutations. DSBs are repaired by 2 prominent repair pathways in mammalian cells, namely, homologous recombination (HR) or non-homologous end-joining (NHEJ) (8). The two repair pathways differ in their requirement for a homologous template DNA and in the fidelity of DSB repair. HR uses an undamaged sister chromatid sequence as a template to faithfully repair the DSB, while NHEJ is a potentially more error-prone pathway that repairs the break through ligating the broken ends together. In mammalian cells, NHEJ is the predominant repair pathway active throughout the cell cycle, while HR is restricted to S/G2 phases, cell cycle stages in which a sister chromatid is available for repair (9-11). Control of these two pathways necessitates the regulation of chromatin/nucleosome modifications that take place surrounding the break. Histone post-translational modifications (PTMs), histones exchange, and nucleosome remodeling complexes participate in altering the chromatin landscape to facilitate DDR activities, which ultimately lead to the repair of the damaged DNA. Whether the damaged lesion is repaired by NHEJ or HR pathway, detection of the damaged DNA and initiation of either of these DSB repair processes requires recruitment of chromatin-modifying enzymes for remodeling of the damaged chromatin. Histone modifications serve as one mechanism that opens or condenses the chromatin structure by changing the nucleosome-DNA, nucleosome-nucleosome and (or) nucleosome/ chromatin protein interactions. ATP-dependent chromatin remodelers alter the chromatin

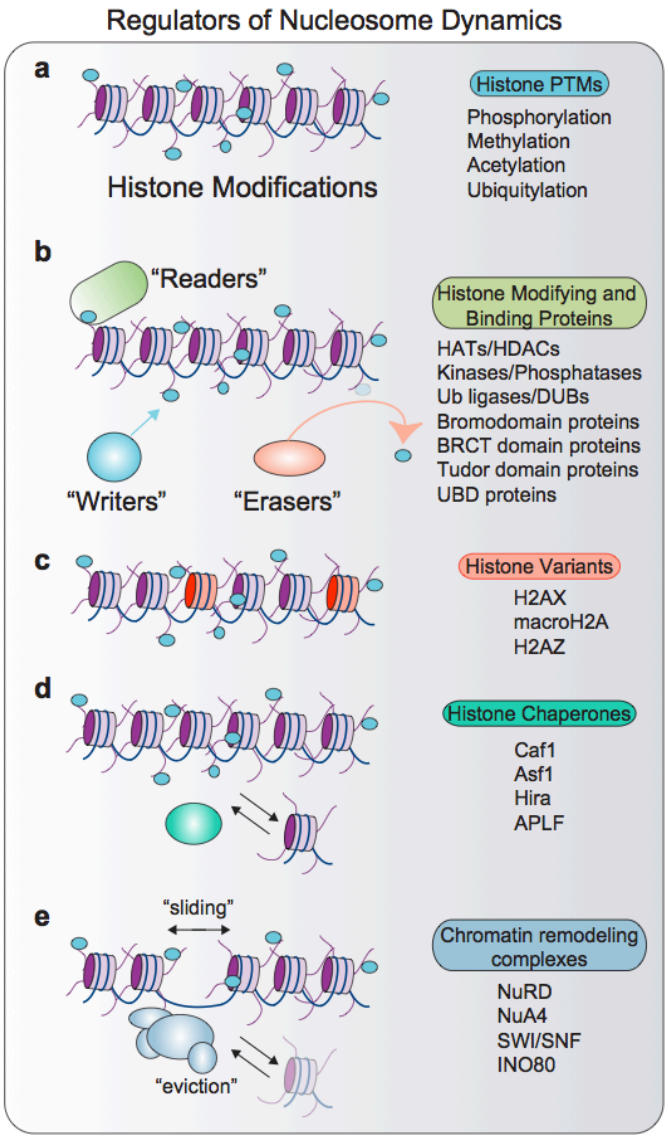

Figure 1.2 Various pathways involved in chromatin dynamics and DNA repair

(A) Histone modifications. (B) Histone PTM modifying and binding proteins that "write," "erase," and "read" chromatin marks. (C) Histone variants. (D) Histone chaperones, and (E) Chromatin remodeling complexes that regulate nucleosome and chromatin dynamics through activities including sliding and eviction of nucleosomes. A limited set of examples for each category is provided (3).

landscape by sliding, evicting, or exchanging histones, including variants or modulating nucleosome–DNA interactions to promote DNA damage signaling and repair (4, 12-16) (Figure 1.2 A-E). The collective utilization of these pathways is essential for maintaining genome integrity and averting diseases including cancer.

HISTONE POSTTRANSLATIONAL MODIFICATIONS (PTMs) IN CHROMATIN REGULATION AND THE DDR

Histone PTMs can impact chromatin structure to provide DNA accessibility to DDR factors to facilitate repair. Eukaryotic genomes contain multiple chromatin states that change depending on cell type and cell-cycle phase as well as the processes that act upon a particular region of the genome at any given time. For example, active transcription correlates with an "open" chromatin configuration (i.e. euchromatin) while transcriptionally repressed regions results in a more "closed" chromatin state (i.e. heterochromatin). A mechanism that regulates chromatin states is the PTMs that decorate histones. The basic charge of histones is due to the high proportion of positively charged lysine and arginine residues that are found in all histone proteins. Negatively charged DNA interacts electrostatically to regions of the histone that contain these amino acids. Modifications of either lysines or arginines have the potential to disrupt DNA/protein and protein/protein interactions by changing the charge of the modified amino acid (17, 18).

Histone PTMs, including phosphorylation, ubiquitination, methylation, and acetylation, can also serve as molecular DSB recognition signals for PTM "reader" proteins that selectively recognize and bind to these modifications on chromatin (4, 12, 19-21). For example, the first histone signaling event identified upon DSB induction was the phosphorylation on serine-139 of the histone variant H2AX (called γH2AX) (22). This modification is triggered by the activation of the DDR kinases, including ATM and DNA-PK that are themselves recruited to and activated by signaling processes that include DNA ends of the DSB. Although initiated at the DSB, the γH2AX modification spreads over a megabase of chromatin flanking the DSB site by an amplification loop involving the binding of γH2AX by the phospho-reader MDC1, which interacts with MRN complex to recruit and further stimulate ATM activity on chromatin (Figure 1.3) (16, 23-30). Focal accumulation of γH2AX promotes the accumulation of DSB factors to the break site, thereby promoting chromatin responses to DNA damage (5, 28, 31-35). In

addition to γH2AX, modification of nucleosomes by other DDR factors act to coordinate the complex signaling events of the DDR network that are involved in DNA repair of DSBs (Table 1.1). Several E3 ubiquitin ligases, including RNF8, RNF168, BRCA1, RNF20/40, RING1B and BMI1 are recruited to DNA lesions and ubiquitinate histones and chromatin factors to promote the DDR (36, 37). For example, phosphorylation of mediator of DNA-damage checkpoint1 (MDC1) protein by ATM recruits RNF8, which

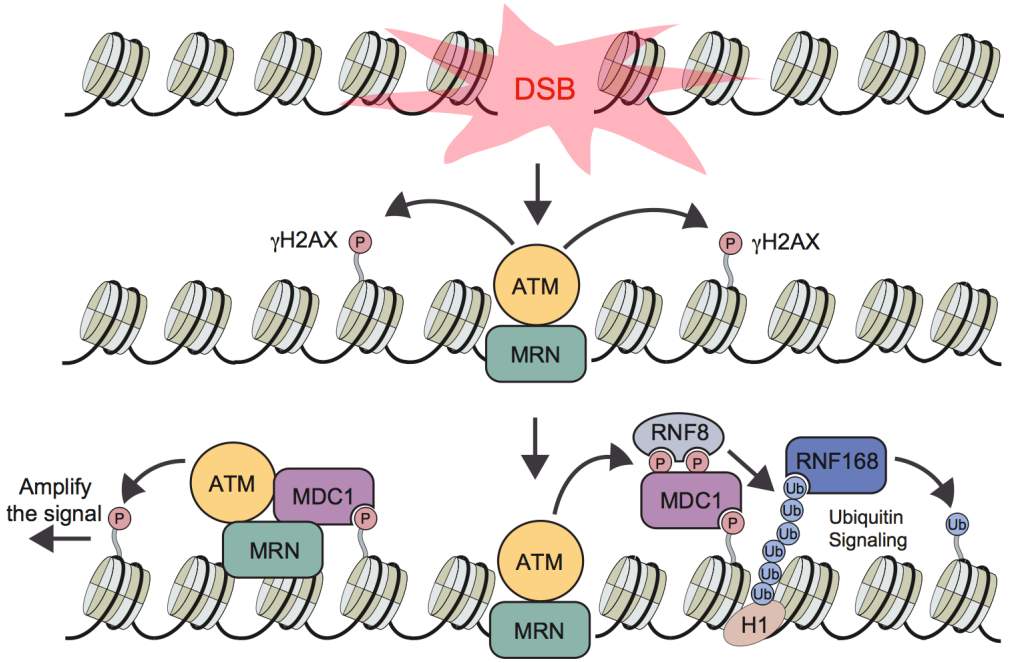

Figure 1.3 DNA damage signaling within chromatin

The MRN complex senses the DSB and recruits and activates ATM resulting in phosphorylation of H2AX (i.e., γH2AX). γH2AX is bound by MDC1, which interacts with MRN-ATM, which sets up an amplification signal on chromatin. Phosphorylated MDC1 recruits the Ubiquitin E3 ligase RNF8 that targets H1 linker histones. Ubiquitinated H1 promotes recruitment of the ubiquitin E3 ligase RNF168. RNF168-dependent ubiquitination of H2A and H2AX promotes accumulation of DSB repair proteins to sites of damage. P = phosphorylation, Ub = Ubiquitination, MRN = Mre11-Rad50-Nbs1 complex (38).

Histones	Modifications	Target residues	Writer enzymes	Functions in DSB repair	References
H2A	Acetylation	K5	Tip60	Involved in early DSB response	(Beck et al., 2006)
	Ubiquitylation	K13/15	RNF8/RNF168	53BP1, BRCA1 recruitment	(Doil et al., 2009; Gatti et al., 2012; Huen et al., 2007; Kolas et al., 2007; Mattiroli et al., 2012)
	Ubiquitylation	K118/119	RING1B/BMI1	Transcriptional silencing at DSBs	(de Napoles et al., 2004; Ginjala et al., 2011; Huen et al., 2007; Ismail et al., 2010; Leung et al., 2014; Wang et al., 2004)
	Ubiquitylation	K127/129	BRCA1	N.D.	(Kalb et al., 2014)
H2AX	Acetylation	K5	Tip60	Regulation of H2AX-Ub, HR repair	(Ikura et al., 2007)
	Acetylation	K36	CBP/p300	Ku recruitment for NHEJ, regulation of IR sensitivity	(Jiang et al., 2010)
	Phosphorylation	S139	ATM, ATR, DNA-PKcs	Check point activation, HR, NHEJ proteins recruitment	(Fernandez-Capetillo et al., 2002; Paull et al., 2000; Rogakou et al., 1998; Stiff et al., 2004)
	Phosphorylation	Y142	WSTF	Switch between DNA repair and apoptosis	(Xiao et al., 2009)
	Ubiquitylation	K13/15	RNF8/RNF168	53BP1, BRCA1 recruitment	(Fradet-Turcotte et al., 2013; Gatti et al., 2012; Huen et al., 2007; Mattiroli et al., 2012)
	Ubiquitylation	K118/119	RING1B/BMI1	Transcription repression at DSB sites, HR and NHEJ repair	(Chagraoui et al., 2011; Facchino et al., 2010; Ginjala et al., 2011; Huen et al., 2007; Leung et al., 2014)
	Sumoylation	N.D.	N.D.	N.D.	(Chen et al., 2013)
H2A.Z	Ubiquitylation	N.D.	RNF168	N.D.	(O'Connor et al., 2015)
H2B	Phosphorylation	S14	Mst1 kinase	Chromatin stabilization and restoration post repair	(Fernandez-Capetillo et al., 2004; Rossetto et al., 2010)
	Ubiquitylation	K120	RNF 20/RNF40	NHEJ and HR proteins recruitment, Chromatin decompaction for repair	(Moyal et al., 2011; Nakamura et al., 2011)
H3	Acetylation	K14	GCN5, requires HMGN	Promotes BRG1 binding to γH2AX NCPs, ATM binding to damaged chromatin, regulates activity of ATM kinase	(Kim et al., 2009; Lee et al., 2010)

(Continued in next page)

H3	Acetylation	K18	CBP, p300	NHEJ repair factor Ku accumulation	(Ogiwara et al., 2011)
	Acetylation	K23	HAT1	Promotes HR repair	(Yang et al., 2013)
	Acetylation	K56	CBP, p300	Promotes NHEJ repair	(Miller et al., 2010; Tjeertes et al., 2009; Vempati et al., 2010)
	Methylation (me3)	K9	Suv39h1/Suv 39h2	ATM activation, Stimulation of TIP60 activity	(Ayoub et al., 2008; Ayrapetov et al., 2014; Bao, 2011; Sun et al., 2009; Xu and Price, 2011)
	Methylation (me2)	K36	Metnase/SE TMAR	NBS1 and Ku accumulation, promotes NHEJ repair	(Fnu et al., 2011)
	Methylation (me3)	K36	SETD2	HR repair of DSBs within transcriptionally active sites	(Aymard et al., 2014; Carvalho et al., 2014; Pfister et al., 2014)
	Methylation (me2)	K79	Dot1L	Recruits 53BP1 to DSB site	(Huyen et al., 2004; Wakeman et al., 2012)
H4	Acetylation	K5, K8, K12	CBP/p300, TIP60 (NuA4 complex)	Ku proteins recruitment for NHEJ repair, chromatin relaxation	(Ogiwara et al., 2011)
	Acetylation	K16	MOF, TIP60 (NuA4 complex)	MDC1 binding to γH2AX, reduced 53BP1 binding to chromatin, BRCA1 recruitment, H2A.Z exchange, transcriptional repression, chromatin condensation, ZMYND8 binding	(Chailleux et al., 2010; Gong et al., 2015; Gupta et al., 2005; Hsiao and Mizzen, 2013; Li et al., 2010; Sharma et al., 2010; Tang et al., 2013)
	Methylation(me1 /2)	K20	PRSET7/Set 8, MMSET	53BP1 recruitment	(Botuyan et al., 2006; Hartlerode et al., 2012; Hsiao and Mizzen, 2013; Oda et al., 2010)
	Neddylation	N-tail	RNF111	RNF168 recruitment	(Ma et al., 2013)
	Ubiquitylation	K91	BBAP	Required for induction of H4K20me to promote 53BP1 recruitment	(Yan et al., 2009)
H1	Ubiquitylation	N.D.	RNF8	Forms K-63 linked Ub chains for RNF168 recruitment	(Thorslund et al., 2015)

Table 1.1 Histone PTMs associated with DSB repair in mammalian cells

N.D. = Not determined. *This table was adapted from (38)*.

has recently been shown to ubiquitinate the linker histone H1 (39). RNF168 is recruited to damage sites through ubiquitin-dependent interactions to promote further ubiquitination of histones by this E3 ligase, which are required to regulate DSB repair by 53BP1 and BRCA1 (5, 24, 37, 40, 41) (Figure 1.3). Interestingly, recognition of damaged chromatin by 53BP1 requires binding to H4K20 methylation as well as histone H2A/

H2AX K15 ubiquitination (17, 42). 53BP1 recruitment to chromatin upon DNA damage is also regulated by histone acetylation. Histones are acetylated by histone acetyltransferases (HATs) and deacetylated by histone deacetylases (HDACs). Many of these enzymes are recruited to DSBs to regulate specific acetylated residues on histones to promote either HR or NHEJ (43). For 53BP1, acetylation of H4K16 at DSBs by the TIP60 HAT occludes the ability of the tudor domain within 53BP1 to recognize H4K20 methylation.

When H4K16 is acetylated, this inhibits 53BP1 binding, which promotes BRCA1 binding and HR (44, 45). Histone marks can also act as high affinity binding sites for proteins that contain binding domains that recognize histone PTMs. Histone binding domains exists for many PTMs including phosphorylation, methylation and acetylation. For instance, twin-BRCT domains can bind phosphorylated histones, chromodomains have binding preferences for methylated lysines and bromodomains can specifically interact with acetylated lysine residues (12, 20, 46). For example, transcription-associated H3K36 trimethylation (H3K36me3) by SETD2 promotes DNA repair by homologous recombination (47-49). H3K4me3 creates a binding site for transcriptional complexes, leading to gene activation and euchromatin formation. Thus, different chromatin states and functions found throughout the genome can be regulated and established by the modification of context specific amino acid residues on histones.

Although the primary function of many histone PTMs in DSB repair signaling are well characterized, it is still unclear how writers of these marks, including ubiquitin E3 ligases and HATs, recognize their histone substrates within the nucleosome to promote site-specific modifications of their target lysine residues (Figure 1.4). Recent studies are beginning to provide mechanistic insights into how nucleosome recognition is achieved to promote chromatin-based DDR events. Accumulating evidence suggests that key stru-

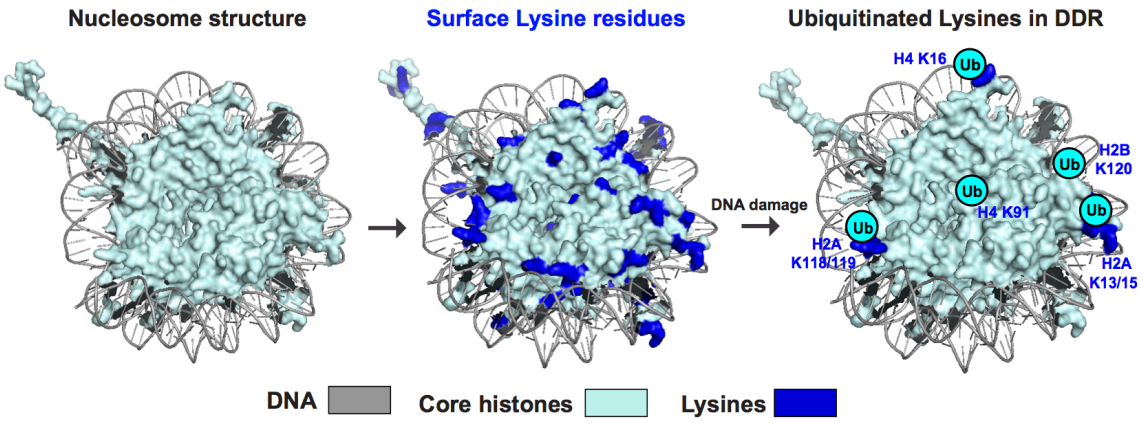

Figure 1.4 Damage-induced histone ubiquitinations on the nucleosome

X-ray crystal structure of a nucleosome core particle of Xenopus was retrieved from protein data bank (PDB code 1AOI) and modeled in Pymol. Locations of lysine residues on the exposed nucleosomal surface are marked in dark blue. Histone tails are structurally unresolved so are not depicted. Known damage-induced ubiquitinated lysines are indicated as Ub. DNA, grey; histones, pale cyan; lysines, dark blue; ubiquitin (Ub), light blue (38).

-ctural features of the nucleosome serve to mediate chromatin targeting by DDR factors to promote DNA damage signaling within chromatin (50-54). This information is starting to reveal important new ideas for how the "histone code" is encoded and read at DSB sites by DDR factors.

THE NUCLEOSOME: BASIC UNIT OF CHROMATIN

In the mammalian genome, billions of bases of DNA are organized by chromatin into the nuclear volume of the cell. Within this environment, specific gene regulatory networks must be highly regulated to maintain cellular function and identity. Dynamic transitions from compact and inaccessible chromatin states to decompacted and accessible structures allow control of gene expression. The presence of DNA damage within these environments necessitates the use of similar chromatin dynamics to coordinate DNA damage signaling and repair. The basic unit of chromatin is the nucleosome, which forms linear arrays of DNA–protein complexes that resemble an extended "beads on a string" structure in its most relaxed state. The nucleosome core

particle (NCP), a structure consisting of a core histone octamer, is composed of 2 copies of each core histone protein H2A, H2B, H3 and H4, containing around 146 bps of DNA (55-57). The overall sequence of histones and structure of NCPs containing the canonical histones is highly conserved from yeast to mammals, suggesting resistance to structural alterations, implying significant functionality for the NCP across different species (58). Histones H2A, H2B, H4 and histone variant H2AX have been shown to be ubiquitinated at distinct lysine residues upon damage induction to signal and activate DSB repair (59-65) (Figure 1.4). However, a mechanistic understanding of how site-specific epigenetic marks on these histone residues are achieved by writer enzymes and how these marks are recognized by their reader proteins within the context of the nucleosome is poorly understood. While most studies have focused on chromatin DDR factors and histone modifications involved in the DDR, very few studies have asked how these pathways are regulated at the level of the starting template, the nucleosome. While many of these protein–nucleosome interactions are mediated by histone PTMs, some regulatory proteins, including writers of these histone PTMs interact with specific residues, surface domains, or structured regions of the nucleosome. One such structured domain is the nucleosome acidic patch present in the histone H2A-H2B dimer (66-69). This indicates that the nucleosome does not merely act as a static packaging mechanism for DNA within cells but rather serves as a dynamic interface for chromatin-mediated processes that regulate the chromatin landscape to orchestrate DNA damage signaling and repair within specialized chromatin surroundings.

NUCLEOSOME ACIDIC PATCH AND DNA REPAIR

Solving the X-ray crystal structure of the NCP using reconstituted *Xenopus* recombinant histones revealed for the first time that in contrast to the largely basic nature of the core histones, the H2A-H2B dimer in the NCP consists of a unique negatively charged region on the surface of the nucleosome called the acidic patch (57). A group of

8 negatively charged residues constitute the acidic patch, 6 residues from histone H2A (E56, E61, E64, D90, E91, E92) and 2 from histone H2B (E102 and E110), all of which are localized on the nucleosome surface (Figure 1.5). Numerous studies suggest that the acidic patch serves as an interaction or recognition site for other chromatin proteins (54, 66, 67, 70). Although the overall structure of the NCP is conserved among species, in higher eukaryotes alternative H2A isoforms exist that can affect chromatin structure and

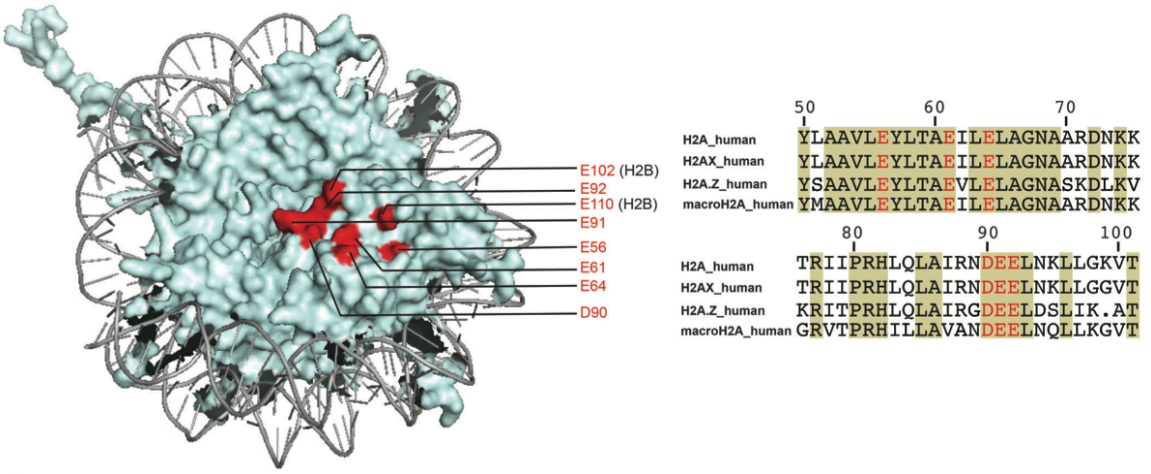

Figure 1.5 Involvement of the nucleosome acidic patch in the DDR

Structural position of the negatively charged acidic patch residues (shown in red) within the nucleosome (PDB 1AOI). The structure was colored and modeled in Pymol. Right panel: Sequence alignment of acidic patch containing segment (50–101 amino acids) of histone H2A and its variants. The acidic patch residues of H2A (E56, E61, E64, D90, E91and E92) are highlighted in red. Residues that are conserved among all the four H2A variants are marked in brown boxes (38).

stability when incorporated into NCPs and in turn regulate the chromatin-association of various factors (71-73). With the exception of H2A.Bbd, the nucleosome acidic patch is conserved in other human H2A variants, including H2AX, macroH2A, and H2AZ (Figure 1.5).

Interestingly, the acidic patch within H2AZ nucleosome is slightly extended as opposed to the other H2A and variant nucleosomes (71, 73, 74), which may alter its functionality, compared to other H2A species. Recent studies have identified the acidic

patch of the nucleosome as a critical chromatin component for DSB sensing and repair. The involvement of the acidic patch in DSB repair was first identified in the Jackson and Miller labs by a systematic mutation screen for H2AX that analyzed over 70 mutations in H2AX and how they affected its PTMs, including phosphorylation, sumoylation, and ubiquitination (50). Surprisingly, mutations within the acidic patch of H2AX or H2A abolished all detectable ubiquitination modifications of the mutant histone protein. However, the functional consequences of these mutations on the DDR require further investigation.

ACETYLATION READER PROTEINS AND THE DDR

Acetylation signaling is an integral component of the DDR machinery in human cells as evident by around 17 histone acetyltransferases (HATs) and 18 histone deacetylases (HDACs) that are recruited to DNA damage to regulate DDR-related acetylation signaling (75). Histone acetylation regulates DNA and histone binding, as shown by H4K16Ac that interrupts histone interactions in order to promote chromatin relaxation (76). The HAT, TIP60 promotes HR by acetylating H4K16 that in turn interferes with chromatin binding of the NHEJ factor 53BP1 to reduce NHEJ (77, 78). Acetylated histone and non-histone proteins can be recognized and bound by specific domains within proteins including BRD proteins, which contain the acetyl-lysine binding bromodomain (BRD) (19, 79) (Figure 1.6).

BRD-containing proteins are involved in a wide range of function such as several of them serve as HATs that catalyze histone acetylation, components of ATP-dependent chromatin remodeling complexes and various other transcription regulators. BRD, the principal acetylation reader domain is present in 42 human proteins containing one or more BRD domains (79, 80). All BRD domains consist of four α-helices (αZ, αA, αB, αC), linked by different loops of various lengths. The ZA and BC loops form a hydroph-

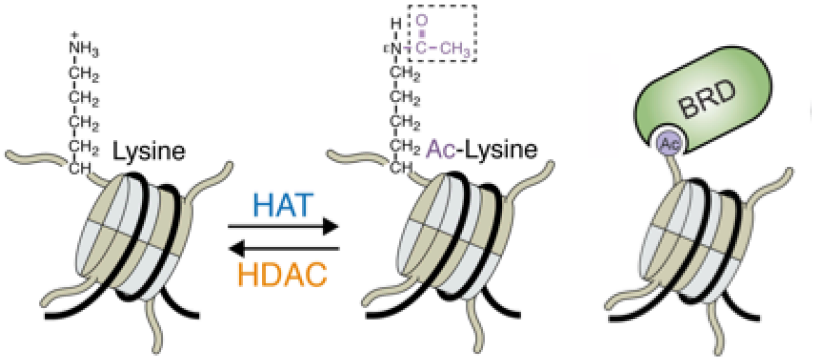

Figure 1.6 Acetylation mark on histones and their readers

HATs catalyze the addition of an acetyl (Ac) moiety on the e-amino group of a lysine residue, and HDACs reverse this reaction. Acetylated lysines on histones is recognized and bound by proteins containing BRD domains and other acetyl-lysine binding domains (not shown here). *This figure was adapted from (81).*

-obic cavity that specifically recognizes acetyl-lysines. BRD proteins are grouped according to their functions such as HATs, components of ATP-dependent chromatin remodeling complexes and transcriptional regulators (79, 82, 83). Mutated or abnormally expressed BRD proteins leading to their dysfunction have been identified in different types of diseases, including cancer (84). BRD proteins represent an attractive drug target due to their unique structure and druggability and efforts to design small molecule inhibitors of these proteins as putative cancer therapies have already been FDA approved or being evaluated in pre-clinical and clinical trials (85-87).

BRD proteins are generally classified as transcriptional regulators and recent studies have shown several BRD proteins (e.g. p300, BAZ1B and BRD4) to be involved in the DDR (88-91). The BRD protein TRIM28 (KAP1) was one of the first identified heterochromatin DSB repair factors (92-94). The Miller lab previously reported the involvement of one-third of the 42 human BRD proteins in the DNA damage response (DDR) (82). They identified ZMYND8 BRD protein as a new DDR factor that recruits to DNA damage and in a TIP60 mediated histone acetylation dependent manner recruits the NuRD chromatin-remodeling complex to damaged chromatin (82) to repress transcription and facilitate DNA repair by HR. Of the newly identified DNA damage

associated BRD factors by the Miller lab, a part of my thesis project focuses on studying the TRIM-BRD proteins (TRIM24-TRIM28-TRIM33) that represent a large family of tripartite motif-containing (TRIM) proteins and have been linked to cancer but their individual or collective roles in the DDR are unclear. Functional analysis of TRIM-BRD proteins in the DDR will help to gain mechanistic insights into chromatin-based DDR through understanding the ability of BRD proteins to read and transmit information contained within acetylated chromatin.

REGULATION OF DNA DAMAGE-INDUCING ANTICANCER TREATMENTS BY CHROMATIN

Although DDR and chromatin pathways cooperate to promote genome stability to suppress mutations that can drive cancer, once the DDR is deregulated, a common situation is cancer cells; it renders the cells chemo- and radio-sensitive. The cytotoxic nature of DNA damage is exploited to kill cancer cells through DNA damage-inducing treatments such as anti-cancer drugs and radiotherapy (95, 96). Indeed, the first chemotherapeutic drug in the 1940s treated cancer by damaging DNA. This pioneering discovery set the stage for developing DNA damaging agents as anticancer drugs that are still amongst the most commonly-prescribed cancer treatment owing to their ability to promote DNA damage and cell death. Based on these successes, genome and epigenome targeting drugs including DNA alkylators, intercalators (actinomycin), cross linkers (cisplatin, mitomycin) etc. represent a large class of compounds being actively developed for therapeutic purposes (97-102). Importantly, different agents are associated with unique drug-induced cell phenotypes that vary between cancers and cell types. Discovery of mutated or dysregulated epigenetic modifiers and altered epigenomes in cancers could contribute to these effects (103). Indeed, the dynamic nature of genome and epigenome makes it challenging to predict and control chromatin-targeting drug responses. Besides, emerging evidence suggests that functional interactions between these small molecule compounds and the genome are non-stochastic and are influenced by a dynamic interplay

between DNA sequences and chromatin states(101). As chromatin regulates transcription through protein targeting at specific genomic loci, these chromatin states can also influence target accessibility and binding of small molecules (Figure 1.7).

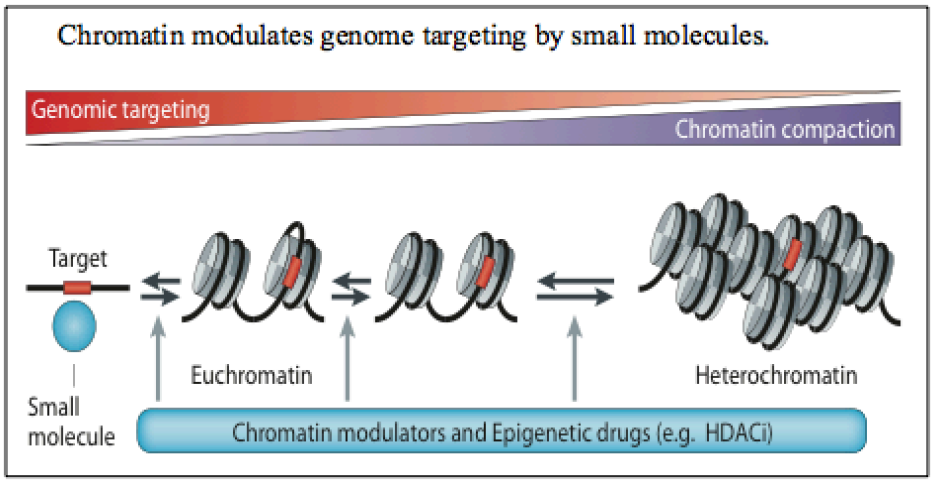

Figure 1.7 Chromatin regulates genome targeting by small molecules

The open state (euchromatin) and closed state (heterochromatin) of chromatin are shown. *This figure was adapted from (104).*

Unbiased genome-wide approaches to identify functional targets of small molecules in cells are being developed to identify drug effects across the genome. For instance, the use of drug labeling and genome-wide sequencing to reveal unanticipated drug mechanisms for a G-quadruplex (G4) binding small molecule, PDS has been shown (105). This work localized G4 structures with a known G4 binding protein, PIF1, which provided the strongest evidence of G4 structures in cells. The use of ChIP-Seq (chromatin-immunoprecipitation followed by sequencing) of DNA damage chromatin mark (γH2AX) identified unanticipated gene targets, including the proto-oncogene SRC that was 90% downregulated by the drug. This study provided a powerful example of how innovative chemical tagging techniques coupled with genome-wide strategies can provide novel insights into drug responses in human cells. Nonetheless, methods such as ChIP–seq and gene expression profiling provide indirect readouts of genomic sites of action of small molecules, which may preclude an in-depth understanding of drug

responses. Another technique, Chem-seq, was developed by the Bradner, Young and Rosenfeld labs that used bulky biotin tagged small molecules to isolate nucleic acids followed by sequencing to identify biologically relevant genomic target sites but there were technical limitations due to drug modifications that reduced the biological activity of the drug(106, 107). These studies highlight the importance of identifying genomic target sites; responses and properties of genome and epigenome drugs and to test the role of chromatin in these processes to better predict and control drug responses as a step towards personalized medicine.

Front line cancer therapies such as platinum drugs including cisplatin treatment readily result in the development of chemoresistance through multiple mechanisms(108). Importantly, cisplatin resistant cancer cells can be resensitized to cisplatin by combined treatment with other epigenetic drugs (109). For example, the two FDA approved epigenetic drugs; histone deacetylase inhibitors (HDACi) and DNA methylation inhibitor 5-azacytidine are being evaluated for combinatorial use with DNA damage for cancer treatments(110). Orchestration of drug targeting by chromatin might also shed light on intrinsic resistance or sensitivity of cancer cells to drug treatments and acquired drug resistance, which represent serious obstacles for therapeutic applications. Taken together, it is critical to evaluate whether chromatin reprogramming can modulate drug target site accessibility and drug responses.

HYPOTHESIS AND AIMS

Ubiquitination of proteins regulate the DDR with at least 6 E3 ubiquitin ligases recruited at DNA damage sites. In particular, the histone H2A/X are ubiquitinated by RING1B/BMI1 and RNF168 on K118/119 and K13/K15 respectively that mediate the chromatin association of both NHEJ and HR repair factors. A mechanistic view of how multiple Ub on H2A/X crosstalk between each other, as well as with other histone marks on H2A/X to coordinate and execute the DDR is undefined. Previous work from the

Miller lab has identified that key functional residues in H2AX that form the nucleosome acidic patch mediates H2A/X ubiquitination. I tested the hypothesis that the chromatin domain, nucleosome acidic patch, is required for both RNF168 and RING1B/BMI1 dependent H2A/X ubiquitinations in response to DNA damage. Secondly, the BRD chromatin reader proteins interact with damage associated acetylation to promote the DDR and genome maintenance. I tested our hypothesis that the TRIM-BRD proteins that are readily detectable as damage-recruited participate in the DDR. These experiments were designed to comprehensively assign functions to the TRIM-BRD proteins through acetylation signaling and their interacting factors. Mechanistic details of the DDR and chromatin would provide insights into novel therapeutic targets and therapies because these pathways are currently targeted by anti-cancer chemotherapeutic treatments in the clinic. Thirdly, chromatin represents a major target of drug substances used to treat cancer. Emerging evidence suggests that functional interactions between small molecules and the genome are non-stochastic and are influenced by a dynamic interplay between DNA sequences and chromatin states. As chromatin regulates transcription through protein targeting at specific genomic loci, these chromatin states can also influence target accessibility and binding of small molecules. In the second part of my thesis project, I tested the hypothesis that genome targeting by DNA-damaging agents is regulated by chromatin, which influences drug targeting, efficacy and responses. This study involved the development of innovative tools and strategies for interrogating chromatin-drug mechanisms, which has the potential to better predict and control these responses in cancer and its treatments as a step towards personalized medicine. These goals were pursued by these projects as outlined below:

Project 1. Investigate the role of nucleosome acidic patch in promoting H2A/X and H2AZ ubiquitination mediated DNA damage signaling. (A) Determine whether both RNF168 and RING1B/BMI1 E3 Ub ligases require the acidic patch for their activity by using a dual approach of *in vivo* and *in vitro* analyses (using reconstituted nucleosomes).

(B) Test whether nucleosome acidic patch interacting peptides (e.g. LANA) inhibit H2A/H2AX ubiquitinations and the DDR by *in vitro* Ub assays and *in vivo* analysis.

Project 2: Determine how chromatin regulates genome targeting of the cisplatin derivative, APPA. (A) Optimize chemical labeling of APPA in cells for visual detection of platinated lesions. (B) Identify how chromatin influences the drug targeting of platinated drugs using combinatorial treatment of APPA and chromatin modulators in cells.

Project 3: Determine the function of human TRIM-BRD proteins in the DDR. (A) Interrogate how damage-recruitment of TRIM-BRD proteins is regulated by upstream factors of the DDR pathway (B) Examine roles of histone acetylation in TRIM24 recognition of damaged chromatin; (C) Identify and validate TRIM-BRD proteins interactome using MS data for functional assignment of TRIM-BRDs in the DDR.

Collectively, these studies have contributed to deciphering chromatin-regulated processes that are paramount for understanding the nuclear pathways that regulate access to, and protection of our genetic and epigenetic information.

SUMMARY

During my graduate studies at the University of Texas at Austin, my dissertation project focused on understanding the mechanisms of chromatin involved in DDR and in chemotherapeutic responses. I also worked on delineating the function of acetylation reader BRD TRIM proteins in promoting chromatin-based DDR. My projects can be divided into several parts as follows:

1. I established methods to biochemically purify recombinant human histones and optimized protocols for reconstitution of nucleosome core particles in order to utilize them for *in vitro* assays. (Chapter 3).
2. I identified that the chromatin domain nucleosome acidic patch regulates both N'- and C'- H2A and H2AX ubiquitination reactions catalyzed by RNF168 and RING1B/BMI1 E3 ubiquitin ligases respectively to promote DDR signaling for efficient DNA repair. (Chapter 3).
3. I studied how chromatin states influence genome targeting of anticancer Pt drugs using a cisplatin analogue (APPA) that can be chemically labeled and visualized in cells. I identified that the clinically approved drug, Vorinostat (SAHA), a known inhibitor of histone deacetylases, when used as a combinatorial treatment with APPA formed clusters of DNA lesions that co-localized with translesion synthesis factors and activated this pathway. I found that the activated damage bypass translesion synthesis pathway no longer acted as a bypass/resistance mechanism but instead promoted apoptosis after cotreatment demonstrating that pharmacological alterations of chromatin reprograms genome targeting with platinum drugs and, concomitantly, the response to these drugs. (Chapter 4).
4. I performed functional analysis of the TRIM-BRD proteins that are recruited to sites of DNA damage. I identified the specific domains in TRIM24 that are required for its recruitment to sites of DNA damage and its dependency on other chromatin associated factors, namely, SUV39H1, KAT6B, TRIM28, TRIM33

that regulate TRIM24 dynamics in the context of DNA damage. I validated some of the interactors of TRIM24, TRIM28 and TRIM33 including the FACT and MCM complex family members to delineate their role in the DNA repair pathway. (Chapter 5).

Knowledge gained from these studies helped to delineate the role of an essential chromatin domain the acidic patch, interplay between three TRIM-BRD reader proteins in the DDR and chromatin-regulated processes that are paramount for regulation and protection of our genetic and epigenetic information. Since mutations in BRD reader proteins including the TRIM family cause genome instability and defective acetylation signaling that has directly been linked to cancer, future investigations to gain mechanistic insights into how these pathways function in regulating the cellular response to DNA damage is warranted. Given the increasing development and potential of epigenetic drugs targeting cancer pathways, these studies could provide additional candidates for development of small molecule inhibitors as well as new therapeutic targets in diseases including cancer. Besides, studies performed on how chromatin influences drug-genome interactions are informative for interrogating drug mechanisms and acquired drug resistance to better predict and control these responses in cancer and its treatments.

In addition to my main projects, I also participated in other collaborative projects, which are not included in this dissertation, but summarized as follows:

1. I identified the H2A histone variant H2AZ to be a substrate of the E3 ubiquitin ligase RNF168.
2. I purified nucleosomes containing the histone variant macroH2A and performed biochemical assays demonstrating that RNF168 and RING1B/BMI1 both ubiquitinate this histone variant.

CHAPTER 2: MATERIALS AND METHODS

CELL CULTURE CONDITIONS AND TREATMENTS

Most of the cell lines used in this study were cultured in standard conditions in Dulbecco's modified Eagle's medium (DMEM) (Invitrogen) supplemented with 10% fetal bovine serum (FBS), 2 mM L-glutamine, 100 U/ml penicillin, 100 μg/ml streptomycin. HEK293T and BOSC23 cells were cultured in RPMI 1640 medium supplemented with 10% fetal bovine serum and 1% penicillin/streptomycin. WT and H2AX deficient MCF10A cells were cultured in DMEM/F12 medium supplemented with 5% horse serum, EGF (20 ng/ml), hydrocortisone (0.5 mg/ml), cholera toxin (100 ng/ml), insulin (10 mg/ml) and 1% penicillin/streptomycin. A2780 cells (cisplatin sensitive) were purchased from Sigma-Aldrich (#93112519) and maintained in RPMI-1640 medium containing 2 mM L-glutamine and 10% FBS. HCT116 RAD18 KO cells were kindly provided by Junjie Chen's Lab (MD Anderson). Cells were kept at 37°C in a humidified incubator containing 5% CO_2. Cells stably expressing GFP-tagged TRIM proteins were established and maintained in medium with 10mg/ml Blasticidin. The chemical drugs and treatment conditions are listed in Table 2.1 on the next page.

Portions of this chapter have been published as follows:

- *Justin W. Leung*, Poonam Agarwal*, Marella D. Canny, Fade Gong, Aaron D. Robison, Ilya J. Finkelstein, Daniel Durocher, Kyle M. Miller (2014) Nucleosome acidic patch promotes RNF168- and RING1B/BMI1-dependent H2AXand H2A ubiquitination and DNA damage signaling. PLOS Genetics* 10(3): e1004178. *(* co first authors*
- *Emmanouil Zacharioudakis[1], Poonam Agarwal[1], Alexandra Bartoli, Nathan Abell, Lavaniya Kunalingam, Valerie Bergoglio, Blerta Xhemalce, Kyle M. Miller* and Raphael Rodriguez* (2017) Chromatin regulates genome targeting with cisplatin. Angew. Chem. Int. Ed. 2017, 56, 1–6. ([1]co first authors, * co corresponding authors)*

Picoplatin, APPA and APP were prepared in the Rodriguez laboratory as described in (111). Suberoylanilide hydroxamic acid (SAHA), cisplatin, MS-275 and hydroxyurea (HU) were purchased from Sigma. Stock solutions of APPA, picoplatin, and cisplatin were prepared at a concentration of 10 mM in DMF for cell viability assay. A fresh stock solution of 1 mM in 0.9% w/v NaCl was freshly prepared for APPA and cisplatin for use

Full name	Abbreviation	Work Conc.	Treatment time
2-aminomethylpyridine (dichloro) platinum (II) azide	APPA	250 μM	3-24 hrs
5-Bromo-2′-deoxyuridine	BrdU	10 μM	24 hrs
Cisplatin	-	10-500 μM	3-24 hrs
Azacytidine	5-Aza	10 μM	24 hrs
Taxol	-	1 μM	6 hrs
Trichostatin A	TSA	1 μM	24 hrs
5,6-Dichlorobenzimidazole riboside	DRB	100 μM	1-2 hrs
KU55933	ATMi	1 μM	2 hrs
Shield-1	-	0.5 mM	3 hrs
4-Hydroxytamoxifen	4-OHT	1 μM	3 hrs
Doxycycline	Dox	1 μg/ml	3 hrs
Olaparib	PARPi	1 μM	2 hrs
5-ethynyl uridine	5-EU	1 mM	1 hrs
Suberoylanilide hydroxamic acid	SAHA	1-10 μM	3-26 hrs
Pyridostatin	-	10 μM	6 hrs
Picoplatin	-	10-100 μM	3 hrs
NU7441	DNA-PKi	2 μM	4 hrs
MS-275		5 μM	5 hrs
GW7647	USP1 DUB	50 μM	3 hrs
Camptothecin	CPT	1 μM	4 hrs
Doxorubicin	-	100 nM	24 hrs
Etoposide	Etop	25 μM	4 hrs
Hydroxyurea	HU	2 mM	3-24 hrs
JQ1	BRD inhibitor	1 μM	5 hrs
Garcinol	HATi	10 μM	24 hrs
Remodelin	-	10 μM	24 hrs
Tranylcypromine	-	10 μM	24 hrs
JIB-04	HDMTi	10 μM	24 hrs
SGC0946	HMTi	10 μM	24 hrs
DZNep	HMTi	10 μM	24 hrs

Table 2.1 Small molecules, chemical drugs and treatment conditions used in this study

in cell imaging and pull-down experiments. Unless stated otherwise, cells were treated with APPA (250 μM) or cisplatin (10 μM). For co-treatments, SAHA (2.5 μM) was added to cells 2 h prior to treatment with APPA or cisplatin.

DOT BLOT ASSAY

U2OS cells were cultured in 15 cm dishes and treated with APP or APPA for 3 h. Total genomic DNA was isolated from cells using DNeasy Blood and Tissue kit (Qiagen; #69506) according to the manufacturer protocol. DNA was reacted with Alexa Fluor 488 alkyne using a click reaction buffer according to the manufacturer protocol (ThermoFisher Scientific; C10337). Labeled DNA was mechanically sheared using a bioruptor (Diagenode), 15 mins, 10 sec on/off at 4°C. DNA was then purified using QIAquick PCR purification kit (Qiagen, #28106) according to the manufacturer protocol. 2 μg of total DNA were loaded on Hybond nylon membranes (GE Healthcare). Samples were air-dried and visualized using a Bio-Rad Molecular Imager ChemiDoc XRS+ system.

DNA PULL-DOWN ASSAY

U2OS cells were treated with APPA alone or in combination with SAHA. After treatment, total genomic DNA of each sample was purified using DNeasy Blood and Tissue kit (Qiagen, #69506). Pure link RNaseA (Invitrogen) was used to remove RNA during genomic DNA extraction. Click-reaction was performed on the isolated DNA using Biotin-PEG4 alkyne (Sigma-Aldrich, #764213) and incubated for 1 h protected from light at room temperature. The click-reaction was quenched using 4 mM EDTA. The DNA was fragmented up to ~ 100-350 bp size using Diagenode Bioruptor 300 and purified using QIAquick PCR purification kit (Qiagen, #28106). To capture the biotin tagged DNA-ACP conjugates, each sample was incubated with Dynabeads® MyOne™ Streptavidin T1 (Invitrogen, #65602) followed by washing with a buffer containing 1 M NaCl, 5 mM Tris-HCl, pH 7.5 and 0.5 mM EDTA. Beads were then washed with 8 M

urea followed by three washes using the above washing buffer with 100 mM NaCl. After washing, beads were incubated in 1.8 M thiourea for 48 h at 37°C. DNA was purified using QIAquick PCR purification kit (Qiagen) and quantified using Qubit.

RNA-SEQ SAMPLE PREPARATION

Total RNA was extracted from cells untreated or treated with APPA, SAHA or in combination of SAHA and APPA using RNeasy Mini Kit (Qiagen, #74106) following the manufacturer's protocol. Residual DNA was removed by DNase I on column digestion. RNA concentration was determined using Nanodrop and sent for RNA-seq library preparation and deep sequencing at the NGS facility, MD Anderson Cancer Center. All datasets were analyzed with FastQC to confirm a lack of sequencing abnormalities. No adapter contamination was detected. rRNA and tRNA sequences were filtered and remaining sequences were aligned to the most recent build of the human genome (hg38) using Tophat2/Bowtie2 with sensitive parameters. Alignments with a mapping quality score of less than 5 or that were flagged as secondary were removed and files sorted and indexed. Read counts per gene were calculated from the remaining alignments using HTSeq with the Gencode v21 comprehensive genome annotation and results were exported into a raw counts expression matrix. Differentially expressed genes were identified using edgeR with default parameters except for two modifications: first, a gene was required to have an expression value of at least 1 count per million reads in at least one sample to be tested and second, a differentially expressed gene was required to have both an absolute fold change of 1.5 or greater and a statistically significant FDR-adjusted P-value <0.01. All final results were exported to Excel and all downstream plotting and analysis was performed with custom scripts in R using the ggplot2 graphics package. The heatmap was generated and hierarchically clustered by row and column using Pearson correlation as a distance metric and mean centered and normalized by row.

TRANSCRIPTION REPRESSION ASSAY

Nascent transcription detection by 5-EU monitoring was performed with 1 mM 5-EU added 1 h post-treatment. 5-EU was detected by Click-iT RNA imaging kit (Invitrogen). Samples were imaged and analyzed with Z-stacked settings using the FV10-ASW3.1 software on a Fluoview 1000 confocal microscope (Olympus).

TRANSFECTION IN MAMMALIAN CELLS AND RETROVIRAL INFECTION

Mammalian expression vectors were transfected into U2OS cells by Fugene HD (Promega) or using lipofectamine 2000 according to manufacturer's instructions. For HEK293T cells, transient transfections were carried out with pEI (Polyethylenimine, Sigma). Analyses for transient plasmid transfection were performed 24-48 h after transfection. HA-Flag-retroviral expression constructs were cotransfected with pCL-ampho in BOSC23 cells using Lipofectamine2000 (Invitrogen). Viruses were harvested and filtered at 48 h and 72 h after transfection. MCF10A H2AX-/- cells were transduced by virus containing medium and selected by puromycin (2 mg/ml). The GFP-LANA (1–32 a.a) or GFP-LANA-8LRS10 constructs were transfected into U2OS cells using HilyMax (Dojindo) following manufacturer's instruction. Transfections for siRNA were carried out with lipofectamine RNAiMax (Invitrogen) following manufacturer's instructions. Analyses for siRNA treated cells were performed 48-72 h after transfection. The sequences of siRNA used in this study are list in Table 2.2.

Target gene	siRNA sequence or Order information	Source
TRIM24	ON-TARGETplus SMARTpool: L-005387-00-0005	GE Dharmacon
TRIM28	ON-TARGETplus SMARTpool: L-005046-00-0005	GE Dharmacon
TRIM33	ON-TARGETplus SMARTpool: L-005392-00-0005	GE Dharmacon
TIP60	ON-TARGETplus SMARTpool: L-006301-00-0005	GE Dharmacon
MOF	GCAAAGACCAUAAGAUUUA	Sigma
LigaseIV	AGGAAGUAUUCUCAGGAAUUA	Sigma
CtIP	GGUAAAACAGGAACGAAUC	Sigma
SUV39H1	ON-TARGETplus SMARTpool: L-009604-00-0005	GE Dharmacon
KAT6B	ON-TARGETplus SMARTpool: L-019563-01-0005	GE Dharmacon

Table 2.2 List of siRNA sequences or order information used in this study

IR treatment: Untransfected cells or 24 h post transfection, cells were treated with 2 Gy IR and processed 2 h post-treatment. A Faxitron X-ray machine (Faxitron X-ray Corporation) was used for gamma irradiation (IR).

CELL VIABILITY ASSAY

Cell viability assays were carried out by plating U2OS human osteosarcoma cells (2,000 cells/well) in 96-well plates. Cells were treated with the relevant drug for 72 h and incubated with CellTiter-Blue® (20 μL/well) for 1 h before recording fluorescence (560(20) Ex/590(10) Em) using a PerkinElmer Wallac 1420 Victor2 Microplate Reader. Experiments were performed in triplicate and the fluorescence of each treated sample was normalized against untreated samples in order to obtain the percentage of viability for each treatment. GI_{50} values (the concentration of drugs that reduces by 50% the fluorescence that is emitted compared to untreated samples) was calculated and plotted on a graph.

CLONING AND PLASMIDS

RNA was extracted from U2OS cells or HEK293T cells for cDNA synthesis. cDNAs of human proteins used in this study were cloned into entry vector pDONR201 by attB recombinant sites. Point mutation or internal deletion constructs of the chosen protein were performed as per the site-directed mutagenesis standard protocols using primers designed for the indicated mutation or deletion. All plasmid inserts and mutations were confirmed by DNA sequencing. WT and mutant human H2AX cDNAs were cloned into gateway compatible entry vector (pDONR201). 5'-biotin tagged 601 nucleotide sequence was generated by PCR using the primer pairs: 5'(Btn) CTGGAGAATCCCGGTGCC (F' primer) and 5'ACAGGATGTATATATCTGACACG (R' primer) to be used for reconstitution of nucleosomes. The N-terminal 32 amino acids of LANA were amplified using PCR with the following primers:

F': 5'TTGTCGACATGGCGCCCCCGGGAATGCGCCTGA-3' and R': 5'-TTTCTAGACTATCTTTCCGGAGACCTGTTTCG-3' and cloned into eGFP-C1 (Clontech) vector using 5'-SalI and 39-XbaI restriction sites to create GFP-LANA (1–32 a.a.). Primers for mutating 8RLS10 to AAA of LANA have been described by a previous study and were used to mutate GFP-LANA (1–32 a.a.) to GFP-LANA-8LRS10 (112). The expression plasmids used in this study are listed in Table 2.3.

Gene name	Expression Plasmid	Vector	Gene Source
H2AX	H2AX-N-SFB	N-SFB-DEST	Dr. Michael Huen Lab, University of HongKong
	H2AXallR-N-SFB	N-SFB-DEST	(52)
	H2AXallR R13/15K-N-SFB	N-SFB-DEST	
	H2AXallR R13/15K E92A-N-SFB	N-SFB-DEST	
	H2AXallR R13/15K S139A-N-SFB	N-SFB-DEST	
	H2AX allR R118/119K	N-SFB-DEST	
	H2AX allR R118/119K E92A-N-SFB	N-SFB-DEST	
	H2AX K13/15R-N-SFB	N-SFB-DEST	
	H2AX K118/119R-N-SFB	N-SFB-DEST	
	H2AX E92A-N-SFB	N-SFB-DEST	
	H2AX S139A-N-SFB	N-SFB-DEST	
	H2AX-His6	pDEST17	
	H2AX E92A-His6	pDEST17	
	H2AX E92D-His6	pDEST17	
	H2AX E92Q-His6	pDEST17	
	H2AX L65A.L93A-His6	pDEST17	
	H2AX I111A.L116A -His6	pDEST17	
H2A	H2A	pET21	(113)
	H2A-E92A	pET21	
H2B	H2B E106R-His6	pDEST17	
	H2B	pET21	
H3	H3	pET21	
H4	H4	pET21	
H2AZ	H2AZ	pDEST17	U2OS cDNA
	H2AZ D94A	pDEST17	
BMI1	BMI1-His6 (1-108)	pET24b (+)	(17)
	BMI1 K62A.R64A-His6 1-108)	pET24b (+)	
RING1B	RING1B (1-116)	pGEX-6P-1	

(Continued in next page)

	RING1B K97E.R98E (1-116)	pGEX-6P-1	
	RING1B K93D (1-116)	pGEX-6P-1	
RNF168	RNF168-N-myc	N-myc-DEST	
	RNF168-His6	pPROEX HTa	
	RNF168 R57D-His6	pPROEX HTa	
LANA	LANA(1-32)-N-GFP	eGFP-C1	cDNA: Sullivan Lab
	LANA(1-32)-8LRS-N-GFP	eGFP-C1	
Polη	Polη-N-Flag	pTRIP-CMV-Flag	pcDNA3.1/Hygro Flag-Polη
TRIM24	TRIM24-N-EmGFP	N-EmGFP-DEST	DNASU:HsCD00005267
	TRIM24-ΔPHD-N-EmGFP	N-EmGFP-DEST	pDONR201-TRIM24
	TRIM24-ΔBRD-N-EmGFP	N-EmGFP-DEST	
	TRIM24 C840W-N-EmGFP (PHD mutant)	N-EmGFP-DEST	
	TRIM24 F979A N980A-N-EmGFP (BRD mutant)	N-EmGFP-DEST	
	TRIM24 C840W F979A N980A-N-EmGFP (PHD and BRD mutant)	N-EmGFP-DEST	
	TRIM24-ΔRING-N-EmGFP	N-EmGFP-DEST	
	TRIM24-C56A C59A-N-EmGFP (RING mutant)	N-EmGFP-DEST	
	TRIM24-N-SFB	pcDNA5/FRT/TO N-SFB	
	TRIM24-N-GFP	pcDNA5/FRT/TO N-GFP	
TRIM28	TRIM28-N-EmGFP	N-EmGFP-DEST	U2OS cDNA
	TRIM28-N-SFB	pcDNA5/FRT/TO N-SFB	
TRIM33	TRIM33-N-EmGFP	N-EmGFP-DEST	Addgene:15734
EGFP-C1	EGFP-C1	pEGFP-C1	Clontech
ZMYND8	ZMYND8-N-EmGFP	N-EmGFP-DEST	(114)
MCM4	MCM4-N-EmGFP	N-EmGFP-DEST	293T cDNA
MCM5	MCM5-N-EmGFP	N-EmGFP-DEST	293T cDNA
MCM6	MCM6-N-EmGFP	N-EmGFP-DEST	U2OS cDNA
MCM7	MCM7-N-EmGFP	N-EmGFP-DEST	293T cDNA

Table 2.3 Expression vectors used in this study

PROTEIN EXTRACTS AND WESTERN BLOTTING

For whole cell extracts, cells were washed once with PBS and collected with 2X Laemmli buffer (4% (v/v) SDS, 20% (v/v) glycerol and 120 mM Tris-HCl, pH 6.8). Samples were sonicated using a Diagenode Bioruptor 300 for 10 min followed by boiling for 5 min at 95°C before loading onto SDS-PAGE gel using 3X protein loading buffer

(4% (v/v) SDS, 30% (v/v) glycerol, 150 mM Tris-HCl (pH 6.8), 350mM beta-mercaptoethanol and 0.075% bromophenol blue). For chromatin fractions, cells were pre-extracted by CSK buffer (10 mM PIPES, pH 6.8, 100 mM NaCl, 300 mM sucrose, 3 mM $MgCl_2$, 1 mM EGTA, 0.5% (v/v) Triton X-100) for 5 min on ice to remove the soluble proteins. After two washes with PBS, chromatin extracts were collected with Laemmli buffer and subjected to sonication and boiling steps before loading. Protein samples were resolved by SDS-PAGE, transferred to nitrocellulose membrane (GE Healthcare), incubated overnight in primary antibodies as indicated, followed by 1h of incubation in HRP-conjugated secondary antibodies. Signal on western blots were detected by standard chemiluminescence (GE Healthcare, Amersham ECL Prime system) using a Bio-Rad molecular imager ChemiDoc XRS+ system. Secondary antibodies used were: anti-rabbit IgG, HRP-linked (Cell Signaling, #7074) and antimouse IgG, HRP-linked (Cell Signaling, #7076). Primary antibodies used in this study are listed in Table 2.4.

Antibody epitope	Host	Source	Catalog No.	Application
PCNA	Rabbit	Abcam	ab18197	IF, WB
TRF1	Mouse	Abcam	ab10579	IF
CENPA	Mouse	Abcam	ab13939	IF
RAD18	Mouse	Abcam	ab57447	IF
H2AX	Rabbit	Millipore	07-627	WB
H4	Rabbit	Abcam	ab7311	WB
Actetyl-Histone H4 (lys 5, 8, 12 and 16)	Rabbit	Millipore	06-866	WB
PCNA	Mouse	Santa Cruz Bio	PC10	WB
PARP	Rabbit	Cell Signaling	9542	WB
RAD18	Rabbit	Cell Signaling	9040S	WB
Fibrillarin	Mouse	Abcam	ab4566	IF
β-tubulin	Rabbit	Abcam	ab6046	WB
γH2AX	Rabbit	Novus	NB100-384	IF, WB
γH2AX	Mouse	Millipore	05-636	IF
γH2AX	Mouse	Cell Signaling	9718	IF
Flag	Mouse	Sigma	F1804	IF
RPA32	Mouse	Abcam	ab2175	WB
p-RPA32 (S4/S8)	Rabbit	Bethyl Labs	A300-245A-5	WB
p-RPA32 (S33)	Rabbit	Bethyl Labs	A300-246A	WB
CHK1	Mouse	Santa Cruz	sc-8408	WB

(Continued in next page)

Phospho-CHK1 (Ser345)	Rabbit	Cell Signaling	2348	WB
Cleaved Caspase-3 (Asp175)	Rabbit	Cell Signaling	9664	WB
H2AX	Rabbit	Cell Signaling	2595	WB
53BP1	Rabbit	Novus	NB100-304	IF
53BP1	Mouse	BD transduction Labs	612522	IF
MDC1	Rabbit	Abcam	ab11169	IF
RIF1 (N-20)	Goat	Santa Cruz	sc-55979	IF
c-Myc	Mouse	Santa Cruz	sc-40	WB
BRCA1 (D-9)	Mouse	Santa Cruz	sc-6954	FACS
RPA32 (9H8)	Mouse	Abcam	ab2175	FACS
p-H3 (Ser10) (D2C8)	Rabbit	Cell Signaling	3377	FACS
Cyclin A (H-432)	Rabbit	Santa Cruz	sc-751	FACS
H4K20me1	Rabbit	Abcam	ab9051	WB
Actetyl-Histone H4 (lys 5, 8, 12 and 16)	Rabbit	Millipore	06-866	WB
CHD4	Rabbit	Active Motif	39289	IF, IP, WB
CHK1	Mouse	Santa Cruz	sc-8408	WB
CHK2	Rabbit	Cell Signaling	2662	WB
CtIP	Rabbit	Cell Signaling	9201	WB
DNA-PKcs	Mouse	Abcam	ab1832	WB
DNA-PKcs S2056p	Rabbit	Abcam	ab18192	WB
Flag	Mouse	Sigma	F1804	WB
GFP	Rabbit	Invitrogen	A11122	IP, WB
GST	Goat	GE Healthcare	27-4577	WB
H2AX	Rabbit	Cell Signaling	2595	WB
H3	Rabbit	Abcam	ab1791	WB
H4	Rabbit	Abcam	ab124762	WB
Phospho-CHK1 (Ser345)	Rabbit	Cell Signaling	2348	WB
Phospho-CHK2 (Thr68)	Rabbit	Cell Signaling	2661	WB
Phospho-p53 (Ser15)	Rabbit	Cell Signaling	9284	WB
TRIM24 (TIF1A)	Rabbit	Bethyl Labs	A300-815A	IF, IP, WB
TRIM28	Rabbit	Santa Cruz	sc-33186	IF, IP, WB
TRIM33	Mouse	Abnova	H00051592-M01	IF, IP, WB
MCM2	Rabbit	Abcam	ab133325	IP, WB
MCM4	Rabbit	Abcam	ab4459	IP, WB
SUV39H1	Rabbit	Abcam	ab155164	IF, WB
SSRP1	Rabbit	Abcam	ab137034	IF, IP, WB

Table 2.4 Primary antibodies used in this study.

IF: immunofluorescence; IP: immunoprecipitation; WB: Western blotting, FACS: Fluorescence assisted cell sorting

LASER MICRO-IRRADIATION AND LIVE-CELL MICROSCOPY ANALYSIS

U2OS cells were plated on glass-bottomed dishes (Wilco Wells). Cells were presensitized with 10 μM of 5-bromo-2' deoxyuridine (BrdU) in normal DMEM medium for 20 h. Laser micro-irradiation was carried out with a Fluoview 1000 confocal microscope (Olympus). Laser setting and protocols were as previous described (113). For quantification of laser damage recruitment, after laser microirradiation, the fluorescence intensity at the damage site as well as an undamaged control region of the same size from the same cell were directly recorded by the FV10-ASW3.1 software in real-time. Variation of the fluorescence intensity was quantified as the difference between the average fluorescence intensity in the damaged region versus the average fluorescence intensity in an undamaged region from the same cell. Each curve corresponds to data obtained from at least 10 independently analyzed cells. Experiments were performed in a heated environmental chamber with 5% CO_2 on a Fluoview 1000 confocal microscope (Olympus).

IMMUNOFLUORESCENCE (IF) ANALYSIS

After incubation with the indicated treatments, cells were washed with PBS (3X) and processed for IF as previously described (52). Briefly, cells were pre-extracted with CSK buffer for 5 min on ice. Cells were then washed with PBS (3X) and fixed with 2% (v/v) formalin (PFA) for 15 min at room temperature. For APPA click labeling with Alexa Fluor® 488 alkyne (Life Technologies; #A10267) was performed based on a previously published procedure (105). Cells were blocked with PBS containing 3% BSA. For specific treatments without pre-extraction, cells were permeabilized with 0.5% (v/v) Triton-X for 10 min between fixing and blocking steps. After blocking, cells were incubated with indicated primary antibodies overnight. Primary antibodies used for IF are listed in Table 2.4. After incubation with primary antibodies, cells were washed with PBS (3X) and incubated with appropriate mouse or rabbit secondary antibodies made in

blocking solution for an hour at room temperature. Secondary antibodies used for IF are as follows: Alexa Fluor 488 goat anti-rabbit IgG, Alexa Fluor 488 goat anti-mouse IgG, Alexa Fluor 594 goat anti-rabbit IgG, and Alexa Fluor 594 goat anti-mouse IgG, Alexa Fluor 594 anti-goat IgG, Alexa Fluor 647 anti-rabbit IgG and Alexa Fluor 647 anti-mouse IgG along with Hoechst 33258 to visualize cell nuclei. After incubations, coverslips with cells were washed with PBS (3X) and mounted on glass slides using mounting medium. Cells were imaged and analyzed with Z-stacked settings using the FV10-ASW3.1 software on a Fluoview 1000 confocal microscope (Olympus). Data were analyzed with ImageJ. For IRIF quantification, >500 or >100 cells were counted for all conditions from at least two independent experiments. Data was analyzed in Prism and graphs were plotted from the data obtained.

FACS ANALYSIS

U2OS cells were transfected with GFP-LANA, Myc-LANA or a control vector for 8 h or with the indicated siRNA. 24 h after plasmids transfection or 72 h of post siRNA transfection, cells were harvested and fixed with 80% ethanol overnight. The fixed samples were washed 3X with PBS containing 1% FCS and incubated with phospho-histone H3 (S10) primary antibody for 2 h followed by incubation of goat anti-rabbit secondary antibody for 2 h at room temperature for the mitotic index assay. For DNA content analysis, the cells were washed and stained with propidium iodide (PI) and processed on a BD Accuri C6 flow cytometer (BD Biosciences) for cell cycle analysis.

***IN VITRO* ASSAYS**

NUCLEOSOME CORE PARTICLE (NCP) RECONSTITUTION

Recombinant human histones were expressed in E.coli BL21 (DE3)/RIL cells from pET21 vectors and extracted from inclusion bodies as described (114-116). All histones were purified under denaturing conditions on 5 ml HiTrap Q and HiTrap SP cation exchange columns (GE Healthcare). Peak fractions were confirmed using SDS-

PAGE and fractions containing pure histones were pooled and dialyzed extensively into 10 mM Tris-HCl (pH 8.0) before lyophilization. Octamers were refolded from purified histones by mixing the four histones in equimolar ratios (10% more of H2A/H2B relative to H3/H4), followed by dialysis into 2 M NaCl and then purified on a Superdex 200 (16/60) size exclusion column (GE Healthcare). NCPs were reconstituted by salt deposition as described (116). The 147 bp '601' DNA was biotinylated and used to wrap the mononucleosomes. NCP formations were confirmed on 6% native TBE gels by gel mobility shift assays.

HUMAN HISTONE PURIFICATION

I. Expression and Purification of Human Histone H2A

Lysis Buffer: 100 mM NaPO4 pH 8.0, 8 M Urea, 10 mM DTT

Wash Buffer: 100 mM NaPO4 pH 8.0, 7 M Urea, 10 mM DTT

Elution Buffer: 100 mM NaPO4 pH 8.0, 1 M NaCl, 7 M Urea, 10 mM DTT

Note: Deionized urea was used to prepare the above buffers by stirring with 25 g/L AG 501-X8 resin (Cat. No. 142-6424, Bio Rad) or Amberlite MB-150 (Sigma A5710) for at least 30 min at RT or over night at 4°C.

For 4 L culture pellet, 100 ml of Lysis buffer, 120-150 ml Wash buffer and 30 ml elution buffer were prepared.

Buffers for FPLC: SAU-200 Buffer: 20 mM Na-acetate pH 5.2, 7 M Urea, 200 mM NaCl, 1 mM EDTA 5 mM β-Mercaptoethanol.

SAU-600 Buffer: 20 mM Na-acetate pH 5.2, 7 M Urea, 600 mM NaCl, 1mM EDTA, 5 mM β-Mercaptoethanol

Note: The above buffers were prepared from a freshly made 8 M urea stock solution that had been deionized. Leftover buffer solution from the gel filtration buffer preparation can be stored over night at 4°C and used the next day to prepare SAU-200 and SAU-600 for the ion exchange purification.

Day 1: H2A Expression: (Procedure for 4 L of culture)

1. Human histone H2A was expressed from pET21b (+) vector by transforming the plasmid into BL21 (DE3)/codon plus RIL cells or streaked frozen stock on LB containing Ampicillin (Amp) plates and incubated at 37°C overnight.

2. Next day in the evening: 40-50 ml LB Amp was inoculated with several colonies and placed on shaker at 37°C overnight.

3. Next day in the morning: 1 L LB Amp/Chloramphenicol was inoculated with 10 ml overnight cultures each. After reaching OD600 = 0.6, histone expression was induced with 0.2 mM IPTG and flasks were incubated at 37°C for 3 h.

4. Uninduced and induced samples on a 15% SDS-PAGE gel by coomassie staining.

5. The culture broth was centrifuged at 5000 g for 15 min at RT and pellet was stored at -20°C. H2A pellet can be frozen and stored at -20°C directly without the addition of buffer or used straight away for the SP-Sepharose capturing step.

Day 2: Capturing H2A from E. coli Extracts on SP-Sepharose Beads and gel filtration

Human Histone H2A does not form inclusion bodies and is captured from E. coli extracts on SP-Sepharose beads and purified by denaturing gel filtration and ion exchange chromatography.

A. In the morning: 1.5 L of SAU-200 buffer was made from a freshly prepared deionized 8 M urea stock solution. Superdex-200 (16/60) gel filtration column (GE Healthcare) was equilibrated first with ~120 ml ddH2O (while preparing urea and buffer) and then with ~150 ml SAU-200 buffer during the day.

B. In the afternoon: H2A was captured from E. coli extracts on SP-Sepharose beads as follows:

1. Cells were harvested or frozen cells were thawed and the pellet was resuspended in 100 ml Lysis Buffer. This results in a final concentration of ~7 M urea.

2. The cell suspensions were distributed into ~25 ml aliquots in 50 ml Falcon tubes and each aliquot was sonicated 4 x 30 sec on ice to prevent samples from heating.

3. The sonicated lysates were centrifuged for 30 min at 20000 g and RT (Beckman JLA-16.25 rotor or equivalent).

4. For 4 L culture broth, 8 ml (bed volume) SP-Sepharose Fast Flow (GE Healthcare) was packed in a 100 ml gravity column by marking 8ml and pouring the slurry up to that mark. Sepharose beads are supplied in 10% ethanol. Hence 8 ml bed volume beads were washed with 10 column volumes (i.e., 80 ml) of water.

5. The column was equilibrated with 10 column volumes of wash buffer.

6. Supernatant (100 ml) was added to the equilibrated SP-Sepharose Fast Flow and rotated for 30 min at RT.

7. The beads were allowed to settle down by loading onto a gravity flow (OR by gently centrifuging the beads at 1000 g and RT) and washed once with 40 ml wash buffer.

8. Excess wash buffer was allowed to drain and then the protein was eluted 5X with 5 ml Elution buffer each time. All elutions/eluate was pooled to a get a total volume of 25 ml.

C. In the evening: The eluted sample was loaded directly onto the gel filtration column. The sample was loaded into a 50 ml super-loop and separated over a Superdex-200 column equilibrated in SAU-200 buffer. Gel filtration (size exclusion chromatography) was done in SAU-200 buffer at 0.5-1 ml/min overnight at RT (or 12°C) by injecting the sample and 2-3 ml fractions were collected using the fractionator.

Note: Deionize urea before use and do not leave proteins in urea buffer for extended periods of time (>24 h) in order to prevent carbamylation of proteins. Purification will also work at 4°C but buffer is close to precipitation at this temperature.

Day 3: Purification

1. The fractions from gel filtration were checked on a 15% SDS-PAGE gel.

2. H2A containing fractions were combined (usually 40 ml total volume).

3. A 5 ml HiTrap Q and a 5 ml SP ion exchange column (GE Healthcare) were set up in tandem (alternatively only a 20 ml SP-Sepharose HP 16/20 column-GE Healthcare can be used). The columns should be arranged so that the protein sample passes through the Q column first.

4. The columns were equilibrated with SAU-200 (can be made using leftover deionized urea from the buffer prep for gel filtration).

5. The combined fractions were loaded directly onto the Q/SP tandem columns at a flow rate of 0.5-1 mL/min with a super loop.

6. Washes were done for several column volumes (at least 15-20 ml) after which the Q column was removed. Elution was done with a gradient from 0% - 100% SAU-600 over 20 CV (Buffer A: SAU-200; Buffer B: SAU-600). 1.5-3 ml fractions were collected.

7. The fractions were checked on a 15% SDS-PAGE gel and pure histone fractions were combined and dialyzed extensively using 7,000 MWCO dialysis tubing against H_20/1 mM DTT overnight at 4°C.

Day 4: Determination of H2A concentration and storage by lyophilization

The concentration was determined by measuring the OD280nm of the undiluted protein solution against water or comparing with known protein concentration by Coomassie staining/Bradford assay. Aliquots of 1.2 ml each were made in eppendorf tubes. Tiny holes were poked using twizzers in the center of the lids of eppendorf tubes containing the histones before lyophilizing to allow moisture evaporation during freeze drying and tubes were freeze dried overnight (For lyophilization, 0.5 L liquid nitrogen was purchased from UT core facility).

Day 5: Lyophilized vials were stored at -20°C and condensed water accumulated in the lyophilizer was wiped clean for the next user.

Expected yields are: H2A: ~20 mg for 4 L of culture

II. Expression and Purification of Histones: H2B, H3 and H4

Buffers and reagents:

1. LB broth supplemented with 34 μg/mL chloramphenicol and 1 μg/mL carbenicillin; 1 M IPTG (isopropyl β-d-1-thiogalactopyranoside).

2. TW buffer for pellet resuspension: 50 mM Tris–HCl (pH 7.5), 100 mM NaCl, 1 mM EDTA.

3. TW buffer for inclusion bodies: 50 mM Tris–HCl (pH 7.5), 100 mM NaCl, 1 mM EDTA, 5 mM β-mercaptoethanol (βME), 1 mM benzamidine, and 1% (w/v) Triton X-100.

4. Urea buffer: 10 mM Tris–HCl (pH 8.0), 7 M urea, 1 mM EDTA, 5 mM βME, and 100 mM NaCl for wt and HA-tagged H2B, 200 mM NaCl for wt and HA-tagged H3 and H4, or 100 mM for all FLAG. Deionize these buffers with 25 g/L AG 501-X8 resin (Cat. No. 142-6424, Bio Rad) for at least 30 min at RT or overnight at 4°C before adding NaCl. A 1.0 mm Whatman paper was used to remove AG 501-X8 resin after deionization.

5. Unfolding buffer: 20 mM Tris–HCl (pH 7.5), 7 M guanidinium-HCl, and 10 mM DTT.

6. Buffer A: 10 mM Tris–HCl (pH 8.0), 7 M urea, 1 mM EDTA, and 1 mM DTT.

7. Buffer B: 10 mM Tris–HCl (pH 8.0), 7 M urea, 1 mM EDTA, 1 mM DTT, 1 M NaCl.

8. Tris dialysis buffer: 10 mM Tris–HCl (pH 8.0) with and without 5 mM βME.

9. Protein purification columns: 5 mL HiTrap Q and SP ion exchange columns, and Superdex 200 (16/60) gel filtration column, all purchased from GE Healthcare.

10. Dialysis tubing: 7,000 MWCO. 11. Lyophilizer (Labconco). 12. Microtip sonicator.

Day 1: Expression of Human H2B, H3 and H4

1. Human histones were expressed from pET21b (+) vector by transforming the plasmid into BL21 (DE3)/codon plus RIL cells and incubated at 37°C overnight. Alternately, E. coli Rossetta strain or BL-21 (DE3) pLysS for protein expression can be used.

2. Bacteria were grown at 37°C in LB broth with 1 mg/mL ampicillin.

3. Induction was performed at OD600 = 0.6 – 0.8 using 200 uL of 1 M IPTG (0.2mM IPTG working stock) per 1 L of culture, and growth was continued for 3 h at 37°C.

4. Cells were harvested by centrifugation at 5000g for 15-20 min at RT. Cell pellet was resuspended in 25 mL TW buffer 1 per 1 L culture and then frozen at –80°C.

5. Samples (uninduced and induced) were analyzed for histones overexpression by SDS-PAGE and Coomassie staining before proceeding to next step.

Day 2: Inclusion Body Purification

The following procedures pertain to wt histones, histones bearing a single FLAG or HA tag, and histone H3 bearing a 3xFLAG tag.

1. TW buffer was added to the cell suspensions up to 35mL total volume and sonicated on ice for 2 min (10 s on and 50 s off) with 40% output.

2. Centrifugation was done at 20,000 × g for 20 min at 4°C to harvest inclusion bodies.

3. The resulting protein pellet was rinsed with TW buffer by resuspending as much as possible with agitation.

4. Centrifugation and resuspension were repeated two more times using TW buffer without Triton X-100 and the protein pellet obtained was frozen at –80°C.

The following procedures pertain to histones H2B and H4 tagged with 3xFLAG.

1. The cell suspensions were sonicated and spun down as described above for WT histones, but this time the supernatant was kept and pellet was discarded.

2. 0.27 g of ammonium sulfate/mL of supernatant was added and stirred at 4°C for 1 h.

3. The suspension was centrifuged at 20,000 × g for 30 min at 4°C and protein pellets frozen at –80°C.

Days 3 – 4: Histone Purification

1. Deionized urea buffer was prepared as mentioned above.

2. To dissolve WT histones, histones with 3XFLAG tag or HA tag, 0.2 ml dimethyl sulfoxide (DMSO) per 1L culture was added and the pellet was minced using a spatula.

3. 6.5 mL unfolding buffer per 1 L culture was added to dissolve the pellets and gently agitated for 1 h at RT.

4. Remaining cell debris was removed by centrifugation at 20,000 × g for 20 min at 4°C and the supernatant was collected. This step can be done by dispensing the suspension in 1.5 ml microfuge tubes.

5. The remaining pelleted material was rinsed again with 1.5 mL unfolding buffer, spun down at 20,000 × g for 20 min at 4°C, and the supernatants were combined.

6. Dialysis of the resulting histones against 1–2 L urea buffer was done using 7,000 MWCO dialysis tubing with two buffer changes for several hours at RT or at 4°C if overnight. For each histone, appropriate urea buffer should be used as mentioned in buffer preparation.

7. Q and SP ion exchange columns were set up in tandem. The columns were arranged so that the protein sample passes through the Q column first.

The columns were equilibrated with 10% buffer B for H2A and H2B and all tagged histones, and with 20% buffer B for wt H3 and H4.

8. Dialyzed sample was loaded onto the Q/SP tandem columns at a flow rate of 0.5–1 mL/min with a superloop and washed with several column volumes. The Q column was removed and protein was eluted over 20 column volumes 10–40% buffer-B for H2B and all tagged histones, over 15 column volumes for 20–50% buffer-B for wt H3 and H4.

Note: H4 is eluted slower than other histones with a flow rate no greater than 0.4 mL/min or 0.2 mL/min if eluted overnight.

9. Peak fractions were confirmed using SDS-PAGE and combined.

10. The histone was dialyzed over several hours against Tris dialysis buffer using 7,000 MWCO dialysis tubing with several times buffer changes at 4°C. The final two buffer changes were done without βME.

11. Protein concentration was measured by taking OD at 280 nm, aliquoted into microfuge tubes and the dialyzed histone was lyophilized. This step can require up to 2 days. The lyophilized histone was store at –20°C.

H2B: ~30 mg for 4 L of culture, H3.1: ~40 mg for 3 L of culture, H4: ~10-15 mg for 3 L of culture.

5'-BTN 601 DNA AMPLIFICATION

For 100 µl reaction: DNA (150 ng), dNTP (10 mM) 2 µl, F' primer (10 mM) 5 µl, R' primer (10 mM) 5 µl, Phusion polymerase 0.5 µl, $MgCl_2$ (50 mM) 2 µl, Water: total to 100 µl. Master Mix can be made for 8 reactions. PCR program: Standard Phusion PCR. Purify using PCR purification kit by using 2 spin columns for purifying 800 µl of the PCR product. Final elution was done in 40 µl (30+10) of water.

NUCLEOSOME RECONSTITUTION

1. The molar concentrations of 601 DNA and octamer were calculated as follows:

a. Concentration of the octamer using nanodrop was noted. For actual conc. of the octamer, added MW of all four histones x 2 = Total MW and sum up if all the individual histones' extinction coefficients was done. The actual concentration was calculated to be = Octamer concentration from Nanodrop X Total MW / Sum of extinction coefficients. The value obtained was then converted into micromolar (µM).

2. The volume of DNA and octamer was calculated to make them equimolar.

To use DNA: octamer = 1:1.7

Total volume = 100 µl which should also include TE with 1.5M NaCl.

3. 10,000 MWCO dialysis buttons were placed in water for 30 min to remove glycine and purified octamer was thawed on ice.

4. A ratio of 1:1.7 :: DNA: octamer in 1X TE (pH 8.0) was mixed with 1.5M NaCl on ice to make a total volume of 100 µl.

5. The mixture was incubated on ice for 30 min and transferred to dialysis button.

6. Gradually the NaCl concentration was reduced by step dialysis at 4°C for 2h in 1X TE (pH 8.0) containing 1M NaCl, 0.8M NaCl, 0.6M NaCl, 0.4 M NaCl.

Reagents for 1 L of each	TE+ 1M NaCl	TE+ 0.8M NaCl	TE+ 0.6M NaCl	TE+ 0.4M NaCl	TE+ 0.2M NaCl
4M NaCl	250 ml	200 ml	150 ml	100 ml	50 ml
1M Tris pH 8.0	10 ml	10	10	10	10
0.5M EDTA	2 ml	2	2	2	2
Water	Make upto 1L	Make upto 1L	Make upto 1L	Make upto 1L	Make upto 1L

Table 2.5 Step dialysis for NCP reconstitution

7. A final dialysis step was done overnight in 1X TE (pH 8.0) with 0.2 M NaCl. Dialysis steps longer than 2h can be done but shorter dialysis times will lower the reconstitution efficiency.

8. The nucleosomes were transferred into 1.5 ml tubes and stored in 4°C for several weeks (upto 6 months).

9. Formation of nucleosome core particles (NCP) was confirmed by running 2-4 µl of the NCP on a 4-6% native polyacrylamide gel.

NATIVE GEL TBE

Native PAGE separations were run in non-denaturing conditions. Detergents are used only to the extent that they are necessary to lyse lipid membranes in the cell. Complexes remain, for the most part, associated and folded as they would be in the cell. One downside, however, is that complexes may not separate cleanly or predictably, since they cannot move through the polyacrylamide gel as quickly as individual, denatured proteins. Recipe for 6% gel is as shown in Table 2.6 below. TBE gel was pre-run for 10 minutes at 80V in 0.5X TBE buffer (see below TBE buffer recipe). This ensures acrylamide would

not react with protein samples and it also heats up the gel so that the DNA stays denatured while running the sample.

Resolving Layer	6% (2 gels)
H2O (ml)	6.15
5X TBE (ml)	0.825
40% Acryl (ml)	1.24
10% APS (ml)	82.5
TEMED (µl)	3.3

Table 2.6 Native gel preparation

Sample loading and gel run: Mix 2-3 µl of NCP + 2 µl 6X non-SDS dye + 3 µl water. Samples are not boiled before loaded onto the gel.

Gel run: The gel is run at 80V for 50-60 minutes. Be sure to watch the solvent front. The gel was removed from the casing and soaked for 15-20 minutes in 0.005% Ethidium bromide (in water). Gel is gooey and was handled with care.

After gel run, the gel was removed from ethidium bromide and rinsed with water 5 times. Gel was let soaked in water for 15 minutes and imaged as done for an agarose gel.

TBE buffer for native gels: 5X stock solution in 1 L of H2O: 54 g of Tris base, 27.5 g of boric acid, 20 mL of 0.5 M EDTA (pH 8.0). TBE was prepared and stored as a 5X or 10X stock solution. The pH of the concentrated stock buffer was adjusted to ~8.3. The concentrated stock buffer was diluted just before use and gel solution and electrophoresis buffer were prepared from the same concentrated stock solution.

Note: Some investigators prefer to use more concentrated stock solutions of TBE (10X as opposed to 5X). However, 5X stock solution is more stable because the solutes do not precipitate during storage. Passing the 5X or 10X buffer stocks through a 0.22-µm filter would prevent or delay formation of precipitates.

To make 1 L of 0.5X running buffer: 100ml of 5X to 900ml of water is to be added.

PROTEIN PURIFICATIONS

E3 Ub ligase enzymes used in the *in vitro* Ub assays were His_6 tagged RNF168 (1–113) construct expressed in Rosetta 2 (DE3) pLysS cells and purified over a Ni-NTA column (Qiagen) and stored in elution buffer (50 mM NaH2PO4, 300 mM NaCl, 250 mM imidazole, pH 8.0) containing 10% glycerol. The pET24b(+)-Bmi1-His_6 (1–108) and pGEX-6P-1-RING1B (1–116) expression plasmids were co-transformed in Rosetta2 (DE3) pLysS cells and the proteins were purified as a complex as described in (117) with exact details provided below:

A. RNF168 expression and purification

1. Lysis Buffer: Preparation 100 ml

50 mM NaH2PO4	0.78 g
300 mM NaCl	(7.5 ml of 4M NaCl stock)
10 mM Imidazole	68 mg

pH was adjusted to 8.0 using 10M NaOH and the volume made up to 100 ml with water.

2. Wash Buffer: 100 ml

50 mM NaH2PO4	0.78 g
300 mM NaCl	(7.5 ml of 4M NaCl stock)
20 mM Imidazole	136 mg

pH was adjusted to 8.0 using 10M NaOH and the volume made up to 100 ml with water.

3. Elution Buffer: 25 ml

50 mM NaH2PO4	0.195 g
300 mM NaCl	(1.875 ml of 4M NaCl stock)
250 mM Imidazole	425 mg

pH was adjusted to 8.0 using 10 M NaOH and volume made upto 25 ml with water.

4. Storage buffer: 50 mM Tris-HCl pH7.5, 1mM EDTA, and 10 % glycerol.

The RNF168 bacterial expression vector (residues 1-113) was cloned into pPROEX Hta (Invitrogen) using the BamH1 and Spe1 sites. His_6-RNF168 (1-113) was purified on Ni-NTA agarose (Qiagen) as follows:

1. RNF168 containing plasmid was transformed into Rosetta or BL-21 cells and plated on LB ampicillin (and chloramphenicol for Rosetta cells). A colony was picked and inoculated in 10 ml LB with antibiotics for overnight incubation at 37˚C.
2. Next day 500mL LB media with antibiotics was inoculated with 5 mL of overnight grown culture to an OD600= 0.6 and then protein expression was induced with 0.5 mM IPTG overnight at 16˚C.
3. Next day, cells were pelleted and can be stored at -20˚C if not processed for the next step immediately.
4. Cell pellet was thawed for 15 min on ice and resuspended in 35 ml of cell lysis buffer.
5. Lysozyme was added to 1 mg/ml and incubated on ice for 30 min.
6. The cell suspension was sonicated on ice using six 10s bursts at 100W with a 10s cooling period between each burst and placed on a shaker at 4˚C for 30 min.
7. The lysate was centrifuged at 10,000g for 25 min at 4˚C to pellet the cellular debris and the supernatant (clear lysate) obtained was collected.
8. 1ml Ni-NTA beads slurry was washed with water and equilibrated with 5 ml of lysis buffer twice.
9. Equilibrated Ni-NTA beads were added to the filtered lysate and nutated for 1h at 4˚C.
10. The mixture was centrifuge at 100rpm/2min and the supernatant was collected. The beads were stored with some supernatant left at 4˚C to avoid drying the beads.
11. 1 ml of pre equilibrated Ni-NTA beads was added to the supernatant and nutated overnight at 4˚C to obtain the remaining previously unbound RNF168 protein in the supernatant.
12. The beads were pooled together by centrifugation and removing the supernatant. The beads were washed twice with 10 ml wash buffer.

13. The protein was eluted thrice with 0.5 ml elution buffer each time and buffer exchange was done into storage buffer via a PD-midi trap G-25 column which was preequilibrated with storage buffer (i.e., final product was obtained in 1.5 ml storage buffer).

Quantity of eluted protein using this method is about ~0.89 mg/ml (64.6 μM)

B. BMI1/RING1B expression and purification

Buffer A: 10 mL of 1 M Tris pH 7.5 (50 mM working stock), 6 mL of 5 M NaCl (150 mM) and 200 μL of 1 M DTT (1mM) to make a total of 200 mL

Buffer B: 2.5 mL of 1 M Hepes, pH 7.5 (50 mM), 1.5 mL 5 M NaCl (150 mM), 50 μL of 1 M DTT (1 mM) to make a total of 50 mL

Buffer C: Buffer B + 0.05% Tween-20

Buffer D: 50 mM Tris pH 7, 150 mM NaCl, 1 mM EDTA, 1 mM DTT

Purification:

1. 2 μl (~100 ng) DNA each of Bmi1-His and GST-Ring1B plasmids were simultaneously cotransformed into Rosetta-1 cells and plated on LB plates containing Ampicillin/Kanamycin/Chloramphenicol antibiotics.

2. Next day, the plates were scraped to inoculate 1 L LB media with antibiotics to an OD600 of ~0.02 and grown at 37°C to reach an OD of about OD600 = 0.6. For induction of protein expression 0.3 mM IPTG was added and the culture was incubated on a shaker overnight at 18°C.

3. Next Day: Cells were pelleted and resuspended in 40 mL Buffer A (+ protease inhibitors). The suspension was sonicated (using six 10 s bursts at 100W with a 15 s cooling period between each burst) to lyse the cells, 21 mg lysozyme was then added to the lysate and nutated for 30 min at room temp (RT).

4. The cell lysate was cleared by centrifuging 18k rpm, 40 min, 4 °C and filtered through a 0.45 μm syringe filter to obtain a clear lysate.

5. 2 mL Ni-NTA slurry was added (Qiagen, and I don't bother washing the storage buffer out of the slurry) to the filtered lysate and nutated for 1 h, RT.

6. The flow through (FT) was collected and beads were washed with 60 mL Buffer A + 30 mM imidazole (0.123 g).

7. The complex was eluted in 15 mL of Buffer A + 250 mM imidazole (60 mL + 1.02 g).

8. Eluted sample was concentrated to 2 mL (30 kDa MWCO) and buffer exchanged into Buffer B via a PD-10 column, pre-equilibrated with 25ml of Buffer B (eluting in 3.5 mL) and stored at 4°C over night.

9. Next Day: The precipitate was spun and 2-3 mL washed glutathione sepharose beads (GE) was added after washes with water and Buffer B. It was nutated at 4°C for 2 h.

FT was collected and beads were washed with 20 mL each of Buffer B, then C, then D. At this point, I ran some of the beads on a gel just to make sure that I had each protein and that it was washed enough.

10. 5 μL of 10 mg/mL Pre-Scission protease was added to beads (still on the column, with about 0.5 mL Buffer D on top of beads) and allowed to cleave overnight, 4°C, on stand (i.e., I did not nutate the sample at this point).

11. Next Day: Some beads (~5 μL) were run on a gel to check for efficiency of cleavage. I observed about 50% cleaved protein, but it made for plenty of protein in the end. FT was collected and beads were washed with Buffer D. The eluted protein (10kDa MWCO) was concentrated and checked on a 15% gel. The preparation was clean and ~1.8 mg of complex was obtained from this 1 L prep.

IN VITRO **UB ASSAY**

Assays were performed essentially as described (17). Briefly, 2.5 mg of recombinant mononucleosomes were incubated in a 50 ml reaction buffer containing 50 mM Tris-HCl, pH 7.5, 100 mM NaCl, 10 mM MgCl2, 1 mM ZnOAc, 1 mM DTT, 30 nM ubiquitin activating enzyme E1 (Boston Biochem), 1.5 mM ubiquitin conjugating enzyme

UbcH5a (Boston Biochem), 4 mM RNF168 (1–113) or RING1B/BMI1 complex, 22 mM ubiquitin (Boston Biochem) and 3.33 mM ATP at 30°C for 4 h. The reaction was terminated by addition of SDS-PAGE loading buffer. Assays with free histones were carried out with 10 mM of H2A or H2AX and the reactions were incubated overnight at 30°C. The samples were boiled and loaded on 15% SDS-PAGE gels, transferred to a nitrocellulose membrane, probed using specific antibodies and detected as described.

IN VITRO METHYLATION ASSAY

2.5 mg of recombinant mononucleosomes were incubated at 30°C for 2 h in a 50 ml reaction containing 50 mM Tris-HCl, pH 7.5, 100 mM NaCl, 10 mM MgCl2, 1 mM ZnOAc, 1 mM DTT, 0.1 mM S-adenosyl methionine (NEB), and 100 ng recombinant human Set8 (Active Motif). The reaction was terminated by addition of SDS-PAGE loading buffer. Western blots were probed using indicated antibodies.

LANA COMPETITION ASSAY

In vitro Ub assays were set up as described above, except with 3, 10, 30, 50, 100 or 150 mM of the indicated peptide. The peptides were synthesized by Bio Basic: LANA (Biotin-Mini-PEG-MAPPGMRLRSGRSTGAPLTRGSY) and 8LRS10 (Biotin-Mini-PEG–MAPPGMRAAAGRSTGAPLTRGSY) and were based on data presented previously (118).

TANDEM AFFINITY PURIFICATION (TAP)

Tandem affinity purification (TAP) was performed as previously described with minor modifications (119). Briefly, HEK293T cells were seeded in 10 cm dishes and transiently transfected with SFB (S-protein, 2xFlag, streptavidin-binding peptide) tagged constructs. After 24 h of transfection, 10 dishes of cells with transfection plus 10 dishes of cells without transfection were collected and combined together. Cells were lysed with NETN buffer (150 mM NaCl, 1mM EDTA, 10 mM Tris-HCl, pH 8.0, and 0.5% NP-40) for 30 min at 4°C. Cell lysates were cleared by 15000 rpm centrifugation for 30 min at

4°C. The supernatants were collected as the soluble fraction. The pellets were digested with NETN buffer containing TurboNuclease (Accelagen) and 1 mM $MgCl_2$ for 1 h at 4°C. Cell lysates were then centrifuged to collect the supernatants as the chromatin fraction. Both soluble and chromatin fractions were incubated with 300 µl of streptavidin beads (GE Healthcare) for at least 1 h at 4°C. Next, the beads were precipitated by 2000 rpm centrifugation and washed one time with NETN buffer. The bound proteins were eluted with 750 µl of NETN buffer containing 2 mg/ml biotin (Sigma) twice. The eluted supernatants were incubated overnight with 40 µl of S-protein beads (Novagen). The precipitated beads were washed three times with NETN buffer. Protein mixtures were eluted by boiling with Laemmli buffer, and resolved by SDS-PAGE. The purification efficiency was checked by silver stain (Calbiochem) following manufacturer's instruction. The remaining samples were subjected to Mass Spectrometry (MS) identification.

MASS SPECTROMETRY (MS) ANALYSIS

For MS experiments, the raw data for TRIM samples were obtained from Dr. Brodbelt's laboratory at the University of Texas at Austin. For MS data analysis in this study, only those proteins identified with at least two peptides for each experiment, were considered as potential interactors.

IMMUNOPRECIPITATION (IP) ANALYSIS

Untreated cells or with indicated treatments were collected and lysed with NETN buffer containing 1 mM $MgCl_2$ and TurboNuclease by nutating on a roller for 1 h at 4°C. Cell lysates were cleared by centrifugation at 15,000 rpm for 30 min at 4°C. Overexpressed SFB tagged proteins were pulled down using 30 µl of streptavidin beads (GE Healthcare) by nutating for at least 1 h at 4°C. Similarly, ectopically expressed GFP tagged proteins were pulled down with 30 µl GFP-Trap beads (Chromotek) by nutating the tubes for at least 2 h at 4°C. Endogenous proteins were immunoprecipitated by adding

1 μg of indicated antibodies or following dilutions suggested in manufacturer's instructions. The lysate-antibody mix was incubated by nutating the tubes overnight at 4°C. Next day, 30 μl of IgG & IgA Dynabeads (Invitrogen) slurry or Protein A beads (Millipore) was added to each tube and nutated at least for 2 h at 4°C. Beads were washed 4X with NETN buffer. Protein mixture was eluted by boiling with Laemmli buffer and then subjected to the standard WB analysis with indicated antibodies (Table 2.4).

CLONOGENIC CELL SURVIVAL ASSAY

U2OS cells (~500 cells per well) seeded in 6-well plates were treated with indicated dosages of different DNA damaging agents such as IR, hydroxyurea (HU), mitomycin C and camptothecin (CPT). Cells were left to form colonies for 10 to 14 days at 37°C. Formation of colonies was checked under the microscope and plates were washed once with 1X PBS and stained with 0.5% (w/v) crystal violet and 20% (v/v) ethanol for 30 min at room temperature. After staining, plates were gently washed with flowing water and let to air dry before the colonies were counted. Results were normalized to plating efficiencies of untreated cells for each treatment.

HOMOLOGOUS RECOMBINATION ASSAY

An integrated HR reporter DR-GFP-containing U2OS cell line was used as described previously [109]. One day after indicated siRNA treatments, U2OS DR-GFP cells were transfected with I-SceI expressing vector (pCAG-I-SceI) or control vector (pCAG). 48 h following I-SceI transfection, cells were trypsinized, washed once with PBS, and then resuspended in Sodium Citrate solution without fixation. Resuspended cells were filled into Falcon 5 ml Polystyrene round-bottom tubes through the cell-strainer caps. The percentage of GFP positive cells was determined by a BD Accuri Flow Cytometer (BD biosciences). All samples were normalized with the siControl sample transfected with pCAG-I-SceI vector.

NON-HOMOLOGOUS END JOINING ASSAY

Experiments were performed as previously described (77). Briefly, 24 h after siRNA transfection, U2OS cells were transfected with linearized pEGFP-C1 (BamHI and XhoI treatment). The next day, GFP positive cells were counted to calculate transfection efficiency. The cells were then trypsinized, counted and plated into two duplicated plates. One plate with 0.5 μg/ml G418 (as NHEJ events), and the other without (as plating efficiency) were incubated for two weeks at 37°C to allow colony formation. Colonies were stained as described in the clonogenic cell survival assay methods. Random-plasmid integration events were calculated using transfection and plating efficiency normalized to siControl.

REVERSE TRANSCRIPTION AND QUANTITATIVE PCR (QPCR)

After indicated treatments, total RNA for each sample was purified using the RNeasy mini kit (Qiagen, 74106) and treated with RNase-Free DNase I (Qiagen) following the manufacturer's protocol. 2 μg of total RNA for each sample was used to synthesize cDNA by the SuperScript III first strand synthesis system (Invitrogen). Quantitative PCR (qPCR) was performed on the StepOnePlus Real-Time PCR system (Applied Biosystems) using SYBR green master mix (Applied Biosystems) with the indicated primers. To analyze mRNA expression levels of candidate genes, gene-specific qPCR primer pairs were designed as obtained. For normalization, the qPCR primer pair for GAPDH (glyceraldehyde-3-phosphate dehydrogenase) was used. The qPCR primer pairs used in this study are listed in Table 2.7 (in the next page).

CRISPR TARGETING FOR GENE KNOCKOUT

USOS cells with TRIM24, TRIM28 or TRIM33 knockout and HeLa cells for TRIM24 or TRIM28 knockout were generated using CRISPR/Cas9 system following standard protocol (120). sgRNA sequences used are: GGCCCGGACTCGGAGCGCGG, CATGCGTGATAGTGGCAGCA for TRIM28 and AGTGCCCACTGAGGCCGCAG

for TRIM33. The Cas9 nuclease vector is pSpCas9(BB)-2A-Puro. Successful knockout of the indicated genes was validated by Western blot.

Target	Sequences
CXCL8	F' TCCTGATTTCTGCAGCTCTGT
	R' AAATTTGGGGTGGAAAGGTT
IL11	F' GGACAGGGAAGGGTTAAAGG
	R' CTCAGCACGACCAGGACC
AREG	F' ACGAACCACAAATACCTGGC
	R' TTTCACTTTCCGTCTTGTTTTG
EREG	F' AGGAGGATGGAGATGCTCTG
	R' CACAGTTGTACTGAGGACTGCC
RRAD	F' CAACAAGAGCGACCTGGTG
	R' CCGCTGATGTCTCAATGAACT
ATOH8	F' TCAGCTTCTCCGAGTGTGTG
	R' ACAGTGGTGGCCTTGGTCTT
UCN2	F' CTGCCTTACCCCAGAAGCA
	R' ACTCTGCCCAACATCAGGAC
DRD1	F' AGCGAAGTCCACATTCCAAG
	R' ATGTCTTCTCGCTCCTCCAA
HTR2A	F' CCGCTTCAACTCCAGAACTAA
	R' GAATCGTCCTGTAGCCCAAA
BMF	F' AAGGTTGTGCAGGAAGAGGA
	R' CAGTGCATTGCAGACCAGTT
GAPDH	F' CAATGACCCCTTCATTGACC
	R' GATCTCGCTCCTGGAAGAT
MDC1-1	F' CTTCATGTTGACTCCACCCC
	R' AATGGCTGTGTAGCCAGGAC
MDC1-2	F' TGGAGGATGAACCTACCCAG
	R' AGAATGGCTGTGTAGCCAGG
KAT6B-1	F' GCCTTCTACCCCATGAGAAA
	R' GCCACAATCTGCACAAGAGA
KAT6B-2	F' TTTGTGTCCCCCTGTTGTTGT
	R' GACTCCATTGGGCTGTAATCAGT
TIP60	F: TCAAGCCGTGGTACTTCTCC
	R: ATCTCATTGCCTGGAGGATG
MOF	F: TCAAGCCGTGGTACTTCTCC
	R: ATCTCATTGCCTGGAGGATG

Table 2.7 qPCR primers used in this study

CHAPTER 3: NUCLEOSOME ACIDIC PATCH PROMOTES RNF168- AND RING1B/BMI1-DEPENDENT H2AX AND H2A UBIQUITINATION AND DNA DAMAGE SIGNALING

Eukaryotic DNA is bound by histone proteins and organized into chromatin, the true in vivo substrate of transcription, replication and DNA repair, processes that are important in preserving genome integrity. Chromatin structure and function are highly regulated by histone post-translational modifications (PTMs) (12). Histones are modified on distinct amino acid residues by different PTMs, such as phosphorylation, acetylation and ubiquitination, including several that are involved in DSB repair (4). Upon DSB formation, H2AX is phosphorylated on Ser-139 within its C-terminal tail by the PIKK family kinases ATM, ATR and DNA-PK, to yield γH2AX (22). γH2AX can be generated over a megabase of chromatin surrounding DSBs, thus creating microscopically-visible ionizing radiation-induced nuclear foci (IRIF) (26, 34). γH2AX creates a binding site for the DNA damage protein MDC1, which promotes the localization of other DNA damage factors to damage sites (4). Numerous E3 ubiquitin ligases including RNF8, RNF168, BRCA1, RING1B and BMI1 are recruited to DNA lesions (121, 122). Collectively, these DNA damage factors orchestrate the DNA damage response (DDR) that is a complex signaling network that is critical in regulating DNA damage signaling and repair (2, 5, 121). Ubiquitin-mediated responses to DNA damage include histone H2A and variant H2AX ubiquitinations (H2A/H2AXub). Indeed, H2A/H2AXub is ubiquitinated by RNF168, which targets Lys-13/15 within the N-terminal tail (17, 59, 62), and RING1B/

Portions of this chapter have been published as follows:

- *Justin W. Leung*, Poonam Agarwal*, Marella D. Canny, Fade Gong, Aaron D. Robison, Ilya J. Finkelstein, Daniel Durocher, Kyle M. Miller (2014) Nucleosome acidic patch promotes RNF168- and RING1B/BMI1-dependent H2AXand H2A ubiquitination and DNA damage signaling. PLOS Genetics* 10(3): e1004178.
  (co first authors)*

BMI1 that ubiquitinates C-terminal Lys-118/119 of H2A/H2AX (60, 123-125). Ubiquitinated histones H2AX and H2A mediate the chromatin association of both the mediator protein 53BP1 and the repair factor BRCA1. These interactions occur through binding to Ubiquitin-interaction motif (UIM) domains in 53BP1 and in the BRCA1-interacting protein RAP80 (126, 127). Thus, site-specific histone ubiquitinations mediate critical signaling events that promote sensing and repair of DNA damage in mammalian cells (4, 121, 128). Although the role of histone ubiquitination is well established in DNA damage signaling, it is unclear how the ubiquitin E3 ligases recognize their specific lysine targets on histones within the context of the nucleosome. Whether the nucleosome itself is involved in mediating the site -specific ubiquitin modifications on histones in response to DNA damage or other biological signals involving histone ubiquitinations has not yet been established. In this study, we find that the nucleosome acidic patch is required for RNF168- and RING1B/BMI1-dependent H2A and H2AX ubiquitination.

RESULTS/DISCUSSION

The acidic patch promotes H2AX/H2A ubiquitination

Ubiquitination of histones has emerged as a critical component of the DNA damage signaling pathway in mammalian cells (121). We previously identified several mutations that reduced H2AX ubiquitin levels in undamaged cells (50). One such mutation, H2AX-E92A resided in the acidic patch region of the nucleosome. Expression of tagged versions of human H2AX and H2A in human HEK293T cells revealed a full-length protein species of predicted size as well as a slower migrating ubiquitinated form for both human H2AX and H2A (Figure 3.1A-B). Mutation of glutamic acid 92 to alanine (E92A) reduced H2AX and H2A ubiquitination (H2AX/H2Aub, Figure 3.1A-B). These results identify the amino acid E92 of human H2AX/H2A as an important residue for H2AX/H2Aub.

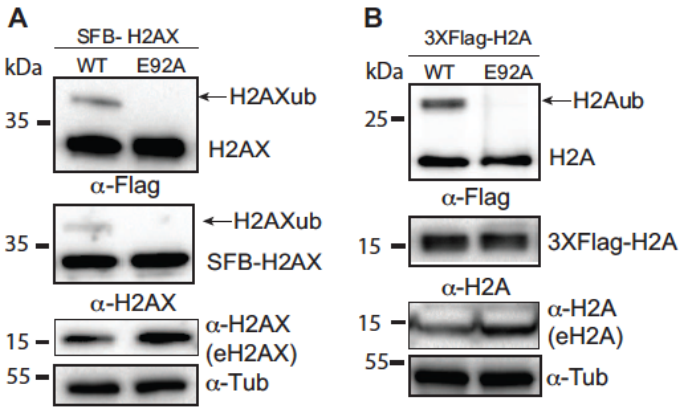

Figure 3.1 Mutation of the acidic patch impairs human H2AX/H2Aub

(A and B) E92A mutation in the acidic patch reduces H2AX/H2Aub. WT or E92A H2AX/H2A constructs were transfected into HEK293T cells and analyzed by western blotting with the indicated antibodies. Arrows indicate ub forms. (SFB = S-tag, Flag epitope tag, and streptavidin-binding peptide tag; e = endogenous; tub = tubulin loading control). Molecular mass (kDa) is indicated on the left of each panel. HEK293T cells were used for all cellular assays. (*This figure was prepared by J.W.L.*)

We next sought to define the contribution of the acidic patch region of the nucleosome towards H2AX/H2Aub and the DDR. H2AX/H2A is specifically ubiquitinated on the N-terminal Lys-13/15 by RNF168 (17, 59, 62), as well as on the C-terminal Lys-118/119 by RING1B/BMI1 (60, 123-125). Therefore, an important question was to determine which sites on H2AX rely on the acidic patch for ubiquitination. To answer this question, we first created a lysine-free human H2AX where all lysine residues were mutated to arginines. These mutations maintain the basic charge at each amino acid location but are unable to be ubiquitinated (Figure 3.2A). As expected, expression of H2AX-allR in HEK293T cells confirmed that this mutant lacked any detectable ubiquitination, similarly to H2AX-E92A (Figure 3.2B). Unlike these H2AX derivatives, mutation of the DNA damage induced phosphorylation site on H2AX (S139) to an unphosphorylatable residue (S139A) did not affect H2AXub (Figure 3.2B). Having identified a mutant H2AX derivative that lacked ubiquitination, we then reverted specific arginine residues in this mutant back to lysine residues that are contained in WT H2AX (Figure 3.2A). This strategy allowed us to unambiguously identify site-specific ubiquitin-

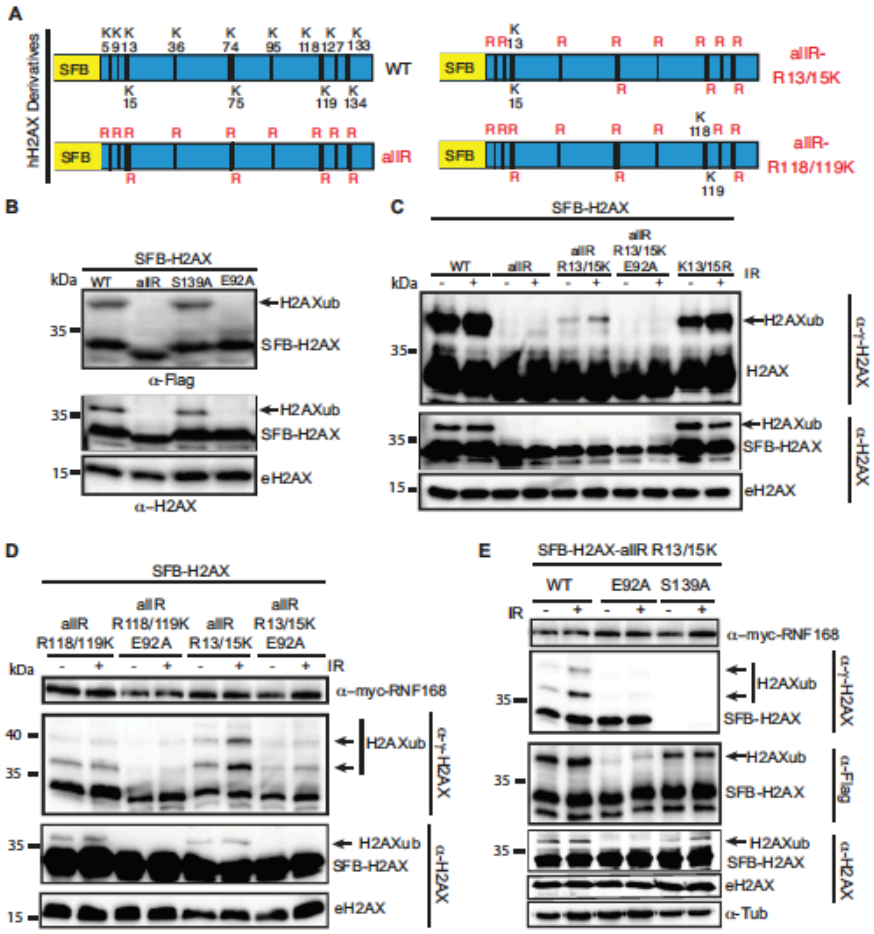

Figure 3.2 H2AX/H2A N'- and C'-ub require functional nucleosome acidic patch

(A) Schematic of all H2AX lysines (K) and mutant derivatives. allR represents an all K to arginine (R) version of H2AX. Additional site-specific reversions from arginine to lysine within the allR H2AX derivate are indicated. (B) H2AX-allR and acidic patch mutation E92A reduces H2AXub. WT or E92A H2AX/H2A constructs were transfected into HEK293T cells and analyzed by western blotting with the indicated antibodies. Arrows indicate ub forms. (SFB = S-tag, Flag epitope tag, and streptavidin-binding peptide tag; e = endogenous). Molecular mass (kDa) is indicated on the left of each panel. HEK293T cells were used for all cellular assays. (C) H2AX-K13/15 dependent ubiquitination requires the acidic patch. H2AX and derivatives were expressed in HEK293T cells (-) or (+) ionizing radiation (IR, 20 Gy). Samples were analyzed as in A 6 hr post-IR treatment. (D) H2AX-K13/15 and K118/119-dependent ubiquitination requires the acidic patch. Cells were co-transfected with H2AX and derivatives along with myc- RNF168 and analyzed as in C. (E) Phospho-competent H2AX S139 is not required in *cis* for H2AX K13/15ub. Cells were analyzed as in C. tub = tubulin loading control. (*This figure was prepared by J.W.L with the assistance of K.M.M.*)

-ations within H2AX. As expected, H2AX mutants lacking K118/119 exhibited a large reduction in mono-ubiquitination (Figure 3.2C). This confirmed previous work showing that these sites on H2AX/H2A are the major lysine acceptor sites for mono-ubiquitination (4, 129). Interestingly, we observed ubiquitination of the H2AX derivative containing only K13/15 as acceptor sites for ubiquitin (Figure 3.2C). We also observed an increase in K13/15ub on this H2AX derivative upon DNA damage, which is consistent with previous studies showing that a small fraction of H2AX becomes ubiquitinated on K13/K15 following DNA damage by the E3 ubiquitin ligase RNF168 (17, 59, 62). To assess the contribution of the acidic patch towards H2AX K13/15ub, we tested whether an E92A mutation would affect H2AX K13/15ub. Combining the E92A mutation within the H2AX derivative that could only be ubiquitinated on K13/15 abolished any detectable ubiquitination at these sites within H2AX (Figure 3.2C). We next tested whether the acidic patch also affected the ubiquitination of K118/119 of H2AX. Analysis of an H2AX derivative that could only be ubiquitinated on K118/119 showed that this protein was readily ubiquitinated and mutation of the acidic patch diminished H2AXub at these specific lysine sites (Figure 3.3).

RNF168 is a limiting factor within the DDR and overexpression of RNF168 increases H2AX-K13/15ub levels but not H2AX-K118/119ub levels (17, 59, 62, 130). In agreement with these studies, we observed that overexpression of RNF168 increased H2AX-K13/15ub but not H2AX-K118/119ub (Figure 3.2D, 3.3). In accordance with our results from Figure 3.2C), mutation of the acidic patch decreased H2AX-K13/15ub levels; even under conditions where RNF168 is overexpressed and not limiting (Figure 3.2D). H2AX-K13/15ub is mediated by RNF168 whose recruitment to sites of DNA damage requires MDC1 and RNF8 (30, 40), which in turn require H2AX phosphorylation on S139 (30, 131-133). Collectively, these findings suggest that γH2AX may be required for H2AX-K13/15ub. To test this possibility, we mutated S139 within the H2AX-allR-R13/15K derivative to monitor specifically H2AX-K13/15ub in either the presence or

absence of S139. While E92A abolished H2AX-K13/15ub, the S139A mutation did not affect ubiquitination at these sites (Figure 3.2E). These results show that S139 is not required *in cis* for H2AX-K13/15ub under these conditions. We note that these experiments were performed in cells containing WT H2AX that could provide functional residues *in trans* for H2AX-K13/15ub. These experiments were done in the presence of overexpressed RNF168, which could bypass the requirement for S139 phosphorylation for its recruitment to chromatin. In overexpression conditions, RNF168 accumulates at sites of endogenous DNA damage marked by 53BP1 (130), which we note requires K13/15ub on H2A/H2AX (17). Regardless, under either limiting or non-limiting conditions for RNF168, we find that the acidic patch is required for H2AX-K13/15ub (Figure 3.2C-E).

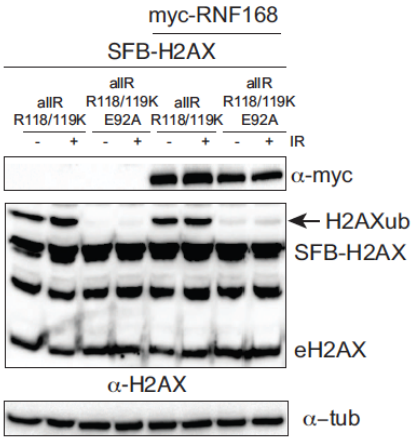

Figure 3.3 H2AX-K118/119ub requires the acidic patch and is unaffected by over expression of RNF168

H2AX derivatives were transfected into HEK293T cells with or without myc-RNF168 and either (-) or (+) IR treated with 20 Gy and allowed to recover for 6 h. Samples were taken and analyzed by western blotting with the indicated antibodies. Arrows indicate H2AXub. (SFB = S-tag, Flag epitope tag, and streptavidin-binding peptide tag, e = endogenous). (*This figure was prepared by J.W.L.*)

Nucleosome acidic patch is required for H2AX/H2Aub *in vitro*

Our results strongly suggested that the acidic patch is required for both K13/15 and K118/119 H2AX/H2Aub. We next sought to test whether the effect of the acidic

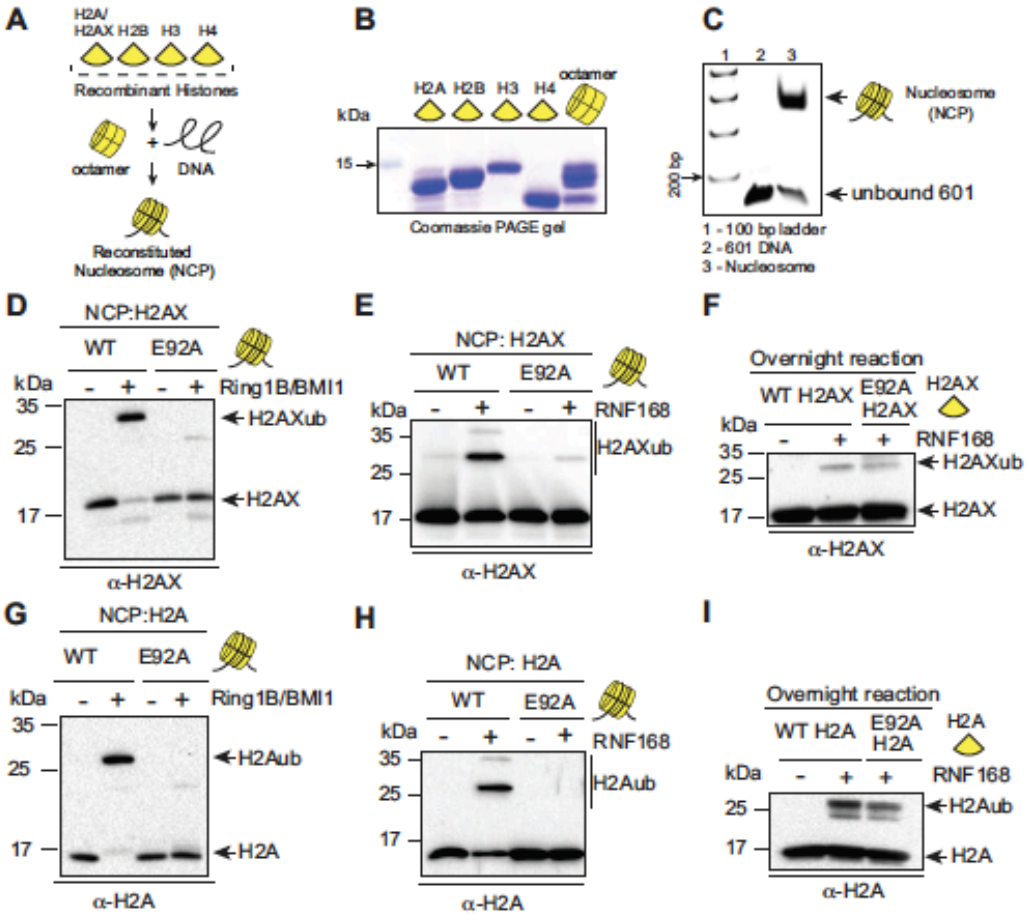

Figure 3.4 RING1B/BMI1- and RNF168-dependent H2AX/H2Aub requires the nucleosome acidic patch *in vitro*

(A) Schematic for *in vitro* reconstitution of nucleosome core particles (NCPs). (B) Bacterially expressed and purified human histones. Histones were expressed, purified and reconstituted as described in experimental procedures. (C) Analysis of *in vitro* reconstituted NCPs. The 147 bp 601 DNA fragment was analyzed alone or after NCP reconstitution. DNA ladder indicates size (bp). (D and E) RING1B/BMI1 and RNF168 readily ubiquitinate H2AX within WT NCPs but not NCPs containing a mutation in the acidic patch (H2AX-E92A). *In vitro* Ub assays (4 h) were performed as described in experimental procedures. (F) RNF168 ubiquitinates WT H2AX and H2AX-E92A similarly when assayed in the context of free histones. Assays were performed as in E except with free histones and reactions were performed overnight. (G and H) RING1B/BMI1 and RNF168 readily ubiquitinate H2A within WT NCPs but not NCPs containing a mutation in the acidic patch (H2A-E92A). Experiments were performed as in D and E using H2A. (I) RNF168 ubiquitinates free WT H2A and H2A-E92A similarly. Experiments performed as in F.

patch mutation on H2AX/H2Aub was direct, as well as to analyze the role of the acidic patch in mediating site-specific ubiquitinations with their associated E3 ligases. To assess these questions, we reconstituted H2AX and H2A nucleosome core particles (NCPs, Figure 3.4A-C) with or without the acidic patch mutation (i.e. E92A) and subjected them to *in vitro* ubiquitination (Ub) assays. Previous studies have established that bacterially expressed and purified RNF168 and RING1B/BMI1 complexes catalyze the specific addition of ubiquitin on H2AX/H2A NCPs at K13/15 and K118/119 respectively (17, 62). Using the same constructs and experimental conditions, we performed *in vitro* Ub assays with H2AX NCPs with or without the E92A acidic patch mutation. As expected, RING1B/BMI1 and RNF168 ubiquitinated H2AX within WT NCPs (Figure 3.4D-E). In contrast, both E3 ligase complexes were unable to efficiently ubiquitinate NCPs containing E92A mutation in H2AX (Figure 3.4D-E). These effects appear to occur within the context of the nucleosome as RNF168 could ubiquitinate the free form of H2AX whether it was WT or contained the acidic patch E92A mutation (Figure 3.4F). We performed identical experiments with H2A WT and E92A NCPs and obtained the same results (Figure 3.4G-I). As another control, we subjected H2AX and H2A WT and E92A NCPs to *in vitro* methylation assays with SET8, a methyltransferase that is active only within the context of the nucleosome for methylating H4K20 (134). The acidic patch mutation did not affect nucleosome specific SET8 methylation suggesting the E92A mutation does not overtly disorder the NCP (Figure 3.5). These *in vitro* results are consistent with our *in vivo* data and demonstrate that RNF168 and RING1B/BMI1 require the nucleosome acidic patch of H2AX/H2A to promote site-specific ubiquitination of H2AX/H2A K13/15 and H2AX/H2A K118/119 respectively.

Nucleosome acidic patch is required for H2AZub *in vitro*

We next performed experiments with NCPs reconstituted with histone H2A variant H2AZ to examine the functional importance of the H2AZ nucleosome acidic patch in

related functions in the DDR. Crystal structure of the H2AZ-containing nucleosome has revealed several unique properties of this H2A variant (73). Compared to other H2A con-

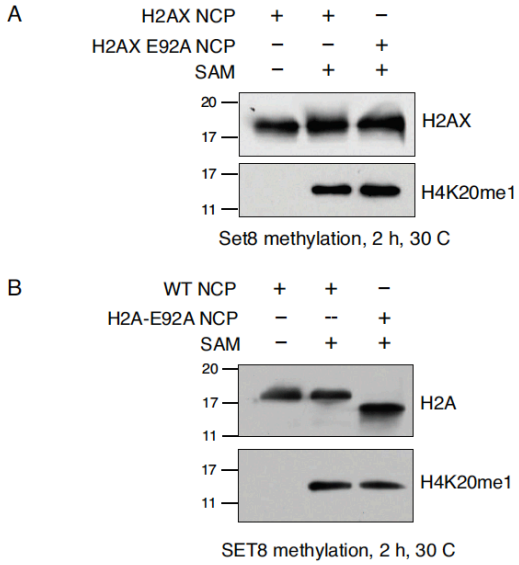

Figure 3.5 The acidic patch does not affect SET8 methylation of NCPs

WT, H2AX-E92A (A) and H2A-E92A (B) NCPs were subjected to methylation assays with Set8. Samples were analyzed by western blotting with specific antibodies against H2AX, H2A and H4K20me1, a SET8-dependent methylation mark. The methylation reactions were performed for 2 h at 20 C. The different apparent molecular weight of WT H2A is due to a 6XHis tag on WT H2A compared to untagged H2A-E92A. SAM = S-Adenosyl methionine. (*This figure was provided by M.D.C.*)

-taining NCPs, the extended acidic patch domain of H2AZ creates an altered acidic pocket on the H2AZ–nucleosomal surface. Mutational studies have shown that this can be functionally significant for DSB repair. For instance, euchromatic H2AZ shows higher chromatin folding than H2A, as a consequence of its extended acidic patch (135). Acetylation of histone H4 tail promotes chromatin relaxation by blocking the binding of H4 tail of one nucleosome to the acidic patch on the surface of an adjacent nucleosome (57, 66, 136, 137). The histone variant H2AZ is transiently loaded into NCPs at DSB sites. This step is mediated by the p400 ATPase subunit of the NuA4 HAT complex to stabilize and maintain a compact chromatin state by increasing the interaction between the H4 tail and the extended acidic patch of H2AZ immediately after DSB induction (51,

138). Since human RNF168 is a key mediator of ubiquitin signaling in DNA double-strand break repair, in collaboration with the Huibregste lab and using the UBAIT technique and MS analysis, we identified H2AZ, a histone H2A variant involved in DNA repair as a new target of RNF168. RNF168 ubiquitinated H2AZ *in vitro* in H2AZ-containing reconstituted nucleosome core particles (NCPs) (Figure 3.15). The D94A mutation in H2AZ disrupts the extended acidic patch in H2AZ that is required for repair activity suggesting that the nucleosome acidic patch region of H2AZ is required for RNF168-dependent ubiquitination (139). The analogous mutation in H2A blocks recruitment of RNF168 to nucleosomes (52), and this mutation also prevented *in vitro* ubiquitylation of H2AZ in NCPs (Figure 3.6).

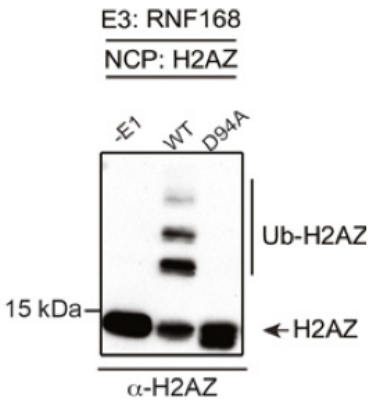

Figure 3.6 RNF168 ubiquitinates H2AZ-containing NCP

Purified WT H2AZ-containing NCPs (first two lanes) were incubated with RNF168, UBCH5a, and ubiquitin, without or with E1 enzyme (lanes 1 and 2, respectively) in an *in vitro* Ub assay. Third lane contains D94A-containing NCPs, incubated with RNF168, UbcH5a, ubiquitin, and E1.

Negative charge and mass of the nucleosome acidic patch is required for histone Ub

In order to further assess whether the charge and/ or mass of the amino acids that comprise the acidic patch plays the critical role in these specific ubiquitin reactions, we substituted the WT acidic glutamic acid E92 in H2AX into another acidic negatively

charged residue, aspartic acid, i.e., E92D to retain the same charge and performed additional biochemical analyses. In addition, for retaining the mass of amino acids similar to the WT glutamic acid (E92), we substituted E92 with glutamine, i.e., E92Q and reconstituted individual nucleosomes with these residues on H2AX (Figure 3.7A). *In vitro* ubiquitination assays showed that RING1B/BMI1 E3 ligase mediated ubiquitination of E92Q containing NCP was completely abolished whereas RNF168 mediated ubiquitination had a marked reduction (Figure 3.7B). These results demonstrate that the

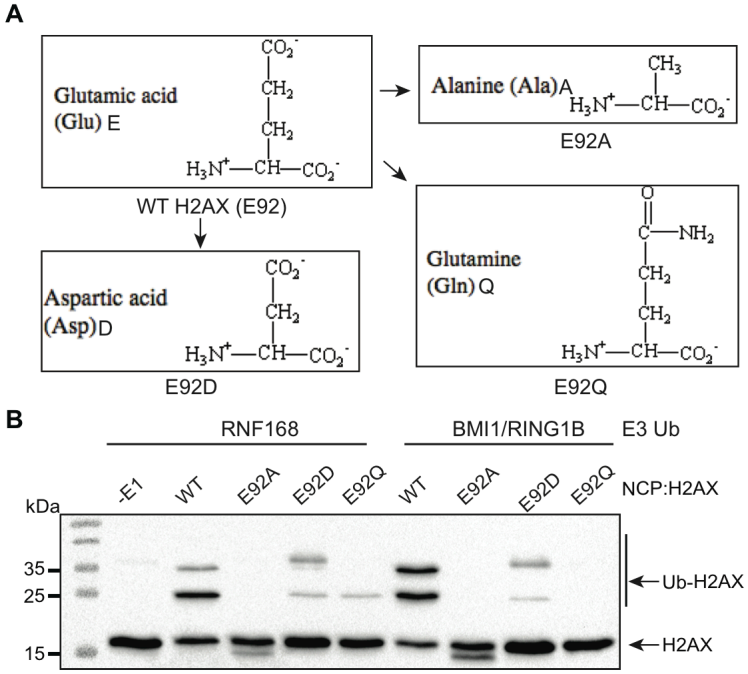

Figure 3.7 Negative charge and mass of the nucleosome acidic patch regulate H2A/Xub

(A) Point mutations of acidic patch were used to analyze the effect of its mass and charge on the histone H2A/X ubiquitinations and DDR signaling. (B) *In vitro* ubiquitination assay using the acidic patch mutants containing NCPs and either of the E3 Ub ligases RNF168 or RING1B/BMI1.

negative charge on the acidic residue glutamic acid is critical for the specificity of the acidic patch mediated chromatin reactions. Substitutions made for maintaining the negative charges and altering mass of the amino acids also showed defective ubiquitinations as compared to WT NCPs mediated by either RING1B/BMI1 or by RNF168. Collectively, these results highlight that both the charge and mass of the acidic

patch residues are determining factors for this chromatin domain to mediate the histone PTMs on site-specific lysines and thereby promote DDR signaling.

Although the acidic patch within H2A-H2B is the most notable interaction platform on the nucleosome, there are other potential structured regions on the nucleosome that may be of functional significance. For instance, investigations of other structural domains on the nucleosomal surface led to novel findings that include the presence of a structured and negatively charged region adjacent to the H2A-H2B acidic patch. This acidic pocket is composed of 3 residues within H3 and one residue from H4 residues (140). Thus, the presence of a distinctive acidic patch region on the nucleosome prompted us to explore the requirement of other structural domains or residues on the nucleosome surface for regulating these ubiquitination reactions. To this end, we used the protein structural biology tool, Pymol, to shortlist 4 residues on H2AX which reside on

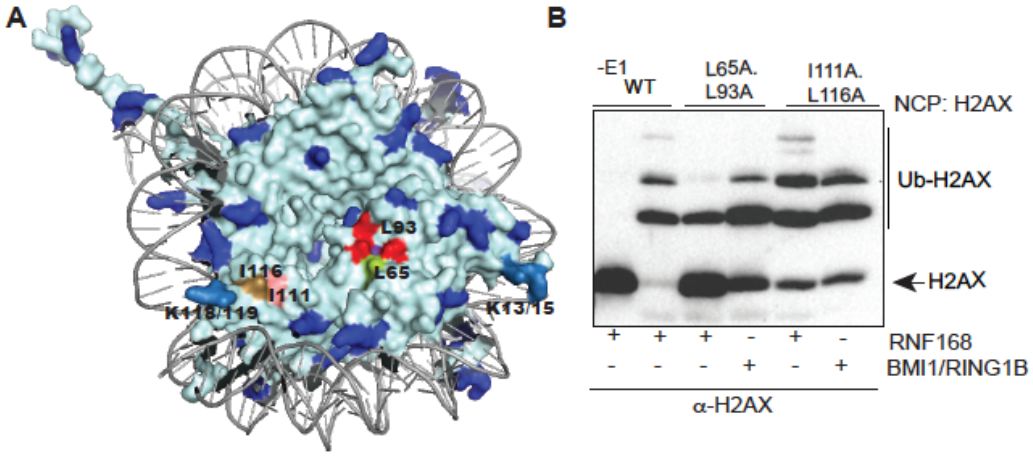

Figure 3.8 Nucleosome surface serves as a chromatin domain to regulate various PTMs

(A) Crystal structure of the NCP highlighting the non-acidic patch mutations on the nucleosome surface. (B) Non-acidic patch mutant L65A.L93A reduces levels of H2AX diubiquitination mediated by RNF168 as compared to control NCP.

the nucleosomal surface to be mutated to alanine and analyze how these modifications would affect H2AX ubiquitination in the NCP (Figure 3.8A). The mutation L65A on H2AX showed reduced monoubiquitination and completely abolished the diubiquitinated H2AX which otherwise is observed in ubiquitination reactions using WT NCPs (Figure

3.8B). On mutating another negatively charged residue in H2B that constitutes the acidic patch to a basic arginine (i.e., H2B E106R) we observed similar results as obtained with the E92A mutant (Figure 3.9).

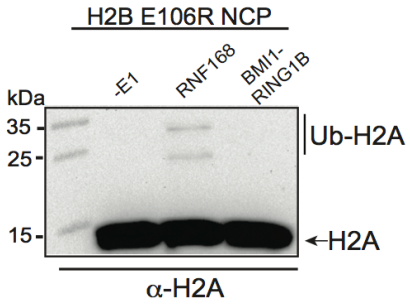

Figure 3.9 Affect of H2B acidic residue mutant on H2Aub

Mutation of acidic patch residue on H2B, E106R reduces RNF168 mediated H2A ubiquitination and completely abolishes RING1B/BMI1 mediated ubiquitination *in vitro*.

Mutations in RNF168 and RING1B/BMI1 affect their E3 ligase activity

Chromatin interaction motifs within both RNF168 and RING1B/BMI1 have been identified. For example, RNF168 contains multiple ubiquitin-binding domains (Figure 3.10A) that target RNF168 to chromatin (141) and the RING1B/BMI1 complex contains DNA binding activity that is critical for histone ubiquitination (117). Similar to the bivalent reading of histone marks by 53BP1, our results suggest that the histone ubiquitin writers, RNF168 and RING1B/BMI1, utilize multivalent chromatin interactions, including the nucleosome acidic patch, to write their "histone code."

Key mechanistic insights explaining these chromatin Ub reactions have been provided by the X-ray structure of the RING1B/BMI1-UbcH5c E3-E2 complex (the PRC1 ubiquitylation module) bound to the NCP. This enzyme–NCP co-crystal structure revealed that the basic residues of RING1B/BMI1 heterodimer interact with the histone surfaces on the NCP, including amino acids within H2A-H2B acidic patch (142). H2A-type histones residue E92 and RING1B residues K97, R98 and to a lesser extent K93 contribute to the RING1B-nucleosomal interface. Validation of the structural predictions

through mutagenesis experiments in solution confirmed that the RING1B residue R98 inserts into the acidic pocket generated by H2A residues E61, D90, and E92, making charged hydrogen bonds with each of the amino acid side chain carboxylates within the acidic patch. Besides arginine R98, other positively charged RING1B residues also interact with the acidic patch extending the RING1B-nucleosome interaction surface. The BMI1 subunit of this E3 ubiquitin ligase heterodimer has weak nucleosome binding affinity but makes contact with the H3 N-terminal tail, which is crucial for binding and proper orientation of the PRC1 complex on the nucleosomal surface (68, 143). Collectively, like RNF168, exposure of the nucleosome surface is necessary for RING1B/BMI1 to make contacts with the nucleosome to promote its site-specific activity on H2A histones. Unlike RNF168, how RING1B/BMI1 are targeted to DNA damage sites is unclear. While RNF168 contains Ub binding domains that recognize damage-induced ubiquitinated targets, it is unclear how the heterodimeric RING1B/BMI1 complex accumulates at damage sites. This question warrants further investigation, as answers to this question could reveal additional mechanistic understanding of how this complex targets damaged chromatin to promote the DDR.

To test the importance of a few basic residues on the E3 ligases RNF168 and BMI1/RING1B, we purified mutant RNF168 and BMI1/RING1 containing aspartic acid or alanine substitutions of their basic residues and performed *in vitro* ubiquitination of H2AX containing NCPs using these as the E3 Ub enzyme. Consistent with previously published reports mentioned above, RNF168 R57D mutant was defective in catalyzing H2AX ubiquitination. However, additional RNF168 mutants that completely abolished or reduced these ubiquitinations on H2AX NCP were detected (R63D, R108D and K112D respectively) (Figure 3.10A-B). Similar results were obtained using BMI1 mutant (K62A.R64A) or RING1B mutant (K97A.R98A or E substitutions) (Figure 3.10C). Taken together, these results highlight the importance of the key residues on the E3s that are critical for perfoming the specific ubiquitination reactions on NCP to mediate DDR.

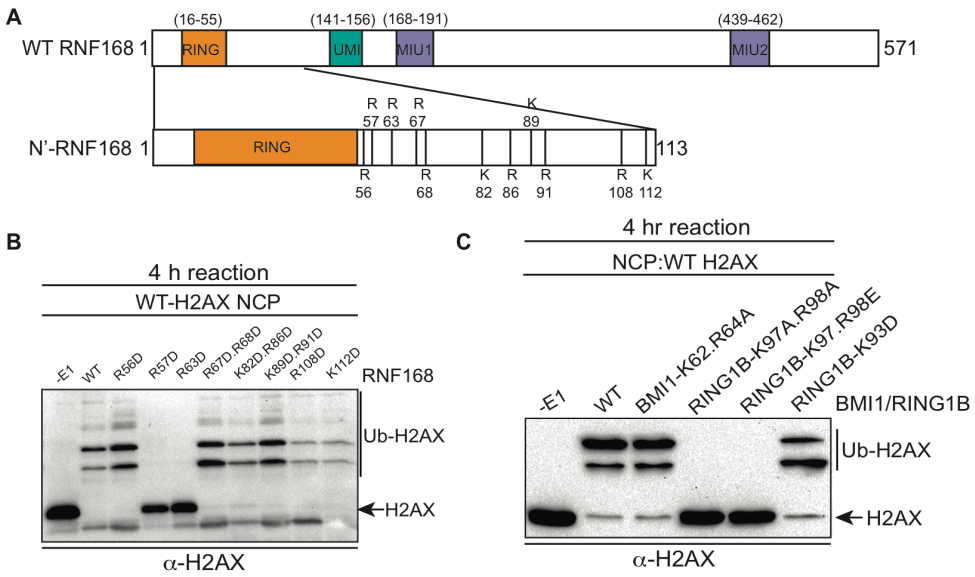

Figure 3.10 Mutations on RNF168 and RING1B/BMI1 residues affect their E3ub ligase activity on nucleosomal substrates

(A) Domain structure of full length RNF168 full length. N'-RNF168 (1-113) is zoomed 3 folds in the schematic. Mutations (aspartic acid substitutions) of amino acid positions are indicated. (B and C) *In vitro* ubiquitination assay using WT H2AX NCPs with (B) RNF168 mutants or (C) RING1B/BMI1 mutants.

Nucleosome acidic patch of H2AX and the DNA damage response

Our findings show that the nucleosome acidic patch mediates both H2AX/H2A K13/15ub by RNF168 and H2AX/H2A K118/119ub by RING1B/BMI1. Several studies have shown that RING1B/BMI1 participates in the DDR although a clear function for H2AX/H2A K118/119ub is as yet unidentified (60, 123-125, 144-146). In contrast, the function of H2AX/H2A K13/15ub by RNF168 was recently elucidated and is well defined (17). Indeed, RNF168-dependent H2AX/H2A K15ub is selectively recognized by the ubiquitination-dependent recruitment motif (UDR) of 53BP1 that, together with its Tudor domain, reads a bivalent ubiquitin-methylation signal at DNA damage sites to recruit the DDR factor 53BP1. A clear prediction of this mechanism is that 53BP1 recruitment to sites of DNA damage would be perturbed in the absence of H2AX-K13/15ub and/or H2A K13/15ub. We chose to next focus on the role of the acidic patch

in regards to RNF168-dependent H2AX/H2A K13/15ub *in vivo* since we could utilize 53BP1 foci formation as an *in vivo* read-out for functional H2AX/H2A-K13/15ub.

Because RNF168 specifically targets H2AX-K13/15, we sought to characterize further our H2AX derivatives where K13/15 are the only lysines available for ubiquitination and to ascertain the contribution of both the acidic patch and RNF168 expression levels on H2AX-K13/15 ubiquitin levels. Expression of SFB-tagged WT H2AX resulted in clearly identifiable mono-ubiquitinated species whose electrophoretic mobility was retarded as expected due to the presence of a 9 kDa ubiquitin protein (Figure 3.11A). Rendering WT H2AX unmodifiable by ubiquitin on all but K13/15 resulted in an almost complete loss of mono-ubiquitinated H2AX (Figure 3.11A). This reduction was also observed when the acidic mutation E92A was added to this H2AX derivative. To analyze the contribution of both RNF168 and the acidic patch on H2AX-K13/15ub, we repeated these experiments in the presence of overexpressed Myc-tagged RNF168. Although we still observed reduced H2AXub in K13/15 only H2AX derivatives compared to WT H2AX, we now were able to specifically detect H2AX-K13/15ub using this H2AX derivative that only contained K13/15 (Figure 3.11A). Interestingly, we were able to detect a small increase in H2AX-K13/15ub upon DNA damage suggesting that this H2AX derivative was functioning within the DDR in cells (Figure 3.11A). Under these optimized conditions for specifically detecting H2AX-K13/15ub, mutation of the acidic patch (i.e. E92A) resulted in a large reduction in H2AX-K13/15ub levels either in the presence or absence of DNA damage (Figure 3.11A). Thus, we could detect DNA damaged induced H2AX-K13/15ub in the presence of RNF168, and in all conditions tested, H2AX-K13/15ub required the acidic patch.

Having now characterized H2AX derivatives for their ubiquitination on K13/15, K118/119 or in the absence of lysines, we sought to determine whether H2AX ubiquitinations were required in vivo for the DDR and more specifically for 53BP1 foci formation. Up to now, all of our experiments analyzing H2AX derivatives were perform-

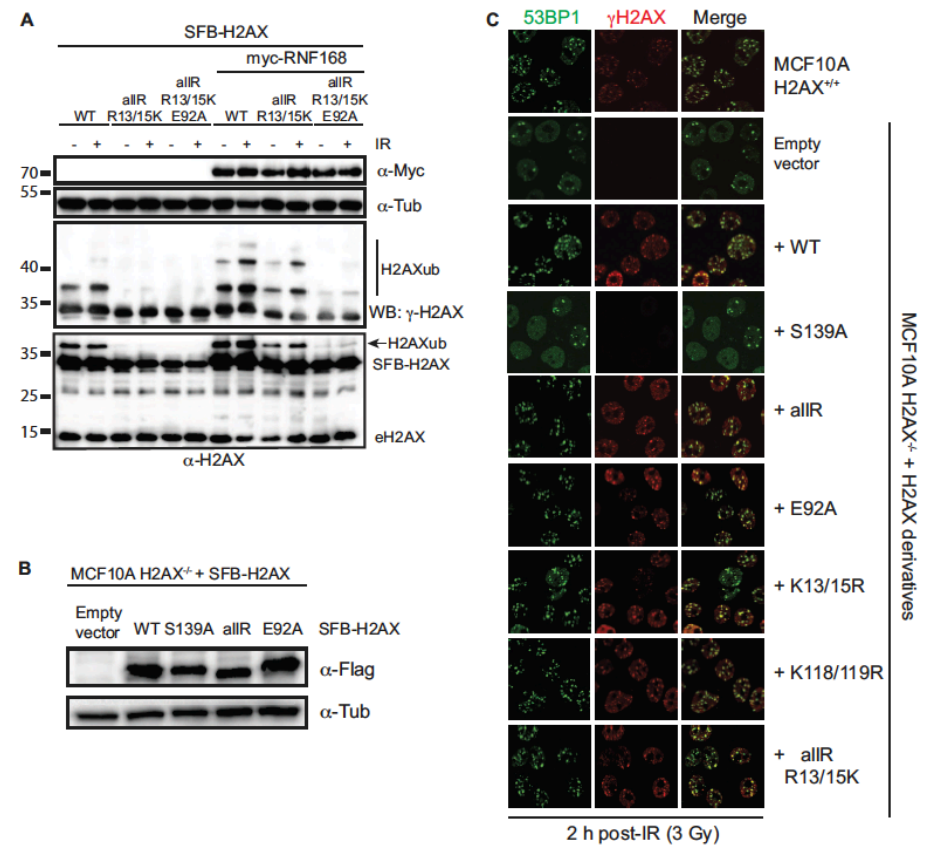

Figure 3.11 The acidic patch regulates H2AX-K13/K15ub by RNF168

(A) Maximum H2AX-K13/15ub levels (-) or (+) RNF168 is dependent on the acidic patch. HEK293T cells were transfected with H2AX and derivatives either (-) or (+) RNF168 and analyzed as in Figure 3.2D. (B) Human H2AX and derivatives reconstituted in MCF10A H2AX-/- cells. Western blot analysis of the indicated MCF10A H2AX-/- stable cell lines. (C) H2AXub is dispensable for 53BP1 foci formation after DNA damage. Reconstituted MCF10A H2AX-/- cells stably expressing H2AX and H2AX mutants were analyzed by immunofluorescence (IF) with the indicated antibodies. Cells were treated with 3 Gy IR and analyzed by IF 2 h post-IR. (*This figure was provided by J.W.L.*)

-ed in the presence of WT H2AX. To overcome this limitation, we turned to a human cell line deleted for H2AX, MCF10A H2AX$^{-/-}$, that we previously characterized (50). In order to test the contribution of H2AXub for 53BP1 IRIF, we stably reconstitutedMCF10A H2AX$^{-/-}$ with WT H2AX and derivatives to compare the ability of site-specific mutations in ubiquitinated sites on H2AX to complement the defect of 53BP1 IRIF that occurs in these cells in the absence of H2AX. We first created stable cell lines expressing H2AX

constructs to be tested and selected clones for each that expressed H2AX in the majority of cells and to similar protein levels as the WT H2AX reconstituted cell line (Figure 3.11B, 3.12 and data not shown). To assess 53BP1 IRIF, we analyzed several H2AX derivatives for their ability to rescue defective 53BP1 IRIF in MCF10A cells lacking H2AX. As we previously reported, MCF10A H2AX$^{-/-}$ and MCF10A H2AX$^{-/-}$ + H2AX S139A are unable to support equivalent recruitment of 53BP1 into IRIF compared to WT MCF10A cells (Figure 3.11C). Surprisingly, all H2AX derivatives tested, including a lysine-less H2AX (allR) that cannot support ubiquitination on either K13/15 or K118/119, were able to fully support 53BP1 IRIF (Figure 3.11C). Thus, although S139 phosphorylation is required for 53BP1 IRIF in these cells, H2AXub (including K13/15 or K118/119), as well as the H2AX acidic patch, is dispensable for 53BP1 IRIF (Figure 3.11C). As DNA damage dependent H2A-K13/15ub also occurs, these results suggest that gH2AX could function in trans to promote H2A- K13/15ub that would be sufficient to mediate 53BP1 recruitment to sites of DNA damage. One hypothesis could be that DNA damage induced H2AX phosphorylation on S139 could mediate an initial ubiquitination on H2AX-K13/15 that would be required to amplify RNF168-dependent H2Aub. Similarly, the nucleosome acidic patch of H2AX could initiate the recruitment and activation of RNF168 that would in turn trigger the start of this ubiquitin-dependent signaling pathway. However, our results argue against these hypotheses and instead suggest that the acidic patch of H2A, as well as H2Aub, can compensate for H2AXub in the DDR to support 53BP1 IRIF. Testing the role of the H2A acidic patch and H2Aub in vivo is extremely challenging due to the unavailability of a mutation system for H2A in human cells. Regardless, our findings establish that the acidic patch of H2AX, as well as H2AXub, is dispensable for 53BP1 IRIF in human cells.

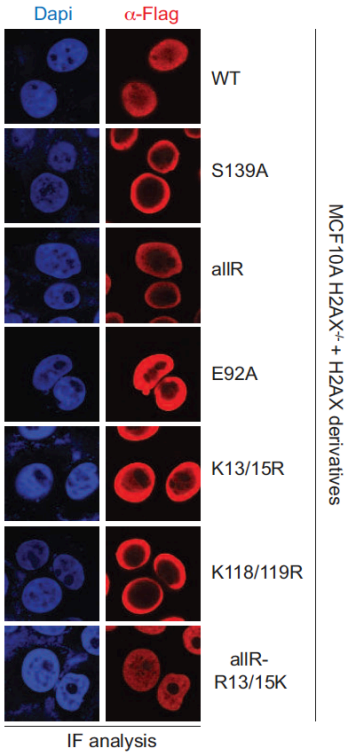

Figure 3.12 IF analysis of H2AX derivatives expressed in MCF10A-/- cells

Cells analyzed in Figure 3.11C were probed with **a**-Flag to detect tagged-H2AX derivatives and DAPI identifies nuclear DNA. Cells were processed for IF as described in experimental procedures (52).

Nucleosome acidic patch is required for the DDR *in vivo*

To overcome the limitations of studying histone mutants in vivo and to validate the requirement of the nucleosome acidic patch in promoting H2AX/H2Aub and subsequent DDR signaling, we sought to identify an experimental approach to target the acidic patch regions of both H2A and H2AX *in vivo*. The nucleosome acidic patch of H2A has been shown to interact with several proteins including histone H4, the Kaposi's sarcoma–associated herpesvirus (KSHV) protein LANA, IL-33, HMGN2 and RCC1 (118, 147-150). The finding that several proteins interact through this nucleosome region has suggested that the nucleosome acidic patch acts as a "chromatin platform" to mediate various cellular signals via their interactions with chromatin through the acidic patch. As our data has identified the nucleosome acidic patch of H2AX and H2A as a requirement

for RNF168- and RING1B/BMI1-dependent H2AX/H2Aub *in vitro* and *in vivo*, we set out to test whether expression of a known acidic patch interacting protein could interfere with these DDR factors. This experimental approach has the advantage of blocking both H2A and H2AX acidic patch regions, a potential necessity for uncovering the function of this nucleosome domain in the DDR. Results from these experiments would further define the role of the nucleosome acidic patch of both H2A and H2AX in the DDR and would allow us to test our hypothesis that the acidic patch of H2A and H2AX functions in the DDR *in vivo*, at least in part by promoting H2AX/H2A-K13/15ub.

The KSHV latency-associated nuclear antigen (LANA) interacts with the nucleosome acidic patch of H2A to tether episomes to chromosomes (118). The first 32 amino acids of LANA comprise the acidic patch interacting region and expression of a GFP fusion with this minimal region in cells is sufficient to target this small truncated region of the protein to mitotic chromosomes (118). Additionally, mutation of the 8-10 amino acid region (named 8LRS10) of this 32 amino acid LANA peptide abolishes the interaction of LANA with the nucleosome acidic patch. To assess whether this acidic patch interacting peptide from LANA could compete with RNF168- and RING1B/BMI1-dependent H2AX/H2Aub, we synthesized the minimal acidic patch interacting peptide from LANA along with the 8LRS10 mutant peptide and analyzed the effects of these peptides on our previously characterized *in vitro* Ub assays.

Interestingly, the acidic patch binding LANA peptide reduced H2Aub that was catalyzed by both RING1B/BMI1 and RNF168 in a concentration-dependent manner (Figure 3.13A, 3.14). The reduction of H2Aub by the LANA peptide required the ability to bind the acidic patch as the 8LRS10 mutant peptide was unable to compete away H2Aub. These results supported our previous findings that the acidic patch was directly promoting histone ubiquitination by these E3 ligases and also suggested that the LANA peptide could interfere with this reaction in cells.

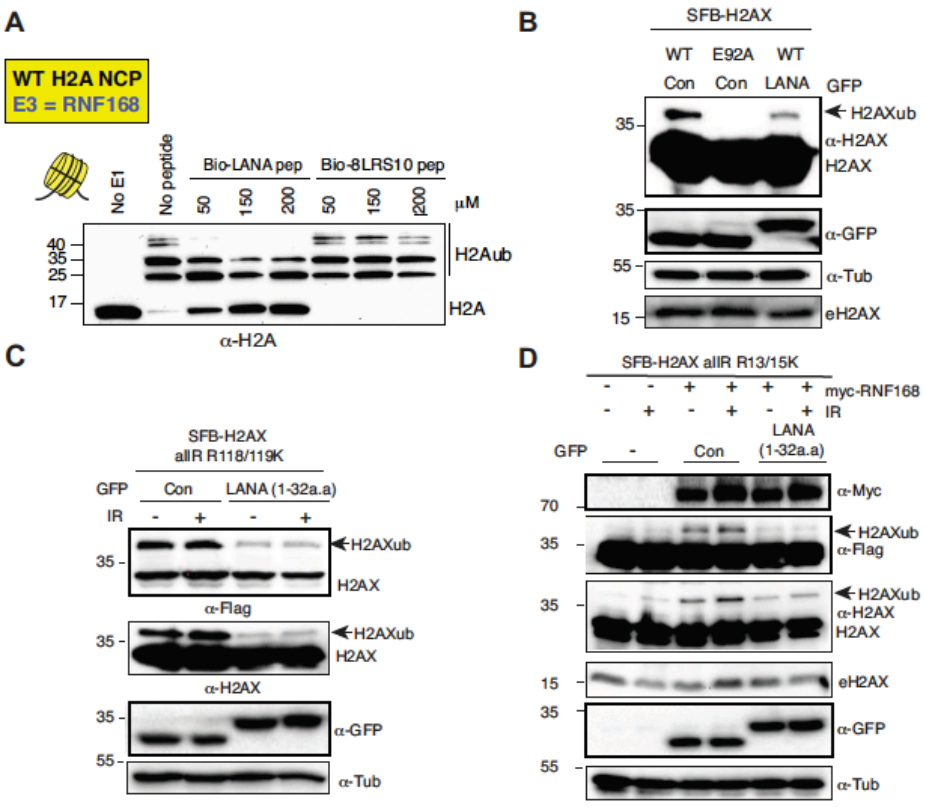

Figure 3.13 The KSHV LANA peptide inhibits histone ub *in vitro* and *in vivo*

(A) The acidic patch interaction region of LANA inhibits RNF168- dependent H2Aub *in vitro*. *In vitro* Ub assays were performed (-) or (+) either LANA peptide or a mutant LANA peptide (8LRS10) that does not interact with the nucleosome acidic patch. Assays were performed as in Figure 3.4 with increasing concentrations of peptides (mM) as indicated (4 h reactions). (B) Expression of GFP-LANA (1-32a.a.) reduces H2AXub. HEK293T cells were transfected with the indicated constructs and analyzed by western blotting as in Figure 3.2B. (C) GFP-LANA (1-32a.a.) reduces H2AXub at K118/119. Experiments were performed as in B using H2AX-allR-R118/119K with or without IR treatment. (D) Expression of GFP-LANA (1-32a.a.) reduces RNF168-dependent H2AXK13/15ub. Experiments were performed and analyzed as in Figure 3.11A with the indicated constructs, with or without IR. Arrows indicate H2AXub protein species. e = endogenous; con = control GFP alone. (*Panels B-D were provided by J.W.L.*)

To begin to address this question, we wanted to ask whether we could observe a decrease in H2AXub in cells expressing LANA peptide. We cloned and engineered a GFP-fusion of LANA containing only the first 32 amino acids (GFP-LANA (1-32a.a.), (118)). Next, we co-transfected our H2AX derivatives with GFP-LANA and analyzed H2AXub by western blotting. We observed that the ubiquitination of WT H2AX, H2AX-

K118/119 only and H2AX-K13/15 only were reduced when co-expressed with GFP-LANA in cells (Figure 3.13B-D). These results are in agreement with both our *in vitro* and *in vivo* data demonstrating that the nucleosome acidic patch of H2AX is required for K13/15 and K118/119 ubiquitination (Figure 3.2, 3.4).

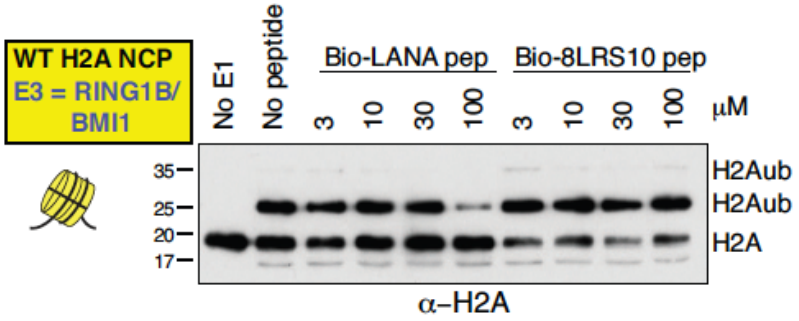

Figure 3.14 The acidic patch interaction region of LANA inhibits H2A ub *in vitro*

Peptides derived from the KSHV acidic patch binding protein LANA compete with RING1B/BMI1-dependent H2Aub. *In vitro* Ub assays were performed (-) or (+) either LANA peptide or a mutant LANA peptide (8LRS10) that does not interact with the nucleosome acidic patch. Assays were performed as in Figure 3.4 with increasing concentrations of peptides (mM) as indicated (2 h reactions).

The ability of LANA to inhibit H2AXub *in vivo* suggested that cells expressing LANA would exhibit impaired DNA damage signaling. If this were indeed the case, a clear prediction would be that cells expressing LANA would exhibit reduced 53BP1 IRIF due to H2AX/H2Aub inhibition from LANA blocking RNF168 through the acidic patch.

To test this possibility, we expressed GFP-LANA in human U2OS and HEK293T cancer cells and analyzed 53BP1 IRIF with and without GFP-LANA. Upon DNA damage, we observed reduced 53BP1 IRIF in cells expressing GFP-LANA compared to GFP alone expressing cells (Figure 3.15A-B, 3.16). Importantly, the upstream DDR factor MDC1, as well as gH2AX, were unaffected by GFP-LANA expression (Figure 3.15A-C). This is consistent with RNF168 inhibition by LANA as RNF168 acts downstream of gH2AX and MDC1 (40, 151). To rule out any potential cell cycle effects due to GFP-LANA

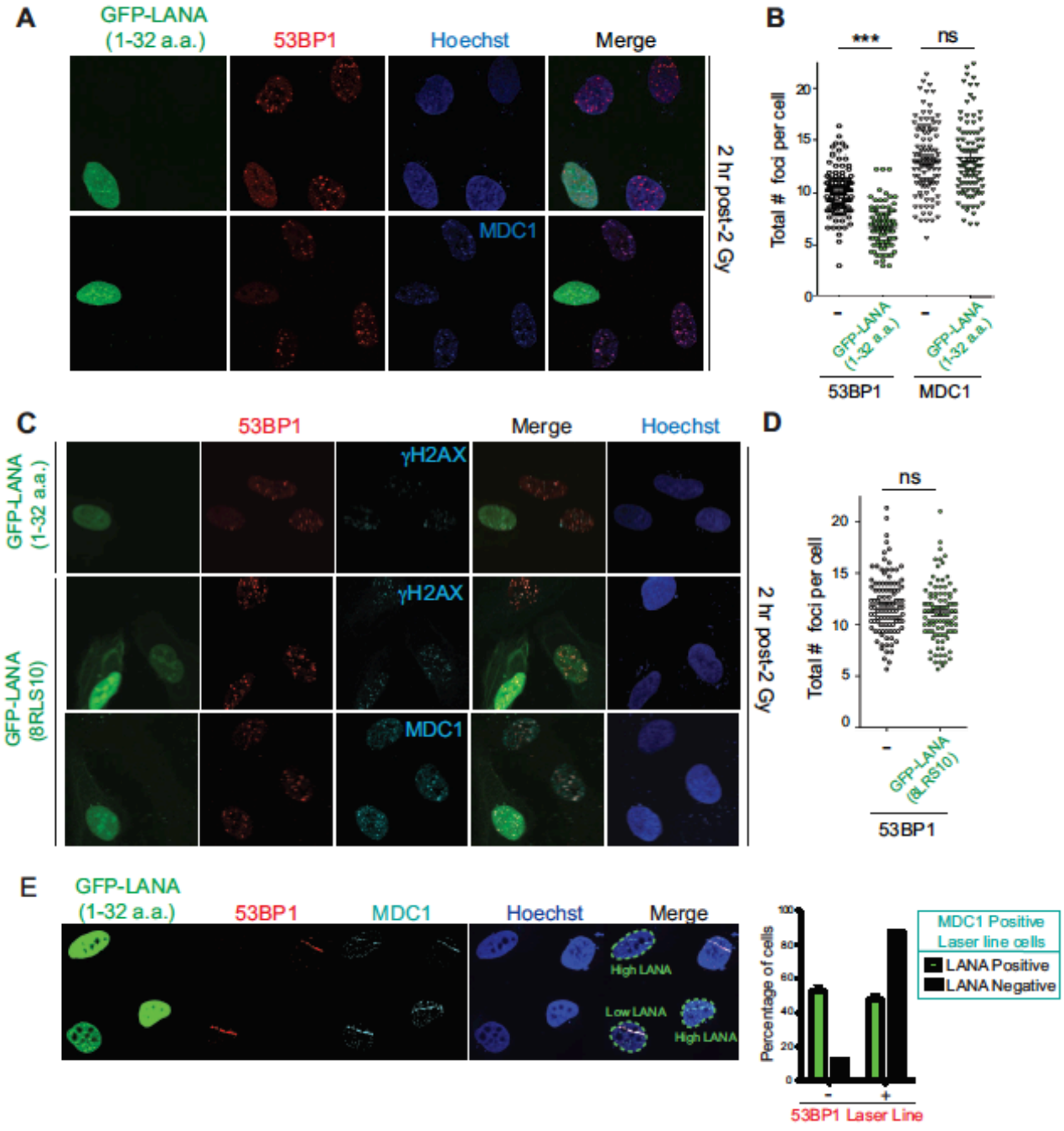

Figure 3.15 Nucleosome acidic patch is required *in vivo* for DDR in human cells

(Figure legend for Figure 3.15 is on next page)

Figure 3.15 (A and B) *In vivo* expression of the acidic patch interacting portion of LANA (1-32 amino acids) reduces 53BP1, but not MDC1, IRIF (ionizing radiation induced-foci). Human U2OS cells were transfected with GFP-LANA (1-32a.a.) followed by 2 Gy IR-treatment. Cells were analyzed by IF with the indicated antibodies 2 h post-IR. Representative IF images are shown. Nuclear DNA was visualized by Hoechst 33342 staining. Quantification of A is shown in B. 53BP1 and MDC1 IRIF were counted and graphed for cells (-) or (+) GFP-LANA (1-32a.a.). N=3, > 100 cells analyzed/experiment, error bars = SEM. Student's t-tests (paired) were performed and results indicated. *** = p-value < 0.001, ns = not significant (i.e. pvalue > 0.05). (C) IF analysis of DDR factor foci formation after IR treatment in GFP-LANA and GFP-LANA-8LRS10 expressing cells. Cells were treated with 2 Gy IR and processed for IF 2 h post-IR. IF analysis was performed as in A. (D) Quantification of 53BP1 IRIF from C. Graph represents values obtained from two independent experiments where foci from >100 cells were scored for GFP-LANA-8LRS10 expressing cells and non-GFP expressing cells. Error bars = SEM. Statistical analysis was performed as in B. (E) GFP-LANA (1-32a.a.) impairs recruitment of 53BP1 to laser damage. U2OS cells were transfected with GFPLANA (1-32a.a.) followed by laser micro-irradiation. Cells were fixed and stained with antibodies as indicated 2 h post-laser damage. Quantification of 53BP1 and MDC1 laser lines were obtained from > 50 damaged cells from two independent experiments. Error bars = SEM. (*This figure was provided by F.G.*)

expression, we analyzed the cell cycle of GFP-LANA expressing cells. Analysis of these cells using FACS, DNA labeling by Hoechst and phospho-Histone H3 (S10) immunostaining, a histone mark specific for mitotic cells, did not reveal any detectable differences in cell cycle stage or DNA staining between control and GFP-LANA expressing cells (Figure 3.17A-D). In addition, expression of mutant GFP-LANA-8LRS10, a mutation that is unable to bind the acidic patch, had no discernable effect on 53BP1 IRIF showing that the effect of GFP-LANA on the DDR required its interaction

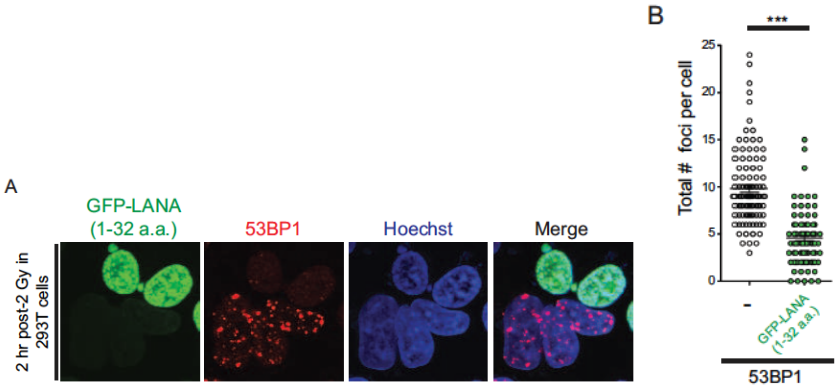

Figure 3.16 *In vivo* expression of GFP-LANA reduces 53BP1 IRIF

Figure 3.16 (A) HEK293T cells expressing GFP-LANA (1-32a.a) were analyzed as in Figure 3.10A. (B) Quantification of 53BP1 IRIF from A. Quantification and statistical analysis were performed as in Figure 3.10. (*This figure was provided by J.W.L.*)

with the nucleosome acidic patch (Figure 3.15C-D). We also confirmed the inhibition of 53BP1, but not MDC1, in GFP- LANA expressing cells by laser micro-irradiation (Figure 3.15E). We observed that cells expressing high levels of GFP-LANA were able

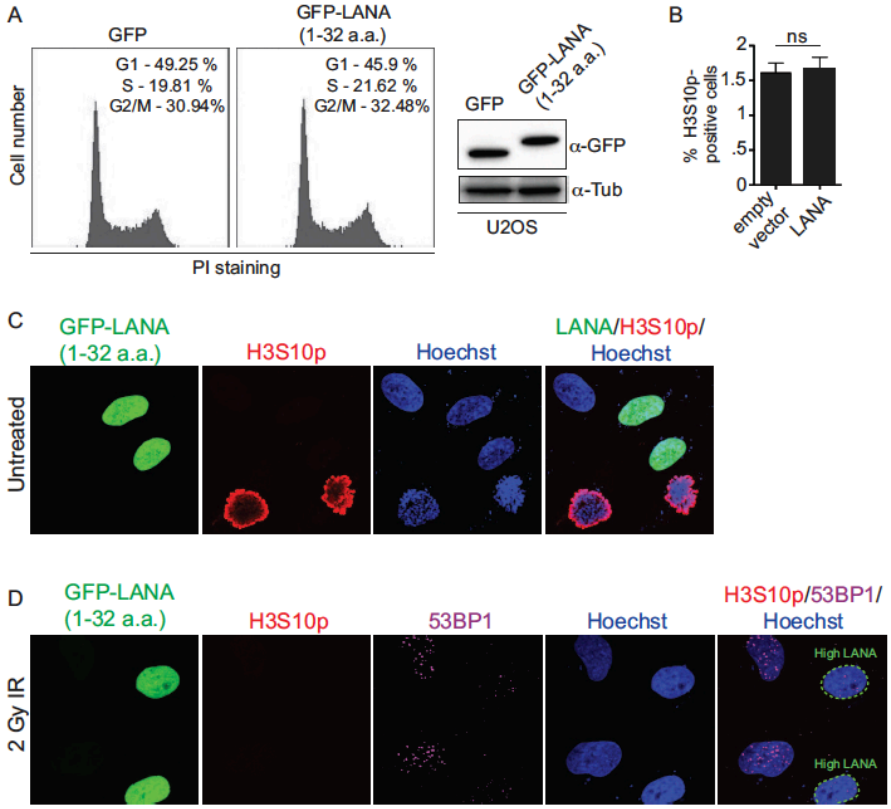

Figure 3.17 GFP-LANA expression does not alter the cell cycle in U2OS cells

(A) Cell cycle distributions of U2OS cells expressing GFP and GFP-LANA (1-32a.a) were analyzed by FACS and percentages of cells in G1, S, and G2/M are shown. GFP and GFP-LANA (1-32a.a) transfected cells were analyzed by Western blotting with indicated antibodies. (B) Mitotic index from empty vector and MYC-LANA (1-32a.a) transfected cells were analyzed by anti-phospho-H3S10 staining and quantified by flow cytometry. Graph represents triplicate experiments. Error bars = SEM. (C-D) U2OS cells expressing GFP-LANA (1-32a.a) do not exhibit detectable changes in H3S10p or nuclear DNA compaction. Untreated or IR-treated GFP-LANA (1-32a.a) transfected U2OS cells were analyzed as in Figure 3.15 with the indicated antibodies and DNA stain. (*This figure was provided by J.W.L. and F.G.*)

to fully inhibit 53BP1 recruitment to laser damage compared to cells expressing lower levels of GFP-LANA (Figure 3.15E). These results are consistent with GFP-LANA targeting the nucleosome acidic patch resulting in inhibition of 53BP1 recruitment to DNA damage.

53BP1 functions in DNA double-strand break repair by both promoting NHEJ and inhibiting HR (reviewed in (152)). 53BP1 recruits the DDR factor RIF1 to DNA damage sites where it inhibits DNA end-resection and acts as the main effector of 53BP1-dependent NHEJ (153-157). Consistent with GFP-LANA inhibiting RNF168-dependent 53BP1 recruitment, we also observed reduced RIF1 accumulation at IRIF in GFP-LANA expressing cells (Figure 3.18A). RNF168 is also required for the recruitment of the HR factor BRCA1 to DNA damage sites (40, 151). Interestingly, GFP-LANA also impaired BRCA1 IRIF in S/G2 cells (Figure 3.18B; S/G2 cells were identified by CyclinA positive staining). Quantification of IRIF in GFP-LANA expressing cells revealed a greater than 50% reduction in cells with greater than 10 foci for either RIF1 or BRCA1 (Figure 3.18C, D). The ability of GFP-LANA to impair IRIF of DDR factors appears to be dependent on expression levels. We observed that high LANA expressing cells displayed a greater reduction in DDR factor recruitment compared to low LANA expressing cells, which explains the incomplete inhibition of DDR factor recruitment to DNA damage sites by GFP-LANA (Figure 3.15E, 3.18B). 53BP1 also inhibits DNA-end resection in G1 to block HR and promote NHEJ (153, 155, 156, 158). Since expression of GFP-LANA impaired 53BP1 foci formation at DNA damage sites, we analyzed whether these cells exhibited functional inhibition of 53BP1 by monitoring DNA end-resection in G1 cells. RPA is recruited to, and binds, resected DNA, which is normally restricted to CyclinA-positive S/G2 cells. As expected, in control cells that do not express GFP-LANA or cells expressing mutant GFP-LANA-8LRS10, RPA foci at laser damage were virtually undetectable using our experimental conditions (Figure 3.18E-F, quantified in G). Interestingly, GFP-LANA expressing cells readily formed RPA foci at laser damage in

CyclinA-negative G1 cells (Figure 3.18E-F, quantified in G). Thus, GFP-LANA expression resulted in DNA end-resection in G1 cells, which supports our previous results showing impaired 53BP1 recruitment to DNA damage by GFP-LANA. Taken together, these results are consistent with a role for the nucleosome acidic patch in promoting both 53BP1 and BRCA1 DDR pathways by mediating RNF168-dependent DNA damage signaling *in vivo*.

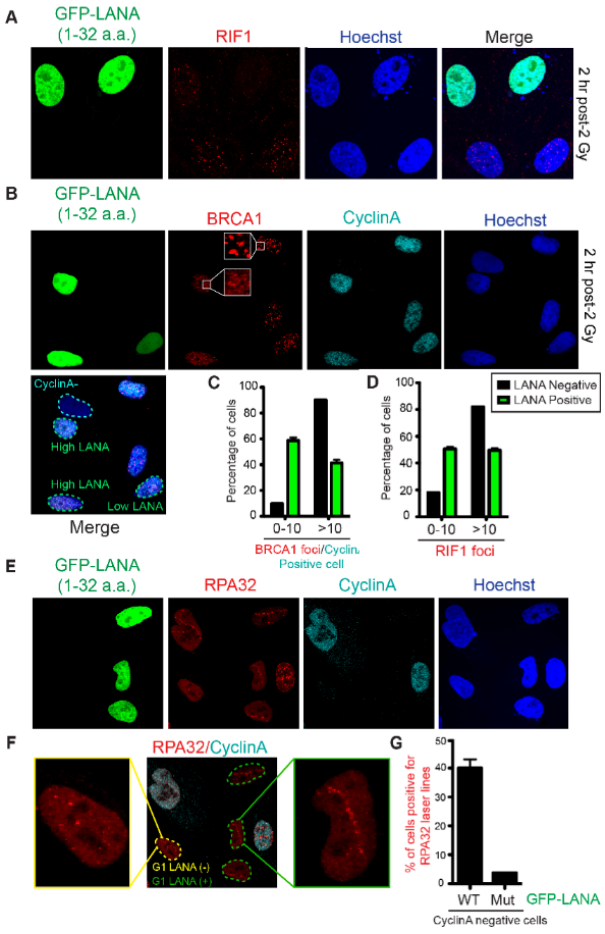

Figure 3.18 Nucleosome acidic patch promotes RNF168-dependent DNA damage signaling and is required to inhibit DNA resection in G1 cells

(Figure legend for Figure 3.18 is on next page)

Figure 3.18 (A and B) RIF1 and BRCA1 IRIF are impaired in GFP-LANA (1-32a.a.) expressing cells. Experiments were performed as in Figure 3.15A. Representative images are shown. CyclinA negative and High/Low LANA expressing cells are indicated in the merged image. Note: CyclinA marks S/G2 cells. (C and D) Quantification of RIF1 and BRCA1/CyclinA-positive IRIF from A and B. Graphs represent values obtained from two independent experiments where foci from >100 cells were quantified. Error bars = SEM. (E) GFP-LANA (1-32a.a.) expressing cells exhibit DNA end-resection as detected by RPA accumulation at laser damage in G1 (CyclinA-negative) cells. Experiments were performed as in Figure 3.10E with indicated antibodies after 4 h of micro-irradiation. (F) RPA32 laser lines in CyclinA-negative cells without or with GFP-LANA (1-32a.a.) expression are indicated by yellow and green dotted lines respectively. Enlarged images from each category are shown. All cells have been laser damaged. (G) Quantification of F and G from either WT GFP-LANA (1-32a.a.) or Mut GFPLANA-8LRS10 expressing cells. Laser damage CylclinA negative cells positive for LANA expression were scored for RPA laser line formation. Graph represents data obtained from >50 cells from two independent experiments. Error bars = SEM. (*This figure was provided by F.G.*)

DISCUSSION

Our results support a model whereby RNF168 and RING1B/BMI1 require the nucleosome acidic patch on H2AX/H2A to target these histones on site-specific lysines and that GFP-LANA can inhibit these processes (Figure 3.19). By overcoming the limitations of mutating the acidic patch of both H2A and H2AX through the expression of GFP-LANA, we have determined that the nucleosome acidic patch functions *in vivo* to promote RNF168-dependent DNA damage signaling. We have also created a novel tool that has the ability to silence DNA damage signaling at the level of RNF168 as well as inhibit RING1B/BMI1-dependent H2AX/H2Aub *in vivo*, which could be useful for studying these ubiquitin-dependent processes in cells. Of note, some viruses inactive the DDR by ubiquitin-dependent degradation mechanisms that target DDR factors, including RNF168 (159, 160).

Our results suggest that viruses, including LANA expressing KSHV, could inactive the DDR through another means by interfering with the nucleosome acidic patch. This potential mechanism would inhibit H2A/H2AX ubiquitination and subsequent DNA damage responses whose inhibition can affect viral transcription and activation of latent viruses in mammalian cells (161). Additionally, other nucleosome acidic patch binding

factors, including RCC1 and HMGN2, could also potentially affect the DDR. RCC1 and HMGN2 have opposing effects on chromatin dynamics with RCC1 promoting condensation of DNA prior to mitosis and HMGN2 decompacting chromatin through interactions with linker histone H1 (67). We envision that these factors could regulate the DDR in multiple ways including chromatin dynamics and/or competition with other nucleosome acidic patch interacting proteins including RNF168 and RING1B/BMI1. Additional studies are warranted to investigate the interplay between nucleosome interacting factors and the DDR.

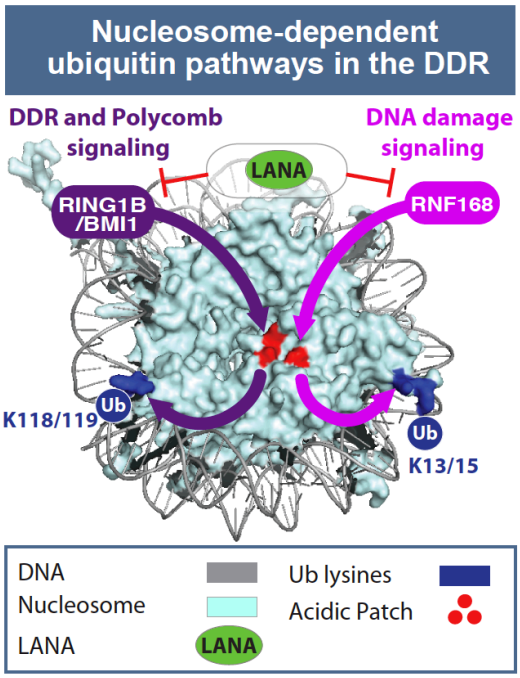

Figure 3.19 The nucleosome acidic patch and histone ubiquitination

Summary of our results within the context of the nucleosome structure. The acidic patch is required for RNF168- and RING1B/BMI1-dependent histone ubiquitination and LANA inhibits these processes. Nucleosome structure was created in Pymol.

To our knowledge, this study has identified the first nucleosome domain that participates in both H2A/H2AXub and the DDR in human cells. Most studies have

focused on the role of histone modifications, including ubiquitination, in the DDR. Our findings provide evidence that the DDR engages the nucleosome acidic patch, which participates in promoting histone ubiquitinations that mediate DDR factor interactions with chromatin including 53BP1. Chromatin interaction motifs within both RNF168 and RING1B/BMI1 have been identified. For example, RNF168 contains multiple ubiquitin-binding domains that target RNF168 to chromatin (141) and the RING1B/BMI1 complex contains DNA binding activity that is critical for histone ubiquitination (117). Similar to the bivalent reading of histone marks by 53BP1, our results suggest that the histone ubiquitin writers, RNF168 and RING1B/BMI1, utilize multivalent chromatin interactions, including the nucleosome acidic patch, to write their "histone code."

CHAPTER 4: CHROMATIN REGULATES GENOME TARGETING WITH CISPLATIN

Emerging evidence indicates that functional interactions between small molecules and genomic DNA are influenced by chromatin features (104, 105). Platinum (Pt) drugs, including cisplatin and its derivatives represent some of the most commonly employed drugs in the clinical management of cancer (162). These drugs form covalent bonds with purine residues to produce toxic DNA-Pt including mono-adducts, inter- and intra-strand crosslinks. Thus, cellular responses to cisplatin are pleiotropic and inherently complex. For example, diverse repair mechanisms including nucleotide excision repair (NER), base excision repair (BER) and DNA crosslink repair involving the Fanconi anemia pathway can process DNA-Pt, and these lesions can also alter the structure of chromatin or be influenced by chromatin features (163). Alternatively, low-fidelity DNA polymerases (e.g. Polh) can bypass DNA-platinum lesions (DNA-Pt) through a mechanism known as translesion synthesis, enabling continued replication in the presence of DNA-Pt, conferring resistance to platinum drugs (164-168).

To study DNA-Pt lesions, we sought to develop a surrogate probe that would allow for the chemical labeling of DNA-Pt crosslinks in cells. Visual detection of DNA-Pt with high resolution at the single-cell level can potentially provide the means to monitor proteins at sites of lesions and to identify small molecules with a propensity to modulate targeting with cisplatin in an unbiased manner. Prior expertise in characterizing

Portions of this chapter have been published as follows:

- *Emmanouil Zacharioudakis[1], Poonam Agarwal[1], Alexandra Bartoli, Nathan Abell, Lavaniya Kunalingam, Valerie Bergoglio, Blerta Xhemalce, Kyle M. Miller* and Raphael Rodriguez* (2017) Chromatin regulates genome targeting with cisplatin. Angew. Chem. Int. Ed. 2017, 56, 1–6.*
  *([1]co first authors, * co corresponding authors)*

mechanisms of action of small molecules prompted us to develop an azide-containing drug to label platinated DNA adducts by means of click-chemistry (105, 112, 169). Previous efforts towards the synthesis of clickable cisplatin derivatives suitable for cell imaging led to the development of an iminoacridine-Pt complex and a flexible alkyl-azide-containing derivative (170, 171).

With this in mind, our collaborators synthesized the cyclic azidoplatinum-containing derivative we named 2-aminomethylpyridine (dichloro) PtII azide (APPA), (patent application no. PCT/EP2016/081166) on clickable cisplatin derivatives and protocols is filed). The design of APPA was inspired from the structures of cisplatin and picoplatin (Figure 4.1A), taking advantage of the aromatic methyl substituent to form a rigid five-membered ring with Pt. Thus, APPA exhibits a structure that can form bulky DNA lesions, where the ring prevents free rotation of the pyridine core chelated to Pt. This structural distinction was considered important given that the chemical nature of ligands bound to Pt at sites of lesions in cells can potentially affect how these lesions are detected and dealt with (172). Like cisplatin and picoplatin, APPA exhibited anti-proliferative properties against human osteosarcoma U2OS cells (Figure 4.1B). Thus, we evaluated the reactivity of APPA towards DNA and our ability to label DNA-Pt with strained or terminal alkyne-containing fluorophores. A 26-mer hairpin-forming DNA oli--gonucleotide containing a single 1,2-GG dinucleotide, prone to form an intra-strand crosslink upon treatment with Pt drugs, was incubated with APPA, purified and then incubated with a strained alkyne containing Alexa 488 (Figure 4.1C) (173, 174). The reaction products were then analyzed and characterized by mass spectrometry. We identified three ion peaks corresponding to the free unreacted hairpin along with the unlabeled and fluorescently labeled Pt adducts (Figure 4.1D). Next, we performed similar experiments in cells using APPA and the control compound 2-aminomethylpyridine (dichloro) PtII (APP, Figure 4.1E), a structurally related active analogue of APPA devoid of azide functionality and therefore not amenable to labeling. Labeled genomic DNA-Pt

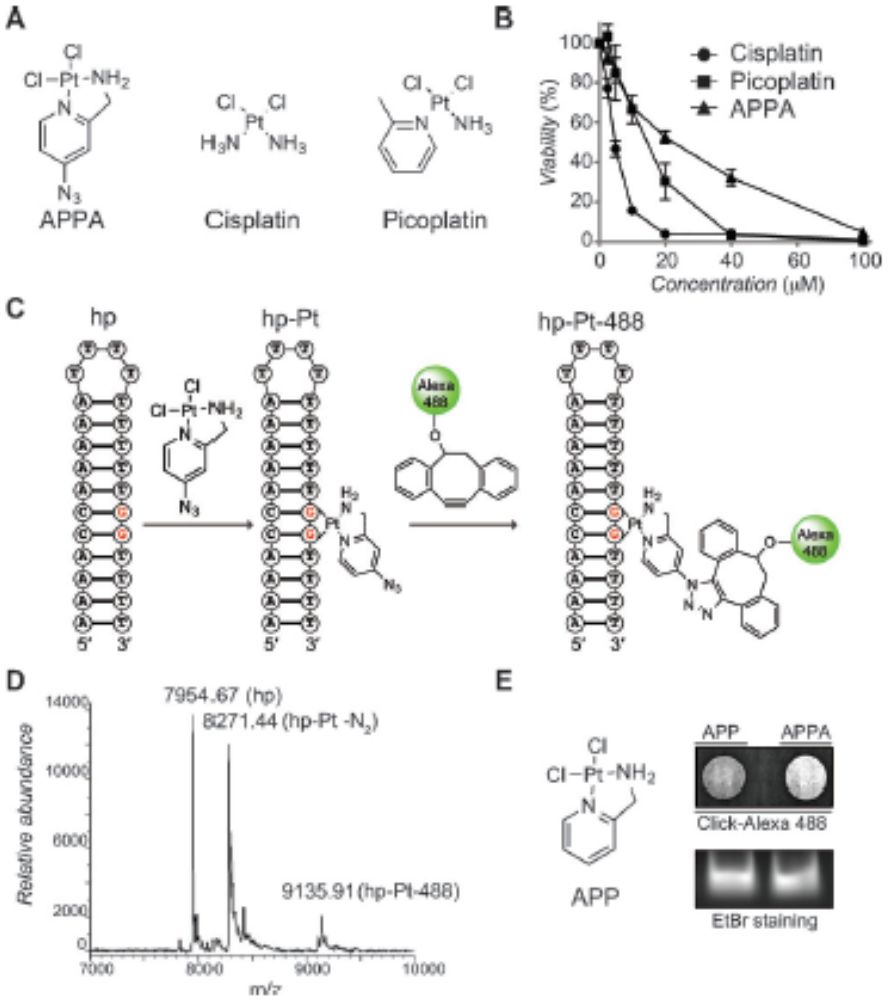

Figure 4.1 APPA forms DNA-Pt cross-links *in vitro* and *in vivo*

A) Molecular structures of APPA, cisplatin and picoplatin. B) Anti-proliferative activity of cisplatin derivatives against U2OS cells. C) Schematic representation of a DNA hairpin (hp), a 1,2-GG intrastrand DNA crosslink (hp-Pt) and chemical labeling of DNA-Pt (hp-Pt-488). For clarity, a single regioisomer is shown for hp-Pt-488. D) Mass spectrometry detection of a free DNA hairpin, the corresponding DNAPt and its labeled counterpart. hp-Pt was observed as the molecular ion peak with loss of nitrogen. E) Molecular structure of APP and detection of genomic DNA platination by dot blot. DNA samples were purified from U2OS cells treated with APP (250 mM) or APPA (250 mM) for 3 h. EtBr (Ethidium bromide) stained gel of input DNA used as loading control. (*Panels C and D were provided by E.Z.*)

obtained from APPA-treated cells displayed increased fluorescence compared to equal amounts of DNA collected from APP-treated cells as monitored by dot blot (Figure 4.1E). This data demonstrated that APPA can form DNA-Pt with genomic DNA in cells.

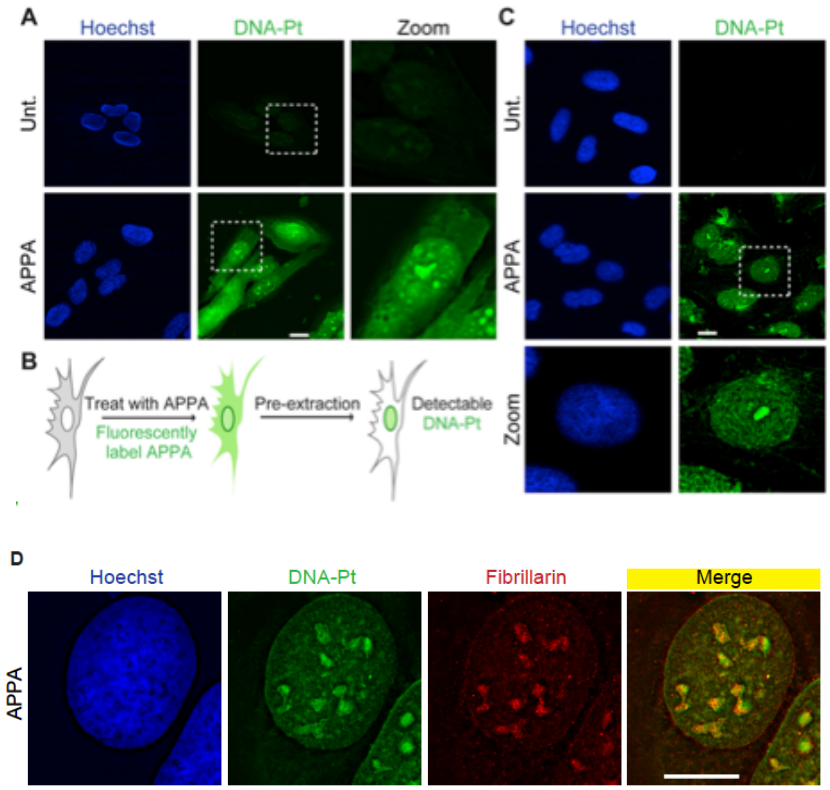

Figure 4.2 Labeling and visualization of DNA-Pt in cells

A) Detection of labeled DNA-Pt in U2OS cells. B) Schematic representation of a strategy for enhancing the detection of DNA-Pt in cells. C) Detection of labeled DNA-Pt in U2OS cells subjected to pre-extraction. Cells were treated with APPA (250 mM for 3 h). Zoomed images are 3X Scale bar, 20 mm. Unt., untreated. D) Visual detection of labeled DNA-Pt by fluorescence microscopy in U2OS cells showing colocalization with the nucleolar marker fibrillarin depicting APPA accumulates in nucleoli. Cells were treated with APPA (250 μM, 3 h). Scale bar, 20 μm.

With this methodology in hand, we investigated the localization of DNA-Pt in cells. To this end, cells were treated with APPA and fixed with formaldehyde prior to labeling DNA-Pt using copper catalysis. Consistent with previous observations (170, 171, 175, 176) labeled DNA-Pt exhibited a diffuse cytoplasmic and nuclear staining (Figure 4.2A), which likely reflected the targeting of nuclear DNA as well as proteins and RNA. As a means to selectively detect DNA-Pt, we implemented a pre-extraction protocol to remove the background linked to soluble proteins and RNA targets of Pt drugs (Figure 4.2B). This protocol allowed for the detection of labeled DNA-Pt in the nucleus with

some sub-nuclear regions displaying increased fluorescence intensity (Figure 4.2C). For instance, labeled DNA-Pt colocalized with fibrillarin (Figure 4.2D), in agreement with the idea that Pt drugs target rRNA in the nucleolus (171). Collectively, these data validated APPA as a functional clickable probe suitable for studying genome targeting with cisplatin derivatives in cells. Next, we searched for small molecule modulators of genomic DNA targeting with cisplatin derivatives, using APPA staining as a readout. We

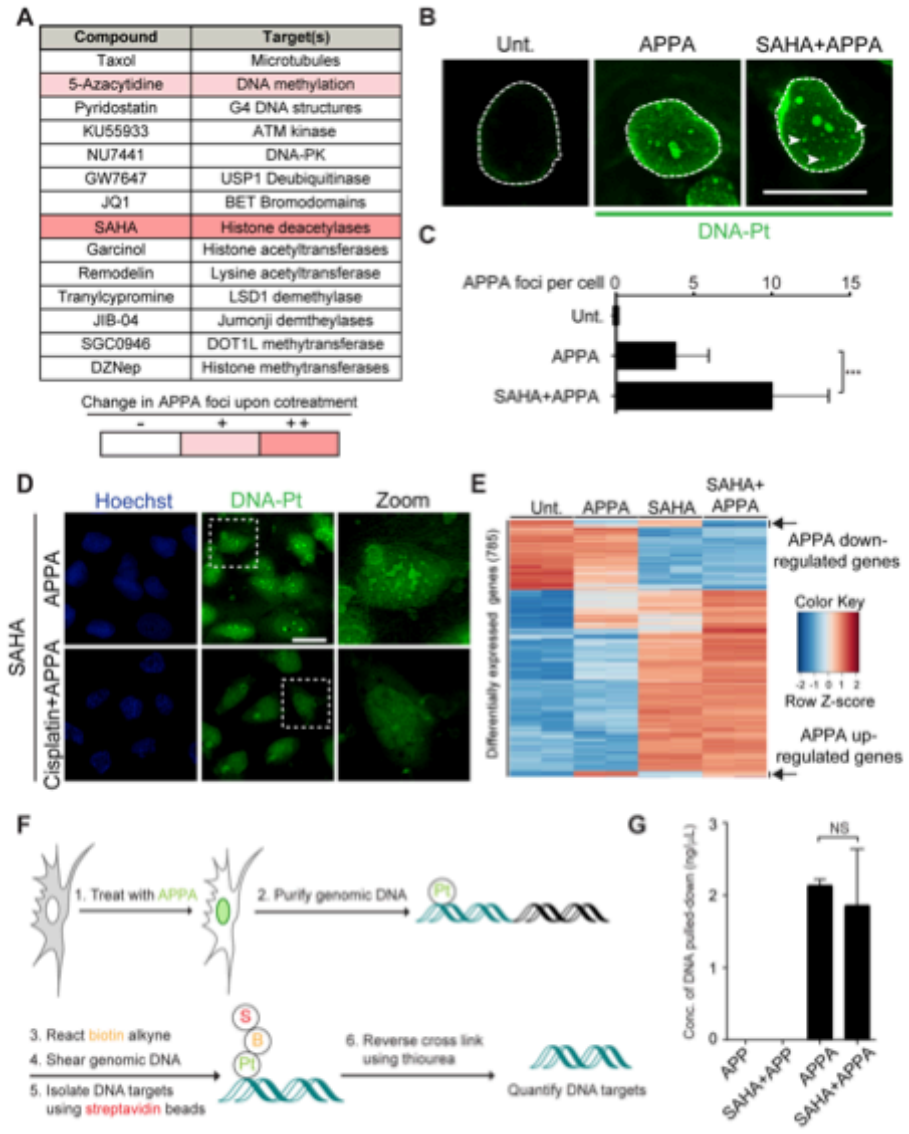

Figure 4.3 Effect on genome targeting with APPA in combination with chromatin modulators

Figure 4.3 A) Small molecules screened for effects on genome targeting with APPA. B) Flourescence microscopy detection of labeled DNA-Pt. Arrows indicate DNA-Pt foci. Scale bars, 20 mm. C) Quantification of B. >100 cells scored per condition; n=3; Foci were counted by means of visual inspection. D) Cisplatin competes with APPA for genome targeting. Zoomed images are 3X Scale bars, 20 mm. E) Heatmap of differentially expressed genes in SAHA and APPA cotreated cells. Genes were selected based on differential expression in SAHA and APPA cotreatment compared to untreated. Data from two independent experiments per condition are shown. Gene expression was monitored by RNA-Seq as described in Supporting Information. F) Scheme of DNA-Pt pull-down methodology. G) Quantification of DNA isolated by pull-down from samples treated as indicated; n=3. All experiments performed in U2OS cells. Cells were treated with APPA (250 mM for 3 h), APP (250 mm for 3 h), SAHA (2.5 mM for 5 h) and cisplatin (500 mM for 5 h). Error bars represent mean ± SD; ***P<0.001, Student's t-test; NS, not significant. (*Panels A and D were provided by E.Z. and panel E was provided by N.A.)*

screened a defined set of small molecules that either operates at the level of chromatin or that are used in cancer treatment in conjunction with Pt drugs (Figure 4.3A). U2OS cells were cotreated independently with each small molecule and APPA, then subjected to chemical labeling and labeled DNA-Pt were analyzed by fluorescence microscopy. Treatment with the clinically approved DNA methyl transferase inhibitor azacytidine (5-Aza) (177) and the histone deacetylase (HDAC) inhibitor SAHA (164, 178, 179) led to the occurrence of foci of DNA-Pt, indicating the presence of targeted clusters of purine residues at these sites that can include mono-adducts, 1,2-GG and 1,3-GTG intra-strand as well as inter-strand lesions (Figure 4.3B-C). Western blotting analysis confirmed that SAHA induced hyperacetylation of histone H4 (Figure 4.4A), an established marker of open chromatin (46). Furthermore, the structurally distinct Class I HDAC inhibitor MS-275 (180) also led to increased number of DNA-Pt foci, implicating further the role of HDACS and chromatin in genome targeting with APPA ((Figure 4.4B). Importantly, the intensity of DNA-Pt foci was reduced when cells were cotreated with a two-fold excess of cisplatin acting as a competitor, indicating that both APPA and cisplatin target similar genomic loci (Figure 4.3D). These data suggested that chromatin relaxation resulting from SAHA treatment revealed *de novo* DNA targets of APPA. Interestingly, DNA-Pt occurring in SAHA-treated cells did not predominantly colocalize with the centromere

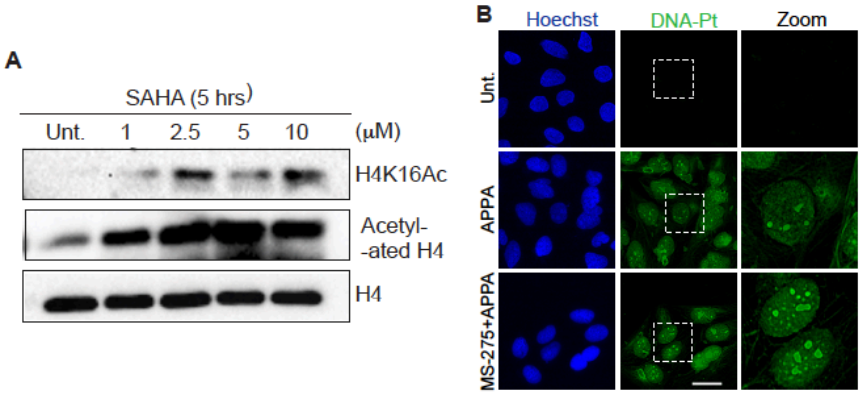

Figure 4.4 SAHA and MS-275 treatment in cells

(A)Western blot analysis of U2OS cells treated as indicated showing SAHA induces hyperacetylation of H4 (B) MS-275 induces the formation of DNA-Pt foci. Visual detection of labeled DNA-Pt by fluorescence microscopy in U2OS cells. Cells were treated with APPA (250 μM for 3 h) and MS-275 (5 μM for 5 h) as indicated. Zoomed images are 3X. Scale bar, 20 μm. (*Panel B was provided by E.Z.*)

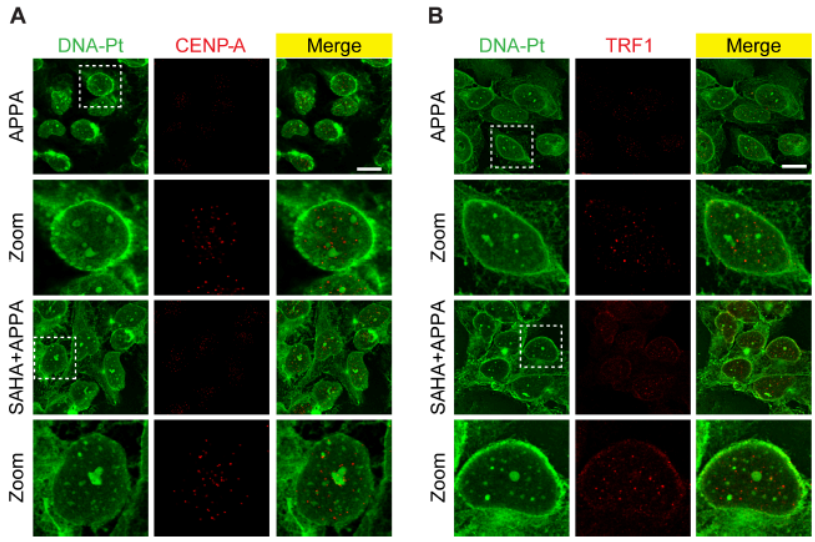

Figure 4.5 DNA-Pt foci do not predominantly form at centromere and telomeres

Visual detection of labeled DNA-Pt by fluorescence microscopy in osteosarcoma U2OS cells co-stained with markers of centromeres and telomeres. (A) Centromeric marker CENP-A. (B) Telomeric marker TRF1. Cells were treated with APPA (250 μM for 3 h) and SAHA (2.5 μM for 5 h) as indicated. Zoomed images are 3X. Scale bar, 20 μm.

and telomere markers CENP-A and TRF1, respectively, excluding these loci-containing repetitive sequences rich in 1,2-purine residues as primary targets of APPA under these conditions (Figure 4.5).

Given that DNA-Pt can alter transcription, (181) we performed RNA-Seq analyses to evaluate whether SAHA treatment affected the transcriptional response induced by APPA. Our analysis identified a subset of genes that were up- or down-regulated by APPA compared to untreated cells (Figure 4.3E, 4.6). Interestingly, the transcriptional changes measured in cells cotreated with SAHA and APPA could be attributed to that observed either in SAHA or APPA independent treatments. This supported the idea that the DNA-Pt clusters detected in cotreated cells did not trigger additional transcriptional effects that were unique to this cotreatment.

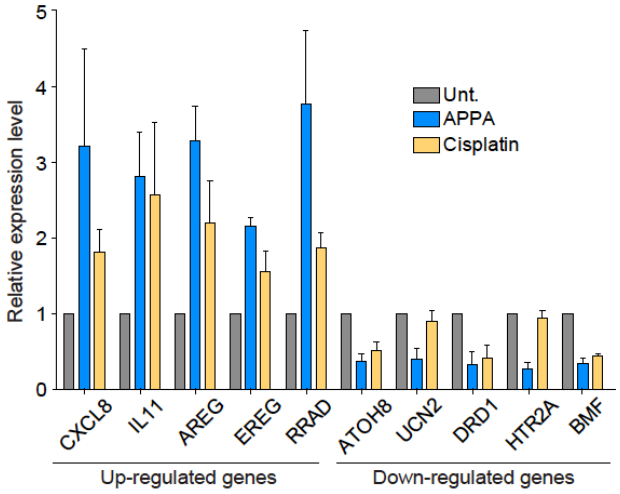

Figure 4.6 Transcriptional analysis in cells treated with platinum drugs

Cisplatin and APPA treatment induce similar transcriptional effects. Analysis of top up- and down-regulated genes in APPA or cisplatin treated cells by qPCR. Bar graph represents data from three independent experiments. Cells were treated with APPA (250 μM for 3 h) or cisplatin (10 μM for 3 h). Error bars represent s.e.m.

Furthermore, qPCR experiments validated that cisplatin induced similar changes in gene expression compared to APPA, providing further evidence that APPA and cisplatin shared genomic targets.

Then, we developed a protocol to isolate DNA targets of APPA from cells (Figure 4.3F). Cells were treated with APPA ± SAHA prior to being subjected to affinity pull-down as previously performed for other classes of molecules (104, 182). The amount of DNA pulled down from cells was similar in both experimental conditions (Figure 4.3G). This result was in line with the idea that SAHA did not solely act by increasing the number of DNA targets per se, but rather induced a redistribution of DNA-Pt throughout the genome, potentiating DNA targeting at particular sites. This was consistent with the idea that chromatin relaxation induced by SAHA altered accessibility of the genome to APPA, providing additional insights into how HDAC inhibitors can sensitize cells to genotoxic drugs (109, 110).

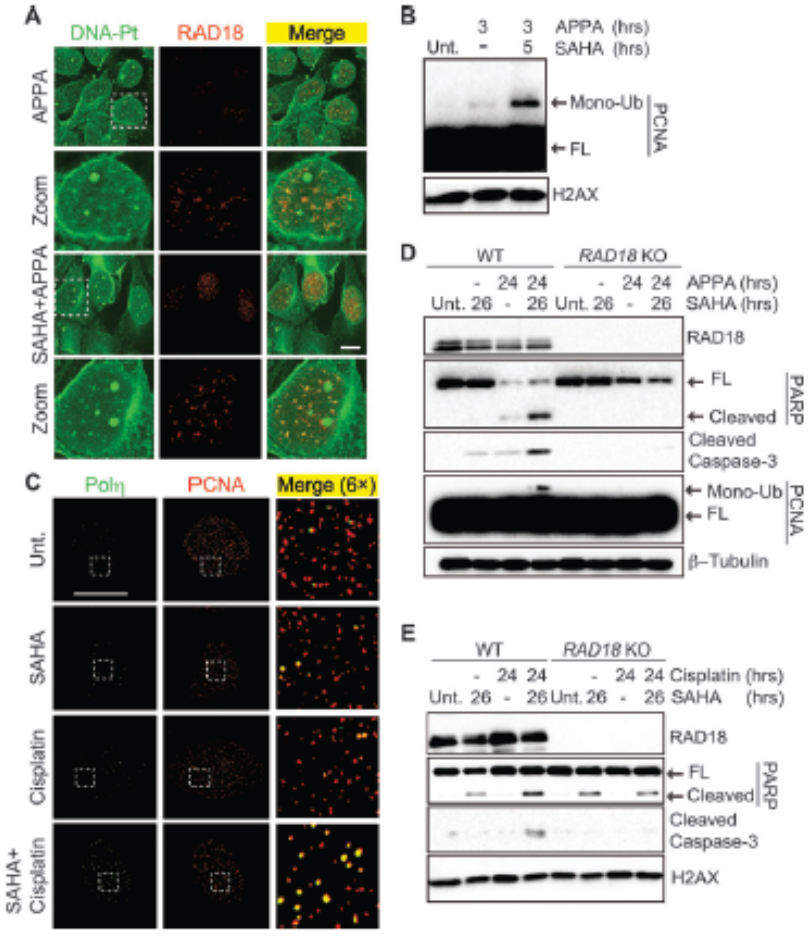

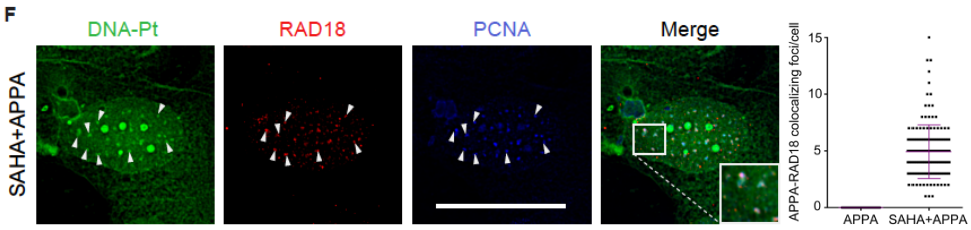

Figure 4.7 Colocalization of labeled DNA-Pt with RAD18 in U2OS cells

A) Cells were treated with APPA (250 mM for 3 h) and SAHA (2.5 mM for 5 h). Zoomed images are 3X. Scale bar, 20 mm. B) Western blot analysis of PCNA mono-ubiquitination in U2OS cells. Cells were treated with APPA (250 mM) and SAHA (2.5 mM) as indicated. C) Focal accumulation of Polη colocalizing with PCNA in U2OS cells. Cells were treated with cisplatin (10 mM for 3 h) and SAHA (2.5 mM for 5 h). Zoomed images are 6X. Scale bar, 20 mm. D) and E) Western blot analysis of apoptotic markers in WT and RAD18 KO HCT-116 cells. Cells were treated with APPA (250 mM), SAHA (2.5 mM) and cisplatin (10 mM) as indicated. (*Panel C was provided by E.Z.*) (F) DNA-Pt colocalize with PCNA and RAD18. Visual detection of DNA-Pt, RAD18 and PCNA by fluorescence microscopy in osteosarcoma U2OS cells. Cells were treated with APPA (250 μM for 3 h) and SAHA (2.5 μM for 5 h) as indicated. Scale bar, 20 μm. Quantification of DNA-Pt and RAD18 colocalizing foci is shown. 50 cells were scored per condition; n = 3. Foci were independently counted by two individuals in double-blinded experiments. Error bars represent mean ± SD. (*Panel C was provided by E.Z.*).

The occurrence of DNA-Pt foci in SAHA-treated cells prompted us to determine whether clusters of lesions could act as physical roadblocks, potentially affecting DNA-templated processes. Strikingly, DNA-Pt colocalized with RAD18, an E3 ubiquitin ligase that mediates mono-ubiquitination of the proliferating cell nuclear antigen PCNA in cells cotreated with SAHA and APPA (Figure 4.7A, F). Moreover, clusters of DNA-Pt also colocalized with PCNA (Figure 4.7F). Cotreatment with SAHA and APPA led to mono-ubiquitination of PCNA (Figure 4.7B), a mark that can promote the recruitment of low-fidelity polymerases involved in TLS, (183) and cells cotreated with SAHA and cisplatin or APPA exhibited increased number of RAD18 foci (Figure 4.8). Furthermore, treatment with SAHA and cisplatin led to the focal accumulation of the TLS polymerase Polη (184) that colocalized with PCNA (Figure 4.7C, 4.9A). Altogether, these data were consistent with the notion that SAHA and cisplatin derivatives activated TLS synergistically.

It is noteworthy that levels of phosphorylated replication protein A (p-RPA) and CHK1 (p-CHK1) were similar in APPA-treated and cotreated cells indicating the absence of additional replication stress (Figure 4.9B). This was in agreement with the notion that HDAC inhibitors promoted a redistribution of DNA-Pt in contrast to a global increase in number of lesions. Remarkably, cotreatment with SAHA and APPA triggered apoptosis signaling as defined by the cleavage of PARP and the activation of caspase 3, in several cancer cell lines including colon carcinoma HCT-116, osteosarcoma U2OS and ovarian carcinoma A2780 cells (Figure 4.7D, 4.10). To evaluate whether RAD18 was directly

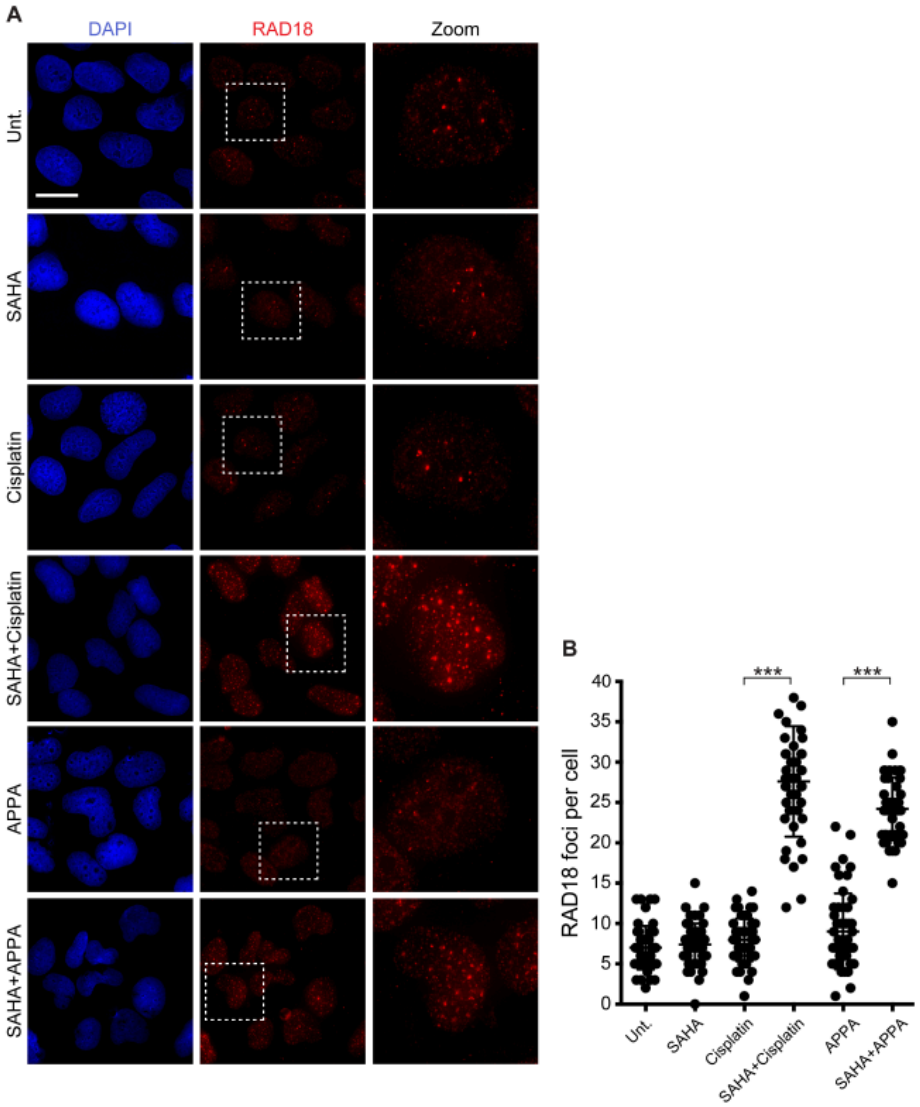

Figure 4.8 SAHA and platinum drugs increase the number of RAD18 foci

Figure 4.8 (A) Visual detection of RAD18 by fluorescence microscopy in osteosarcoma U2OS cells. Cells were treated with cisplatin (10 μM for 3 h), APPA (250 μM for 3 h) and SAHA (2.5 μM for 5 h) as indicated. Zoomed images are 3X. Scale bar, 20 μm. (B) Quantification of A. 25 cells were scored per condition; n = 2; Foci were independently counted by two individuals in double blinded experiments. Error bars represent mean ± SD; ***P < 0.001, Student's t-test. (*Panel B was prepared together with E.Z.*)

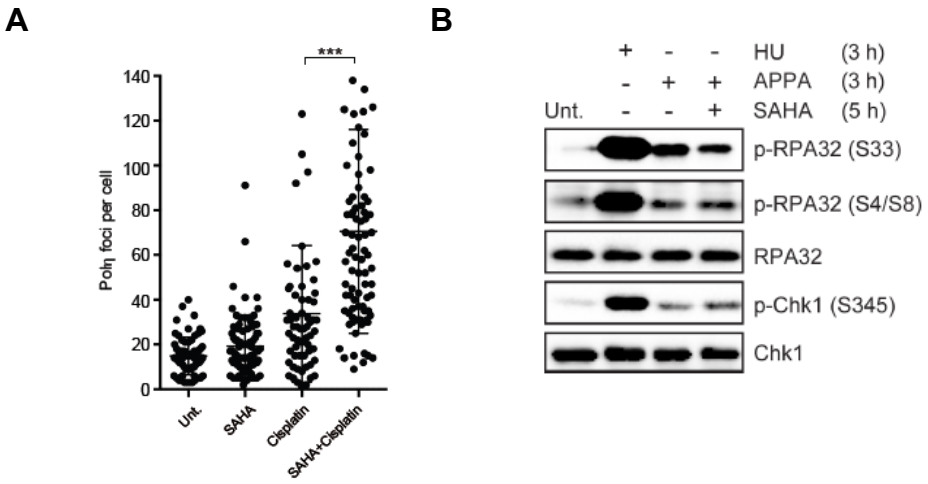

Figure 4.9 Quantification of Polη foci and effect of replication stress

A. U2OS cells were treated as indicated in Figure 4.7C. > 25 Polη positive cells were scored per condition; n = 2; Foci were computationally scored using Fiji software and the Analyze Particles function Error bars represent mean ± SD; ***P < 0.001, Student's t-test. (This figure was prepared together with E.Z.). (B) SAHA and APPA induce similar replication stress compared to APPA. Western blot analysis of osteosarcoma U2OS cells treated as indicated showing markers of replication stress. Cells were treated with HU (2 mM), APPA (250 μM) and SAHA (2.5 μM) as indicated.

involved in apoptotic signaling under these conditions, we performed similar experiments with matched HCT-116 RAD18 knockout (KO) cells. Western blotting indicated that cells devoid of RAD18 did not display PCNA mono-ubiquitination in response to SAHA and APPA cotreatment (Figure 4.7D). Additionally, markers of apoptosis were not detected in HCT-116 RAD18 KO cells even though DNA-Pt foci formed similarly in WT and RAD18 KO cells cotreated with SAHA and APPA (Figure 4.7D, 4.11). These results, along with the RAD18-dependent PCNA mono-ubiquitination implicated RAD18 in promoting apoptosis signaling in response to SAHA and APPA cotreatment. Comparable results were observed in SAHA and cisplatin cotreated WT and RAD18 KO cells,

demonstrating that this response was a common feature of these cisplatin derivatives (Figure 4.7E). Although the induction of apoptosis signaling by RAD18 could be potentially counterintuitive owing to the well-established role of this factor in DNA repair processes and TLS, (164-168) HDAC inhibitors have been shown to re-sensitize cancer cells refractory to cisplatin (109, 110). Therefore, our results suggested that the

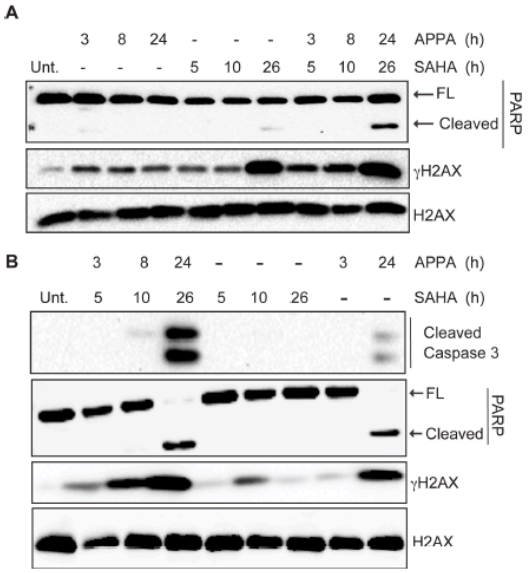

Figure 4.10 SAHA and APPA induce apoptosis signaling

Western blot analysis of cancer cells treated as indicated showing apoptotic markers. (A) Osteosarcoma U2OS cells. (B) Ovarian A2780 cells. Cells were treated with APPA (250 μM) and SAHA (2.5μM) as indicated.

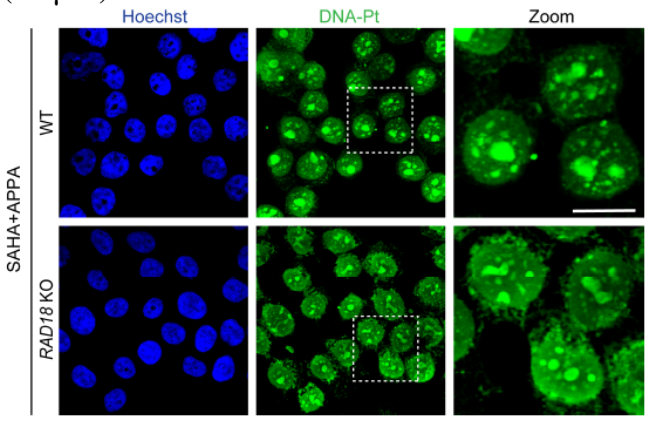

Figure 4.11 RAD18 KO does not prevent the formation of DNA-Pt foci

Figure 4.11 Visual detection of labeled DNA-Pt by fluorescence microscopy in colon carcinoma HCT-116 WT and HCT-116 RAD18 KO cells. Cells were treated with APPA (250 μM for 3 h) and SAHA (2.5 μM for 5 h). Zoomed images are 4X. Scale bar, 10 μm.

higher level of apoptosis signaling observed in RAD18 expressing cells in response to SAHA and cisplatin derivatives is due to the inability of polymerases to efficiently bypass DNA-Pt clusters. For instance, it is possible that chromatin relaxation mediated by SAHA favored the formation of 1,3-GTG intrastrand lesions, which have previously been shown to block TLS polymerases (185, 186). It is also conceivable that HDAC inhibition promoted lesion bypass at the expense of DNA repair (187), thereby leading to detectable clusters of DNA-Pt prone to trigger apoptosis through other mechanisms.

DISCUSSION

Engagement of the replication machinery with DNA-Pt can promote DNA breaks and cell death. However, cells can employ DNA damage tolerance pathways involving specialized low-fidelity polymerases to mono-ubiquitinated PCNA to bypass DNA-Pt (164-168, 188). These processes play a critical role in resistance to Pt drugs (108, 189-193). To overcome these mechanisms, cisplatin derivatives containing bulkier ligands, or combination therapies with other drugs have been identified (194). Here, we have developed a versatile strategy to visualize DNA-Pt in cells with high resolution. This methodology has allowed unbiased identification of small molecule modulators of genome targeting with cisplatin derivatives. In particular, we have discovered that treati--ng cells with the HDAC inhibitor SAHA and APPA resulted in detectable clusters of DNA-Pt and activation of a DNA damage response at these sites (Figure 4.12). While we cannot rule out a putative role of template switching and homologous recombination that could also be mediated by RAD18, the increase of Polh foci in cells cotreated with SAHA and cisplatin is consistent with activation of TLS. Thus, the response observed in these conditions comes in agreement with reports showing that clustered DNA lesions can impair DNA damage response pathways (195-197). This study has uncovered

unanticipated insights into how chromatin alterations can affect the targeting of genomic DNA and sensitization of cancer cells to cisplatin derivatives, establishing a robust exper-

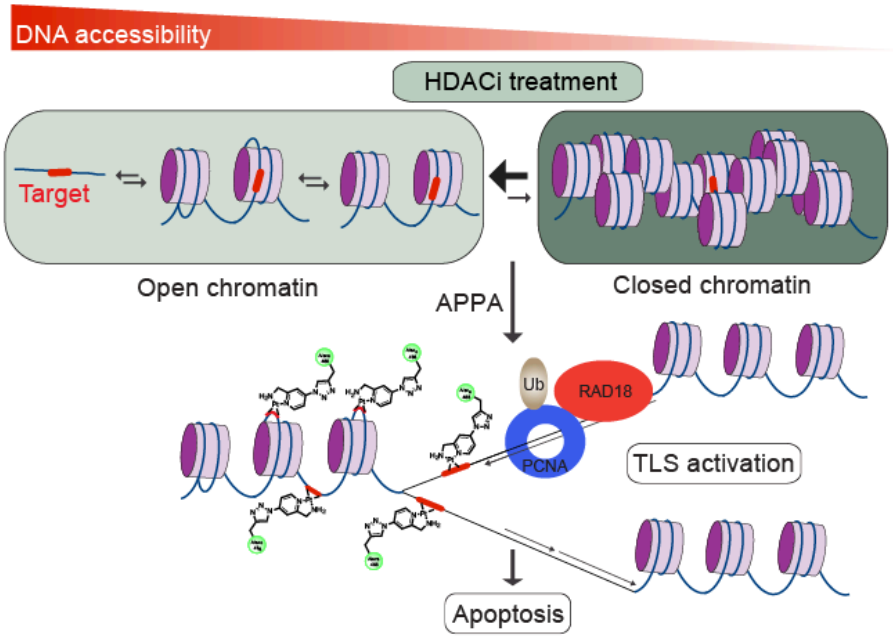

Figure 4.12 Model depicting influence of chromatin on genome targeting

Treatment of cancer cells with cisplatin derivatives and a histone deacetylase inhibitor leads to the production of clusters of platinated DNA lesions that synergistically activate translesion synthesis and apoptosis signaling. These findings provide evidence for a role of chromatin in regulating genome targeting with cisplatin derivatives and associated cellular responses (111).

-imental platform for basic and translational research relying on chromatin-targeting small molecules (98, 102). It is conceivable that these methods could be extended to the study of patient-derived xenografts, a step towards personalized medicine.

CHAPTER 5: FUNCTIONAL ANALYSIS OF TRIM BROMODOMAIN PROTEINS IN THE DNA DAMAGE RESPONSE

INTRODUCTION

Histone posttranslational modifications (PTMs) are an integral part of the DDR machinery in human cells. One such PTM is acetylation and deacetylation of histones which is carried out by the concerted action of HAT (histone acetyltransferase) and HDAC (histone deacetylase) enzymes that recruit to sites of DNA damage to regulate and promote repair by modulating the chromatin states by altering interactions between DNA and histones. A class of proteins containing the conserved bromodomain (BRD) reader domain recognize and bind to acetylated lysine residue on proteins (79). Since BRD containing proteins also read the DDR-specific acetylation marks at sites of DNA damage, these have recently gained immense interest as an area of extensive research in current drug development. For instance, in addition to the existing pool of clinically approved small molecule inhibitors against HATs (eg. Curcumin) and HDACs (eg. Vornistat, Romidepsin) that target acetylation signaling, a wide range of small molecule inhibitors of that target proteins of the BRD family (e.g. BRD4 inhibitor JQ1, I-BET762, etc.) have been clinically approved for targeting DDR and tested for therapeutic applications for various cancer types including leukemia, myeloma, glioma and prostrate cancer (87, 89, 198-202).

Given the increasing potential of diverse screens for discovering novel DDR factors that could be effective anticancer drug targets, our group performed a comprehensive analysis of the dynamics of all the 42 human BRD-containing proteins which revealed that a third of these proteins relocalized upon DNA damage (82), some of which are known to be involved in various aspects of the DDR including reading specific acetylation changes at DNA damage sites (89, 91, 94, 203). They also found that 3 out of the 4 TRIM family BRD containing proteins, namely, TRIM24 (TIF1α), TRIM28 (TIF1β or KAP1) and TRIM33 (TIF1γ), which are generally classified as transcriptional

cofactors and constitute a Transcriptional Intermediary Factor 1 (TIF1) family, are recruited to sites of laser induced DNA damage (82). This is consistent with the previously known involvement of TRIM28 (92, 204) and TRIM33 proteins (205) in the DDR.

In this study we investigated the DDR associated role and regulation of the TRIM BRD proteins, with a primary focus on TRIM24. Our data provides evidence that the multidomain protein TRIM24 binds acetylated chromatin and is involved in the DSB repair process in a TRIM28 and TRIM33 dependent manner. Damage recruitment of TRIM24 is mediated by histone acetylation by the HAT KAT6B to facilitate DNA repair in a PARP and SUV39H1 dependent manner. These functions require the bromodomain, PHD as well as the RING domain of TRIM24 revealing the potential importance of acetylation and ubiquitin signaling in this pathway. These findings will aid in gaining mechanistic insights on how acetylated chromatin and their reader domain containing TRIM-BRD proteins orchestrate DDR pathways, which can facilitate our understanding of how these proteins and pathways can be targeted for therapeutic purposes.

RESULTS

TRIM24 DNA damage recruitment is dependent on its RING, PHD-BRD domains

One of the methods we implemented to study the TRIM DDR factors kinetics and localization upon induced DNA damage in live or fixed cells is by utilizing laser microirradiation followed by visualization of fluorescently tagged TRIM proteins by fluorescence confocal microscopy (Figure 5.1A). The TRIM-BRD proteins including TRIM24 are characterized by the presence of distinct structural features such as an N-terminally located **R**ING domain, two **B**-box zinc-binding domains and a leucine zipper coiled coil (**CC**) domain (also called RBCC family) and a plant homeodomain finger and a bromodomain at the C-terminus (Figure 5.1B). These domains are involved in protein-protein and protein-DNA interactions as characterized in other chromatin associated

proteins and transcription regulators (206, 207). Linked histone PTM reader modules such as tandem PHD finger and bromodomain are found frequently in proteins that interact with histones but not much is known about their mechanisms of action. Although several BRD proteins recruit to the sites of DNA damage, the requirement of BRD for its accumulation at damage site vary widely. For instance, the BRD containing TRIM28 which shares many structural features with TRIM 24 recruits to DNA damage sites independent of BRD since it lacks acetyl-lysine binding (208). In contrast, the plant homeodomain (PHD)-BRD tandem domains of TRIM24 and TRIM33 can read methylated or acetylated histones (209, 210). Therefore we sought to investigate which domains in the newly identified DDR factor TRIM24 are required for its recruitment to damaged chromatin. We first observed that endogenous TRIM24 is rapidly recruited to sites of laser induced DNA damage marked by γH2AX (Figure 5.1C). By testing several ectopically expressed N-terminal GFP tagged TRIM24 constructs, for instance, WT TRIM24, PHD finger binding pocket mutant (C840W), bromodomain binding pocket mutant (F979A/N980A) or both PHD-BRD mutant (C840W/ F979A/N980A) (210) we found that TRIM24 rapidly accumulated to sites of laser induced damage and that TRIM24 required both PHD-BRD for this damage association (Fig 5.1D-E). TRIM24 is also reported to have E3 ubiquitin ligase activity, which modifies the tumor suppressor protein p53 mediated by its RING domain (211). We next tested whether deletion of the RING domain had an affect on its damage recruitment. However, RING deletion led to mislocalization of the nuclear protein TRIM24 in the cytoplasm (Figure 5.1 B, F-G). We therefore generated the catalytic dead RING mutant (C56A/C59A) to test its effect on damage recruitment (Figure 5.1B). TRIM24 RING mutant is localized in the nucleus but has defective recruitment to DNA damage sites (Fig 5.1 H-I). Thus, these results indicate TRIM24 as a new DDR factor reliant on its RING, PHD-BRD domains for binding to damaged chromatin.

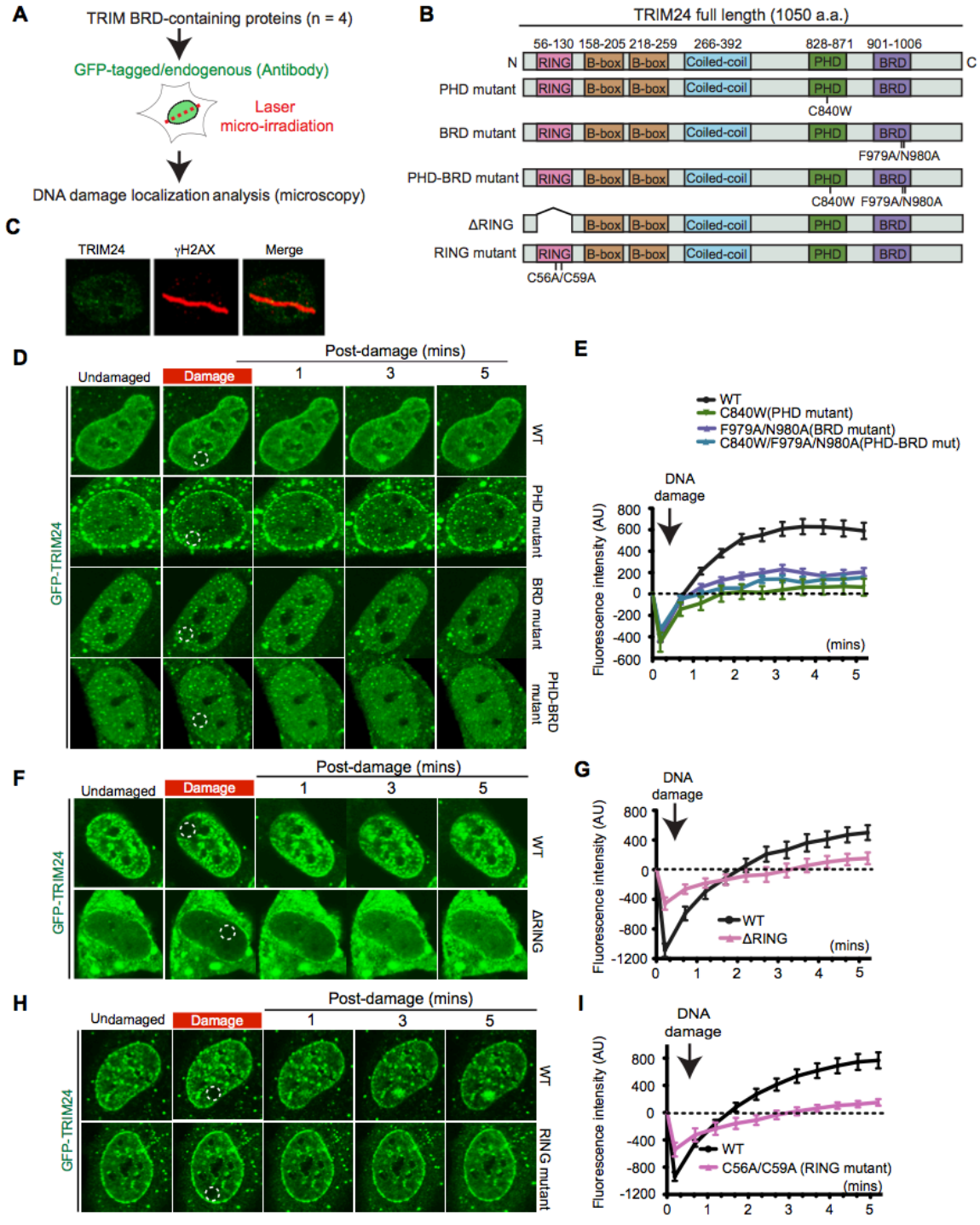

Figure 5.1 TRIM24 recruitment to damage requires its RING, PHD and BRD domains

(Figure 5.1 legend is on the next page)

Figure 5.1 (A) DNA damage localization was studied using laser-induced damage and fluorescence microscopy (B) Domain structure of human BRD protein TRIM24 and generation of various mutants and deletion constructs. (C) Endogenous TRIM24 is recruited to laser induced damage sites and colocalizes with γH2AX. (D-I) TRIM24 damage recruitment requires BRD, PHD and RING domains. White dashed circle represents laser induced DNA damage site (error bars represent S.E.M., n>10).

TRIM24 is involved in maintaining genomic stability

Our initial results showing that TRIM24 associates with damaged chromatin prompted us to further test its role in DNA damage signaling. TRIM24, also known as transcription intermediary factor 1-α (TIF1α), has been identified as a negative regulator of transcription factors including nuclear factors and p53 in human breast cancers (212). High levels of TRIM24 mRNA and overexpression negatively correlate with survival of breast cancer patients (210, 213). TRIM24 is abundantly localized in the nucleus of embryonic stem cells whose expression is downregulated during differentiation and organogenesis (214). A few reports highlight deregulation of TRIM24 expression as well as genomic alterations in human tumors such as papillary thyroid carcinoma and acute myeloid leukemia suggesting its functional significance (215-217). Moreover, the rapid recruitment of endogenous and GFP tagged TRIM24 to γH2AX-marked laser induced DSB sites (Figure 5.1C-D) indicated its role in another chromatin templated process, namely DNA repair. These results corroborated with another method as endogenous TRIM24 increased chromatin association following DSB induction by ionizing radiation (IR) (Figure 5.2A). We then sought to characterize the role of TRIM24 in the DDR in human osteosarcoma U2OS cells by producing a TRIM24 knockout cell line (here referred to as TRIM24 KO and the parental cells (referred to as WT) using the CRISPR-Cas9 technique. The TRIM24 knockout efficiency and specificity was confirmed by Western blotting (Figure 5.2B). TRIM24 knockout cells exhibited similar and comparable cell cycle profiles to parental U2OS cells containing TRIM24 (Figure 5.2C).

Further analysis showed that TRIM24 KO cells are hypersensitive to irradiation (IR), DNA cross-linking agent mitomycin C (MMC), topoisomerase I inhibitor camptothecin (CPT) and replication stress inducing compound hydroxyurea (HU), implicating that the

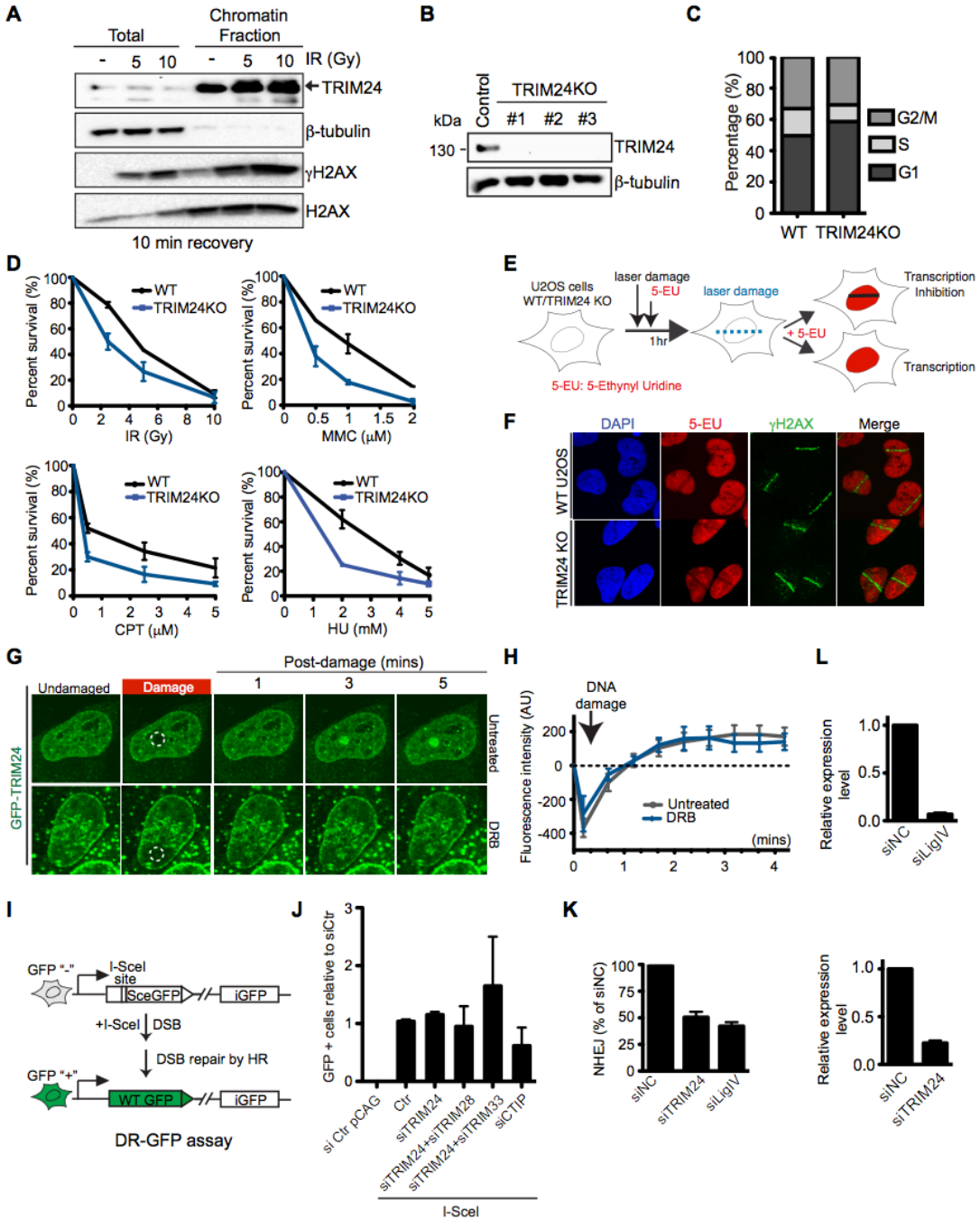

Figure 5.2 TRIM24 participates in DNA damage repair

Figure 5.2 (A) Endogenous TRIM24 accumulated on chromatin following IR induced DNA damage. (B) TRIM24 KO cells verified by western blot. (C) Cell cycle distribution of
WT and TRIM24 KO cells (D) Colony formation assays reveal hypersensitivity of TRIM24 KO cells in response to various DNA damaging agents (error bars indicate S.E.M., n=2) (E) Schematic of EU-labeling assay for nascent transcription analysis post damage (F) TRIM24 is not involved in transcription repression following laser induced DNA damage (G) TRIM24 recruitment is unaffected by DRB treatment (H) Quantification of G (Error bars = S.E.M., n>10) (I) Schematic for DR-GFP assay used to analyze HR efficiency (J) TRIM24 depletion alone or in combination with TRIM28 or TRIM33 does not impair HR-repair. siCtIP was used as a positive control for defective HR (error bars are S.E.M., n=3) (K) Random plasmid integration assay for analyzing NHEJ repair efficiency in WT and TRIM24 depleted U2OS cells. Data was normalized to siControl cells (siNC) and siLigaseIV (NHEJ factor) was used as a positive control for defective NHEJ (error bars, S.E.M., n=2). (L) Efficiency of siTRIM24 and siLigaseIV was assessed by quantitative PCR. *Panel B TRIM24 KO U2OS cell line was made by F.G. Panel E was modified from* (82). *Panel I was adapted from* (82).

DDR and DNA repair pathways are compromised in the absence of TRIM24 (Figure 5.2D). These results confirm similar defects reported previously in cells depleted of TRIM28 and TRIM33 proteins which supports the involvement of these TRIM-BRD proteins in the DDR (94, 205).

Since the TRIM family of proteins are generally classified as transcriptional regulators, this led us to hypothesize that this class of TRIM-BRD protein family members may have a role in transcription repression after DNA damage, a phenomenon known to occur as part of the DDR machinery to avoid conflicts between the transcription and repair pathways which can lead to genome-epigenome instability. We, therefore, tested whether TRIM24 repressed transcription after damage by utilizing EU-labeling technique to monitor nascent transcription (Figure 5.2E) (82). We found that TRIM24 KO cells did not exhibit a reduction in transcription silencing at damaged sites (Figure 5.2 F). As both TRIM28 and TRIM33 have previously been demonstrated to be damage recruited, we assessed their roles in transcription inhibition following DNA damage as well. However, similar results were obtained using TRIM28 KO and TRIM33 KO cells suggesting these DDR factors are not involved in transcription silencing at DNA damage sites (data not shown). We next examined whether TRIM24 required

transcriptionally active chromatin to mediate its recruitment to DNA damage. For these experiments, WT U2OS cells were treated with 5,6-dichlorobenzimidazole riboside (DRB), a chemical compound that inhibits transcription elongation, and TRIM24 damage recruitment was assayed. TRIM24 accumulation at sites of DNA damage was unaffected by DRB treatment indicating that its recruitment was not specific to transcriptionally active chromatin state in particular (Figure 5.2G-H).

To further assess the role of TRIM24 in specific DSB repair pathways, we analyzed the efficiency of HR repair upon depletion of BRD-TRIM proteins using a HR reporter assay. As compared to control cells, there was no remarkable defect in HR efficiency following depletion of TRIM24 only or in cells co-depleted of TRIM24 and TRIM28 or TRIM33 (Figure 5.2I-J). This data is consistent with previous analysis of HR repair where 11 out of the 42 BRD proteins when depleted showed > 30% reduction of HR efficiency (data not shown). Using a random plasmid integration assay for NHEJ repair, we found that TRIM24 depletion impairs NHEJ repair (Figure 5.2K-L). Therefore, these preliminary data provide strong support for the involvement of TRIM24 in the DDR. However, further analyses to complement these findings through alternative experiments are warranted.

TRIM24 regulates MDC1 expression levels in cells

One of the distinctive features of DDR proteins is their discrete localization to the break sites that are microscopically detectable as foci. Since MDC1 (Mediator of DNA damage Checkpoint I) is one of the early DDR factors which promotes binding of DNA damage checkpoint and repair proteins to break sites, we investigated the focal accumulation of MDC1 to laser damage sites in TRIM24 depleted cells. Interestingly, we found a marked reduction in the number of MDC1 foci in TRIM24 KO cells. This defective MDC1 foci formation was also observed upon siRNA-mediated depletion of TRIM24 in U2OS cells. We then checked whether this decrease in MDC1 foci is due to a

reduction in the total levels of MDC1 produced. Both RNA analysis using qPCR and western blot using cell lysates from TRIM24 KO cells revealed a decrease in MDC1 mRNA and protein levels respectively suggesting TRIM24 may play a role in regulating MDC1 expression. The formation of MDC1-γH2AX complex mediates retention of DDR factors in the vicinity of DNA lesions (30). As phosphorylation of histone H2AX (γH2AX) levels strongly increase following DNA damage to provide an initial signaling mechanism in the maintenance of DNA stability we expected to find higher levels of the γH2AX in TRIM24 KO cells exposed to genotoxic stresses. Unexpectedly, when TRIM24 KO and control U2OS cells were irradiated, or treated with HU, accumulation of γH2AX at various time points post-exposure was strongly reduced in the TRIM24 deficient cells as compared to the WT cells indicating these cells have a defect in the DDR pathway (Figure 5.3F-G). The reduced γH2AX may be a downstream effect of the

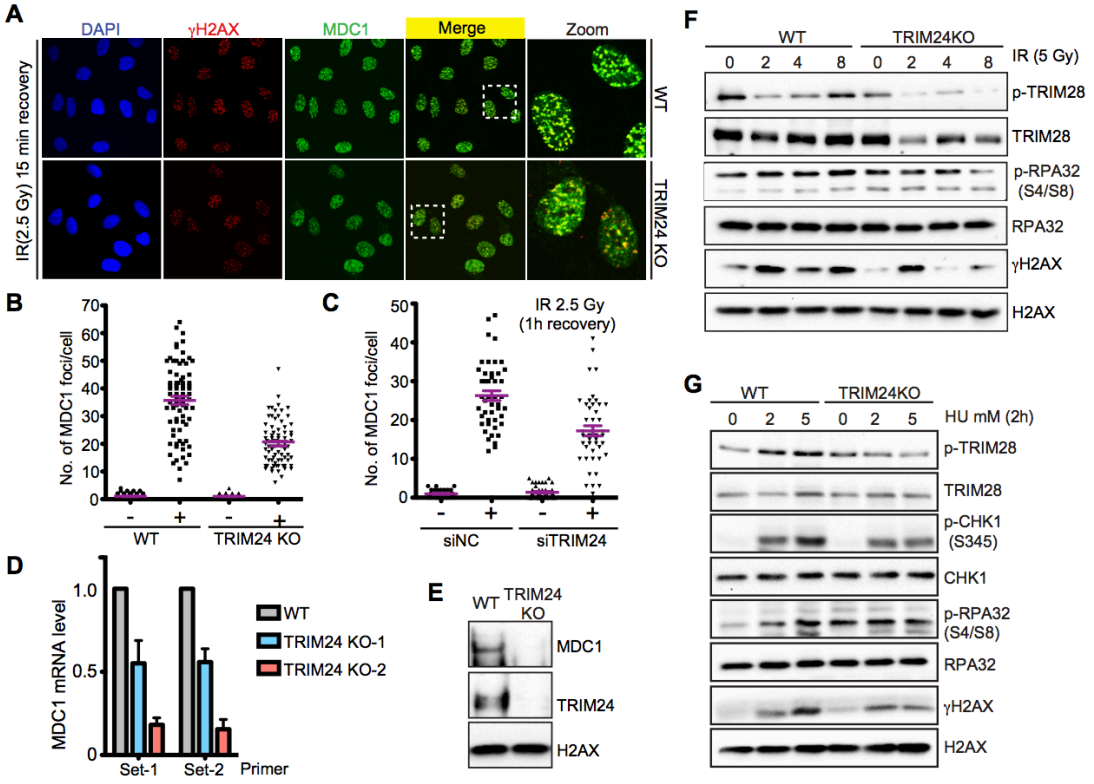

Figure 5.3 TRIM24 regulates MDC1 expression and foci formation

Figure 5.3 (A) MDC1 foci formation is partially defective in TRIM24KO cells upon laser damage treatment but not affected in WT cells (B) Quantification of A (P value <0.0001, n>50). (C) Quantification of MDC1 in siControl and siTRIM24 treated U2OS cells (P value <0.0001, n=85) (D) qPCR analysis for MDC1 mRNA levels using two different primer pairs (error bars = S.E.M., n=2). (E) Western blot for total MDC1 protein levels in WT and TRIM24KO U2OS cells. H2AX is used as a loading control. (F) Western blot for DNA damage signaling markers post IR damage.

decreased MDC1 levels we observed in these cells as some studies implicate that MDC1 masks the C-terminal region of γH2AX against premature dephosphorylation for efficient DNA repair to occur (30, 218). In TRIM24 KO cells, we observed reduced RPA2 phosphorylation and ATM kinase mediated TRIM28 phosphorylation compared with wild- type cells after IR and HU treatment and reduced Chk1 phosphorylation after HU treatment (Figure 5.3F-G). Taken together, our data demonstrated a requirement of TRIM24 in maintaining genome integrity, which further highlights its relevance in the DDR.

TRIM24 recruitment is PARP and ubiquitination dependent

We next sought to determine the mechanisms that control TRIM24 recruitment to DNA lesions. We tested for the contribution of two important enzymes involved in early steps of the DDR: PARP and ATM. As known for a multitude of transcription factors that localize to damaged chromatin in a PARP dependent manner, we observed that recruitment of TRIM24 to damaged sites was partially PARP dependent (Figure 5.4A-B). This is in line with previously reported PARP dependency of TRIM33 recruitment as these three TRIM-BRD proteins are implicated to form heteromeric complexes (205). However, use of the ATM inhibitor KU-55933 revealed that ATM is dispensable for TRIM24 recruitment to damage sites (Figure 5.4C-D). Similar results were obtained for ATM related kinase ATR inhibition (data not shown). We then tested whether regulatory ubiquitination events contributes to accumulation of TRIM24 on the damaged chromatin, we treated cells with the proteasome inhibitor MG132 which triggers translocation of the nuclear pool of ubiquitin-protein conjugates to the cytoplasm and subjected to laser

microirradiation (219). Remarkably, depletion of nuclear ubiquitin abrogated accumulation of TRIM24 recruitment to damaged sites suggesting regulatory ubiquitination is required for promoting recruitment of TRIM24 (Figure 5.4E-F).

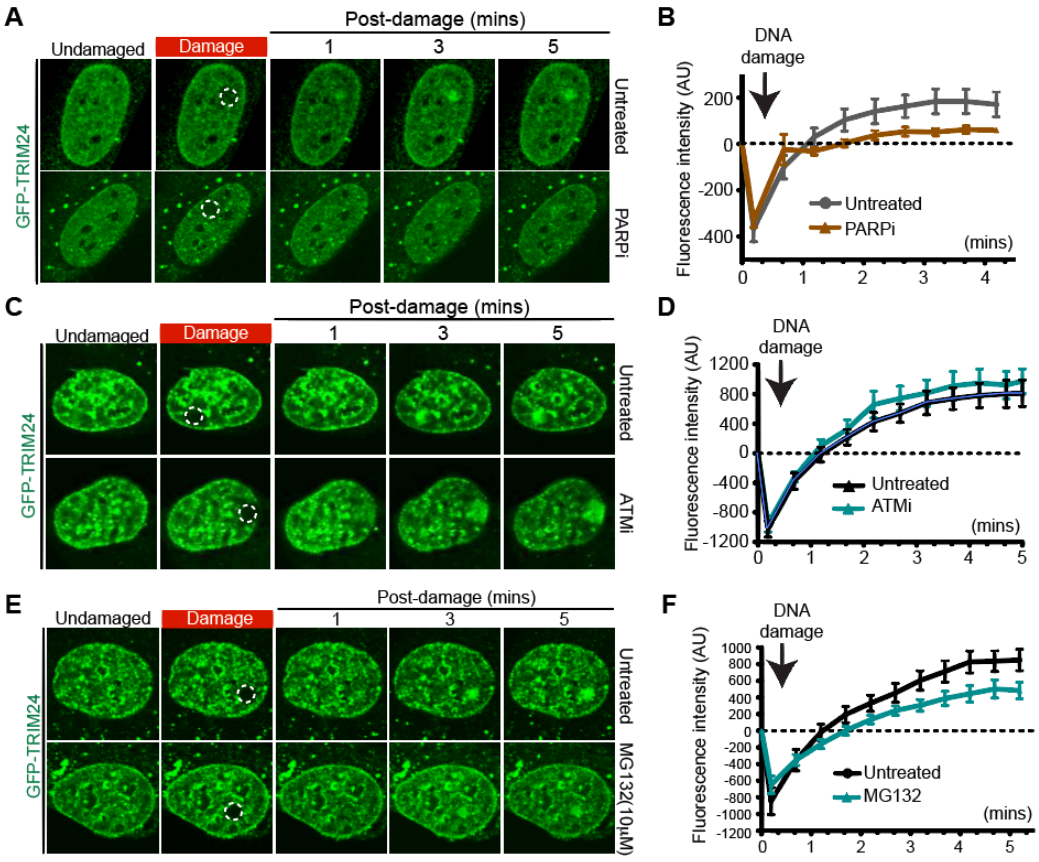

Figure 5.4 Factors affecting TRIM24 recruitment at damage sites

(A and B) Accumulation of GFP-TRIM24 to sites of laser microirradiation is attenuated upon PARPi treatment but not affected by (C and D) ATMi treatment (E and F) Treatment with MG132, proteasome inhibitor reduced TRIM24 DNA damage recruitment.

TRIM24 accumulates to damaged chromatin in a SUV39H1 dependent manner

Although the overall architecture of TIF1 family members including TRIM24, TRIM28, TRIM33 are similar, the extent of their functional similarity in the DDR pathway is not known. One function of TRIM28 is its association with heterochromatin-associated factors HP1α, HP1β and HP1γ to promote the silencing of euchromatic genes

(220). In response to DNA damage, ATM kinase phosphorylates many histone and non-histone proteins including the transcriptional regulator TRIM28 (94, 221-223). Phosphorylated TRIM28 promotes HR repair of DSBs in heterochromatic regions by chromatin decompaction, which allows the repair factors to access damaged sites (92, 224). This is achieved by the formation of TRIM28-HP1-SUV39H1 complex, which rapidly recruits to damaged chromatin. H3K9 trimethylation is mediated by the methyltransferase SUV39H1 to promote additional binding of the TRIM28-HP1-SUV39H1 repressive complex at DSB sites through interaction of H3K9me3 with HP1 chromodomain, which facilitates the formation of heterochromatin and gene repression (225, 226). H3K9me3 activates the HAT TIP60, which then acetylates ATM and H4 (212). This acetylated ATM activates the ATM kinase activity to promote DSB repair (227). siRNA-mediated depletion of TRIM28 blocked the recruitment of SUV39H1 to DSBs and vice versa. A high throughput histone peptide pull-down interaction screening platform to map the chromatin readers of the key activating and repressive histone modifications that serve as binding platform for the chromatin-associated proteins revealed that all the three TRIM-BRD proteins are specific binders of the repressive mark H3K9me3 which is mediated by SUV39H1 (228). These studies support our premise to interrogate whether the TRIM-BRD proteins work in collaboration to orchestrate the DDR and therefore we examined the affect of SUV39H1 knockdown on TRIM24 recruitment. Consistent with previous findings (212), both TRIM24 and TRIM28 recruitment to DSBs required SUV39H1 (Figure 5.5A-F). However, using the knockout cells that we generated for TRIM24 and TRIM28, we observed no defect in SUV39H1 recruitment upon laser damage indicating SUV39H1 is an upstream factor that regulates the recruitment of TRIM-BRD proteins to the damaged chromatin (Figure 5.5D-E).

TRIM24 recognizes H3K23Ac catalyzed by KAT6B for damage recruitment

Biophysical experiments by Tsai et al. showed that TRIM24 recognizes dual histone modifications, specifically, unmethylated H3K4 (H3K4me0) and the non-canonical histone mark H3K23Ac through its tandem PHD-BRD domain (210). In addition, immunohistochemical analysis of breast carcinoma samples showed that the levels of

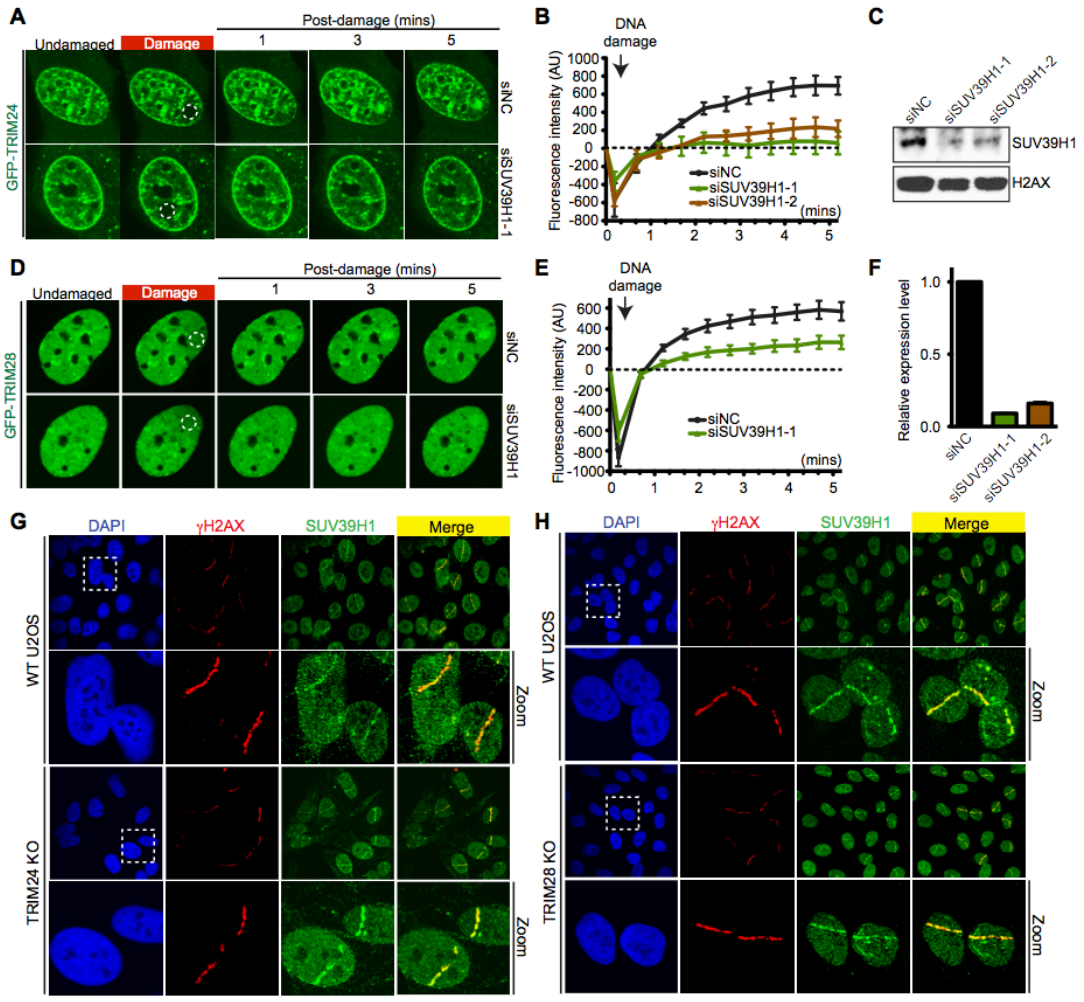

Figure 5.5 SUV39H1 regulates recruitment of BRD-TRIM proteins

(A) U2OS cells were transfected with control siNC or siRNA to SUV39H1. Knockdown of SUV39H1 impairs TRIM24 to DSBs (B) Quantification of A (Error bars = S.E.M., n>10) (C and F) Western blot and mRNA levels showing siSUV39H1 efficiency (D and E) Depletion of SUV39H1 reduces TRIM28 recruitment to laser damage (Error bars = S.E.M., n>10) (G and H) Conversely, SUV39H1 recruitment is not affected in TRIM24 or TRIM28 depleted cells.

TRIM24 expression positively correlated with H3K23Ac levels (229). A similar PHD-BRD multivalent chromatin reader module was discovered in TRIM33 that recognizes histone H3 tail that is unmethylated at K4 and R2 and acetylated at two consecutive lysines, for instance, K18 and K23 (209). The histone mark H3K23Ac is catalyzed by the tumor suppressor HAT KAT6B (230). In order to assess whether these epigenetic marks are crucial for damage recruitment of the TRIM proteins, we depleted the cells of the HAT KAT6B and quantified their accumulation to damage sites. Notably, we observed a marked decrease in TRIM24 and TRIM33 accumulation upon KAT6B depletion (Figure 5.6A-D). However, this dependency on KAT6B mediated H3K23Ac was not observed

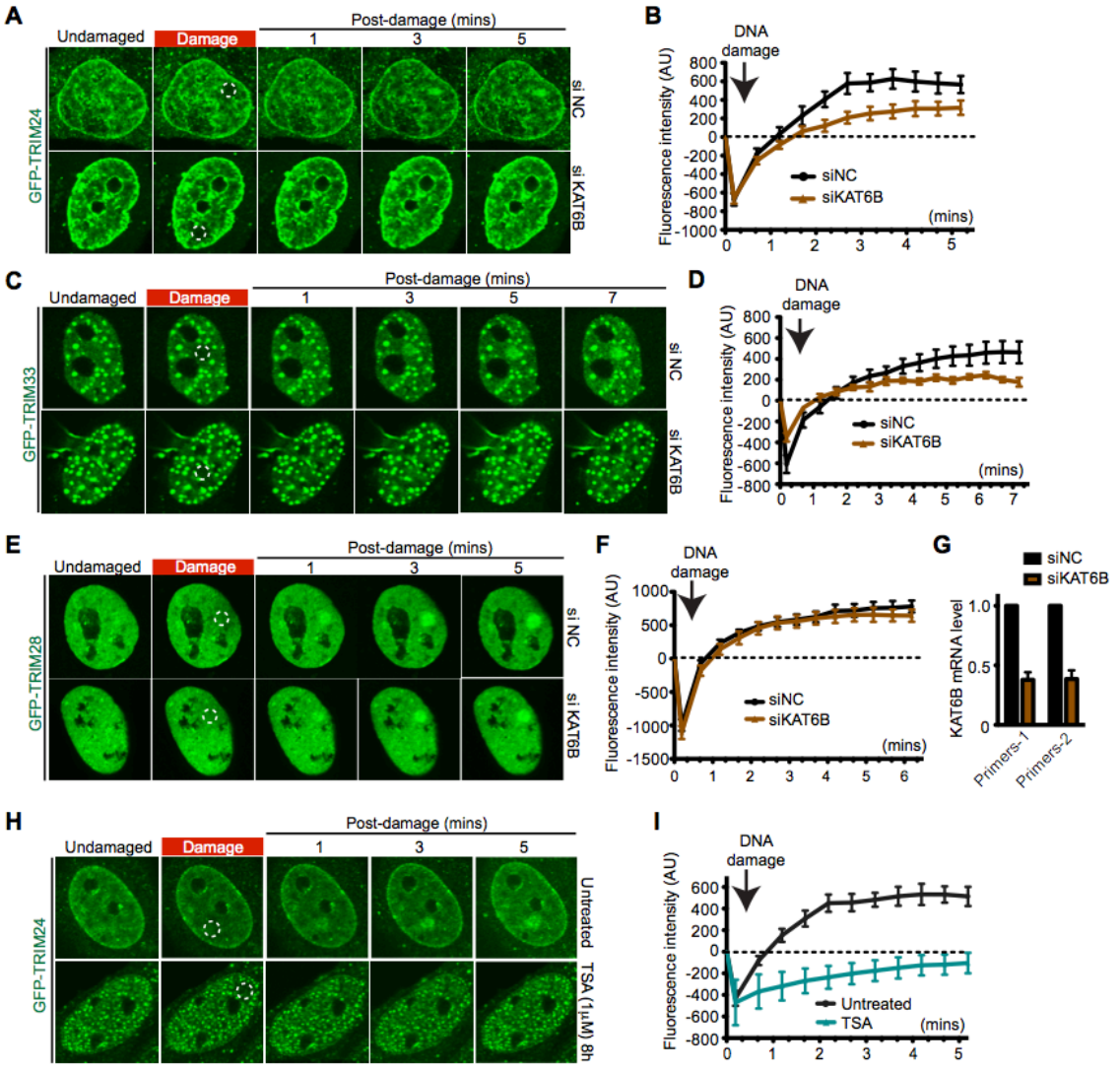

Figure 5.6 TRIM24 recognizes KAT6B mediated H3K23Ac mark for damage accumulation

Figure 5.6 (A and B) Knockdown of KAT6B HAT reduces the recruitment of TRIM24 and (C and D) TRIM33 whereas (E and F) TRIM28 recruitment is not affected by depletion of KAT6B. (G) Quantification of qPCR showing efficient knockdown of KAT6B. (H and I) Cells treated with HDACi, TrichostatinA has impaired TRIM24 accumulation to sites of damage.

for TRIM28 recruitment to DNA lesions which is in line with previously identified non-BRD reader module recognition for TRIM28 to accumulate to damage sites (Figure 5.6E-G). In striking contrast to the above data for TRIM24 and TRIM33 recruitment via KAT6B mediated acetylation recognition, chemical inhibition of HDACs (histone deacetylases) using Trichostatin A (TSA) completely abrogated TRIM24 accumulation at sites of laser induced damage (Figure 5.6H-I). This might be due to a drastic increase in the global acetylation levels on chromatin as a result of TSA treatment, which alters the TRIM-BRD association with damaged chromatin. Taken together, these data suggest that the recruitment of TRIM-BRD proteins to DNA damage sites is context specific and influenced by the damage site associated microenvironment.

The TRIM-BRD proteins functionally interact to promote the DDR

Several non-DNA damage repair studies have shown that TRIM24, TRIM28 and TRIM33 have distinct functions (5-14). This is substantiated by the observation that TRIM28 and TRIM33 null mice are embryonic lethal at E8.5 and E9.5, respectively (15,16) whereas TRIM24 germline knockout mice are viable. Herquel *et al*. showed that HeLa cells overexpressing HA-tagged TRIM24 co-immunoprecipated TRIM28 and TRIM33 as interacting partners along with HDACs 1 and 2 and the HP1 proteins (17). In order to examine whether these 3 TRIM proteins interact functionally in the context of DNA damage to promote DDR signaling and repair, we generated TRIM28 KO and TRIM33 KO U2OS cell lines (Figure 5.7A-B). Over expressing GFP-TRIM24 in both TRIM28 KO and TRIM33 KO cells resulted in defective TRIM24 accumulation at laser damage sites (Figure 5.7C-D). Besides, TRIM28 recruitment was significantly reduced in the TRIM24 KO cells (Figure 5.7E-F). Our co-IP analysis using SFB-tagged TRIM33 stably expressing 293T cells copurified TRIM24 and lower levels of TRIM28 (Figure 5.7G), similar to previous reports where TRIM24 was found to be stoichiometric with TRIM33 in the complex but less abundant than the TRIM24, TRIM28 and TRIM33 tri-

member complex (17). We then sought to identify whether the interaction between TRIM24 and TRIM28 is mediated by TRIM33. To this end, we performed endogenous IP using the WT and TRIM KO cell lines. TRIM24 and TRIM28 interaction was not dep-

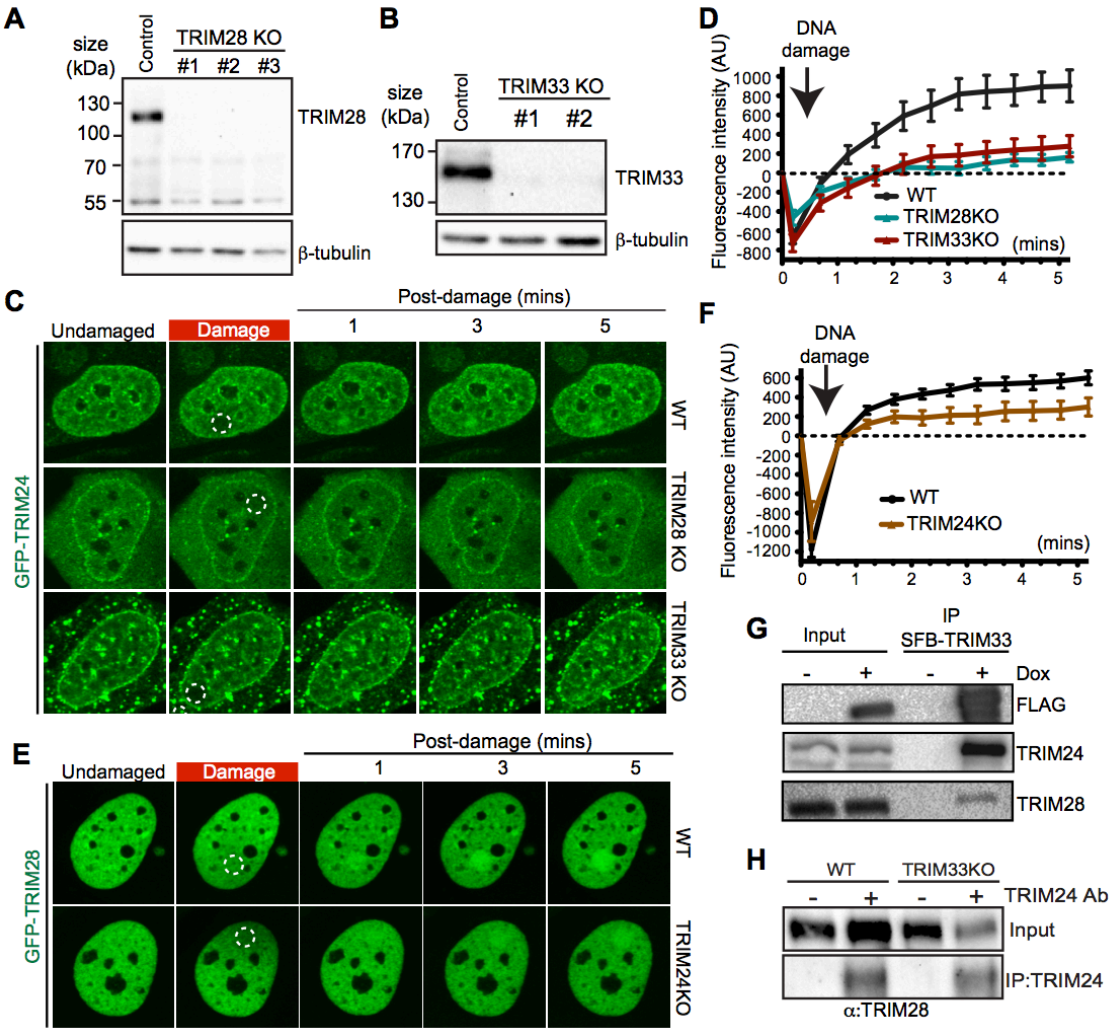

Figure 5.7 TRIM24 damage accumulation is TRIM28 and TRIM33 dependent

(A and B) Western Blot to confirm TRIM28 and TRIM33 KO U2OS cell lines generated using CRISPR-Cas9 respectively. (C and D) TRIM24 accumulation at damage sites is impaired in TRIM28 KO and TRIM33 KO cells (Error bars = SEM, n>10). (E and F) TRIM28 recruitment is reduced in TRIM28 KO cells (Error bars = SEM, n>10). (G) Over expression of SFB-TRIM33 and affinity purification to validate that the 3 BRD-TRIM proteins interact with each other. (H) Endogenous TRIM24 interacts with TRIM28. Western blot analysis of co-IP with TRIM24 antibody from WT and TRIM33KO U2OS cells. (*Panel A-B, TRIM28 and TRIM33 KO U2OS cell lines were generated by F.G. Panel G was provided by P.C. and panel H was prepared with assistance from M.K.)*

-endent on the presence of TRIM33 as revealed by equal levels of TRIM28 co-purified from WT and TRIM33 KO U2OS cells (Figure 5.7H). Thus, we ascertained that the interaction between TRIM24 and TRIM28 was not mediated via TRIM33 and this interaction could be either direct or through other common partner proteins such as HP1. Sequential immunoprecipitations using TRIM24 KO and TRIM28 KO cells are warranted to test whether TRIM24 is required for TRIM28-TRIM33 interaction and TRIM28 requirement for TRIM24-TRIM33 interaction respectively. Further investigations are required to test whether the affinity between the individual TRIM proteins increases upon damage induction. These results implicate that the 3 TRIM-BRD proteins function as a complex and might act interdependently in the DDR.

MCM complex interacts specifically with TRIM24

To better understand the molecular function of TRIM24 in the DDR, we sought to identify its interacting protein partners. Expression vectors containing N'-SFB (S protein, 2X flag, biotin) tagged TRIM-BRD genes were generated for TRIM-BRD proteins and stably expressed in HEK293T cells. Pull down of TRIM24, TRIM28 or TRIM33 interacting proteins was carried out by a previously described two-step tandem affinity purification (TAP) method using streptavidin and S-protein beads (82) and purification efficiency was checked by silver stain (Figure 5.8A). These samples were then analyzed by mass spectrometry (MS) to identify the specific interactors of each of the TRIM-BRD proteins. Consistent with our identification of the TRIM-BRDs as chromatin interacting proteins, we identified all the core histones, H2AX, macroH2A in our MS results for BRD-TRIMs. We shortlisted ~15 proteins as potential TRIM24 interactors using the CRAPome database (a contaminant repository for affinity purification mass spectrometry data) to filter out common contaminants of MS analysis (Figure 5.8B). Consistent with previous findings and our analysis of TRIM proteins interactions and complex formation among TRIM24, TRIM28 and TRIM33, each of these proteins peptides appeared in the MS results for one another. Interestingly, we observed that, except for MCM5, peptides

corresponding to members of the hexameric MCM complex (e.g. MCM2, MCM3, MCM4, MCM6 and MCM7) were present as interactors of TRIM24 exclusively but not found in the TRIM28 or TRIM33 interactome. The eukaryotic MCM (minichromosome maintenance complex) proteins form a heterohexameric ring consisting of MCM2-MCM7 that possesses DNA helicase activity and is activated during replication to unwind DNA and recruit DNA polymerases at the replication fork (231-233). In addition to its role in forming the pre-replication complex, the MCM complex has been implicated to be involved in DNA repair (234-237). The subunits MCM3 and MCM7 have been identified substrates for checkpoint kinases, ATM and ATR (238). A study showed that excess MCM complex bound to the chromatin safeguards the genome integrity under replication stress (239). A proteomics screen to identify proteins interacting with the MCM complex following etoposide induced DNA damage revealed ASF1 as an MCM2 interactor, the levels of which increased upon DNA damage (235). Based on our MS results, we validated the MCM complex interaction with TRIM24 using GFP pull down experiments from cells over expressing GFP-tagged MCM4 (Figure 5.8C). In order to rule out the over expression effects, we confirmed these interactions with endogenous TRIM24, TRIM28, TRIM33, MCM2 and MCM4 from HEK293T cells (Figure 5.8D). In addition, we validated MCM complex interaction with reciprocal immunoprecipitation of endogenous TRIM24 (Figure 5.8E). Future work is required to map these interactions within the TRIM-BRD and MCM complex. It will be interesting to analyze whether the replicative helicase MCM complex cooperates with TRIM24 to promote signaling and repair of collapsed replication forks.

FACT complex interacts with TRIM24 and TRIM33

Our MS analysis also revealed interactions between the TRIM-BRD proteins and the histone chaperone complex FACT (Facilitates Chromatin Transcription) which is composed of the subunits, SUPT16H and SSRP1(240). We validated this interaction

using streptavidin immunoprecipitation from inducible HEK293T cells stably expressing SFB-TRIM33 (Figure 5.8F). Besides, our preliminary results indicate that SSRP1 is recruited to sites of DNA damage in WT U2OS cells but not in the TRIM33 or TRIM24

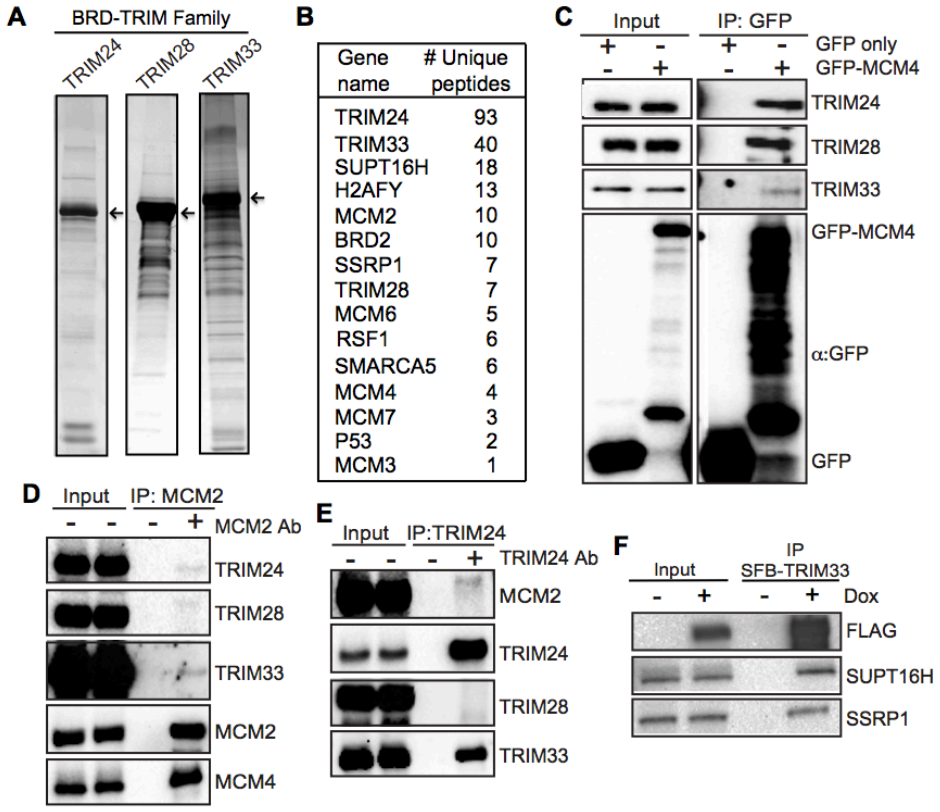

Figure 5.8 TRIM24 interacts with the MCM and FACT complex

(A) Identification of BRD-TRIM proteins interacting factors by mass spectrometry. (B) List of top proteins identified as TRIM24 interactors in MS analysis from three experiments. (C) MCM4 interacts with BRD-TRIM proteins, TRIM24, TRIM28 and TRIM33 directly or indirectly as analyzed by co-IP from HEK293T cells overexpressing GFP-MCM4. (D) Endogenous TRIM24 interacts with MCM2 and MCM4, core components of the MCM-complex. (E) WB analysis of endogenous reciprocal co-IPs with TRIM24 antibody from HEK293T cells. (F) TRIM33 interacts with FACT complex subunits, SSRP1 and SUPT16H (*Panel A and F was provided by P.C.)*

KO cells (data not shown). It is conceivable that TRIM24 and TRIM33 are the upstream factors that regulate the accumulation of FACT complex to damaged chromatin. As discussed earlier, we validated that TRIM24 interacts with TRIM33 and that both TRIM24 and TRIM33 interact with the FACT and the MCM complex. We also

confirmed that SSRP1, a FACT complex component, reciprocally interacts with TRIM-BRD proteins and the MCM complex. Previous data indicate that functional association of FACT-MCM complexes on DNA replication origins promotes replication initiation and DNA unwinding (241, 242). The functional basis of TRIM-BRD proteins interaction with the FACT and MCM complexes requires further investigation but it is possible that this interaction facilitates a very site-specific recruitment of the TRIM-BRD complex to active replication forks. Additional studies are required to evaluate how these complexes in association with TRIM-BRD proteins is involved in orchestrating their DDR function. It will be important to analyze any changes in abundance of the FACT and MCM components in the TRIM KO cell lines or changes in their interaction ability upon DNA damage to assess whether TRIMs are involved in regulating turnover of either complex. Besides, a host of zinc finger family proteins were also identified in the MS data some of which overlap among the three TRIM-BRD proteins. To better characterize the involvement of these factors in mediating the DDR functions of TRIMs, it is important to examine the effects on TRIM recruitment to DNA damage upon depletion of each putative TRIM-BRD interacting protein including MCM complex components and subunits of FACT complex.

DISCUSSION

Our work provides, for the first time, some preliminary insights into the role and regulation of TRIM24 in the DDR. Here we uncover that similar to previously known functions of TRIM28 and TRIM33 in promoting DNA repair, TRIM24 is a novel DDR factor. Specifically we have shown that TRIM24 accumulates at DNA damage sites and requires its PHD-BRD as well as the RING domain. Based on previous biochemical and structural studies indicating TRIM24 as a bivalent chromatin reader that recognizes unmodified H3K4 and H3K23Ac mediated by histone acetylation by the HAT KAT6B, we found that both TRIM24 and TRIM33 DNA damage recruitment is dependent on this

histone signature. This finding reveals the importance of acetylation signaling in the TRIM-BRD mediated repair pathway. Since this TIF1 family of proteins is categorized as transcription regulators, we first analyzed whether the TRIM-BRD protein family members were involved in transcription repression post DNA damage in order to avoid conflicts between the transcription and repair pathways and thereby promote the DDR. Strikingly, loss of TRIM24 did not reduce transcriptional silencing at damage sites indicating its involvement in other pathways. Further analysis revealed that TRIM24 deficiency resulted in defective NHEJ repair efficiency, increased sensitivities to different damaging agents and had lower levels of the master regulator protein MDC1. Our work highlights how the newly identified TRIM24-dependent damaged chromatin recognition pathway is regulated to promote DNA repair.

Future work is required to explore and comprehend mechanistically how these TRIM proteins orchestrate the DDR pathway in conjunction with the potential common and specific interactors of the TRIM-BRD proteins including MCM complex, FACT complex and Zn-finger proteins identified through proteomic analysis. Moreover, RNA-seq and ChIP-seq analyses could reveal how TRIM-BRDs are involved in regulation of genes that are essential for cancer cell survival. ChIP-seq will allow to map the TRIM-BRD occupancy throughout the genome. Nevertheless, it is important to analyze whether mutations in these three TRIM-BRD proteins that have been identified in cancer effect DNA damage repair by HR or NHEJ, which could point towards therapeutic opportunities. Detailed genetic and biochemical analysis to clarify functional redundancy between TRIM proteins would improve our understanding of the role of TRIM proteins in DDR. All these studies would provide a framework for elucidating chromatin-based DNA damage responses involving TRIM-BRD proteins that promote DNA repair and the DDR. It remains to be addressed whether the TRIM-BRD proteins act as key chromatin modulators of the DDR via a novel yet unidentified pathway to orchestrate the DDR in a

context specific damage associated microenvironment, for instance, active replication forks or heterochromatic DSB repair as implicated for TRIM28 (243).

Our analysis of TRIM-BRD multi-protein complex as putative DDR factors has important implications for targeted anticancer therapy. Given the fast-paced development and clinical success of small molecule inhibitors of BET family of bromodomain proteins and increased application of DDR proteins targeted therapeutics, a comprehensive analysis of TRIM-BRD proteins in the DDR is potentially relevant to cancer. Two different groups have developed potent and selective small molecule inhibitors for TRIM24 BRD and BRPF1 family of proteins (244, 245), which can aid in further elucidating the DDR roles of TRIM24 and thereby utilize these inhibitors to target TRIM-BRD for anticancer therapy. Thus, knowledge gained from this study will be a stepping-stone towards therapeutic strategies for targeting TRIM-BRD proteins as mediators of DDR signaling.

CHAPTER 6: DISCUSSION

CHROMATIN AND THE DNA DAMAGE RESPONSE

Chromatin and the DDR participate in promoting cellular responses that are crucial for repairing damaged DNA across the chromatin landscape to ensure genome stability and cellular homeostasis. My thesis dissertation has contributed to this field in several ways. The first part of my thesis dissertation project identified the chromatin domain, the nucleosome acidic patch, as a critical region that modulates H2A and H2AX ubiquitinations that regulates DDR signaling. Secondly, altered chromatin dynamics occurring in diseases including cancer is known to influence DNA repair. This has been especially well established in cancer treatments as DNA damaging agents are used as frontline therapies to treat this disease and chromatin-based mechanisms have been identified as mediators of these responses. For example, cancer cells resistant to DNA damaging agents including cisplatin can be reversed to a drug-sensitive state through the reprogramming of chromatin by using the epigenetic drug that inhibits histone deacetylases (109). To gain mechanistic insights into how these events occur, the second part of my thesis focused on delineating how the chromatin modulator, SAHA (HDACi) in combination with the platinum drug influences genome targeting. These and other studies provide evidence that epigenetic drugs are promising anticancer agents and that

Portions of this chapter have been published as follows:

- *Poonam Agarwal and Kyle M. Miller (2016) The nucleosome: orchestrating DNA damage signaling and repair within chromatin. Biochemistry and Cell Biology 94: 1–15. (Contributions: P.A. and K.M.M. wrote the manuscript together.)*
- *Poonam Agarwal and Kyle. M. Miller (2016) Book chapter: Chromatin Dynamics and DNA repair in Chromatin Regulation and Dynamics, Elsevier (Contributions: P.A. and K.M.M. wrote the manuscript together).*

drugs that alter chromatin dynamics have the potential to be combined with DNA damaging agents as novel therapeutic strategies to kill cancer cells (2, 97-99, 102, 104). Lastly, I have been focusing on characterizing the functions of TRIM-BRD proteins, which have currently gained importance as novel DDR factors.

NUCLEOSOME ACIDIC PATCH

Although our studies identified the nucleosome acidic patch as a key nucleosome feature that is utilized by the DDR factors RNF168 and RING1B/BMI1 to promote DNA damage signaling and repair, there are still numerous unanswered questions remaining about this chromatin region that need to be investigated. Several E3 ubiquitin ligases and other DDR factors promote the recruitment of RNF168 to damage sites. For example, RNF8 recruitment generates K-63-linked ubiquitin chains on H1 linker histones that are recognized by RNF168 via its UDM1 module, thus recruiting RNF168 to DSBs (39). Once on chromatin, RNF168 ubiquitinates histones, including H2A and H2AX on K13/15, which promotes the binding of the DDR factor 53BP1 to facilitate DSB repair by NHEJ (40, 41, 59, 62) (Figure 6.1A).

RING1B/BMI1 catalyzes monoubiquitination of H2A/H2AX on the C-terminal lysines, K118 and K119 (129, 246) (Figure 6.1B). It is part of the Polycomb repressive complex1 (PRC1) that compacts chromatin to promote transcriptional repression at various gene loci (129, 247, 248). In the DDR, several studies have shown that RING1B/BMI1 are recruited to sites of DNA damage (61, 123, 124, 249, 250). We and another group showed that the nucleosome acidic patch mediates the activity of the E3 ligase complex, RING1B/BMI1 (52, 142) (Figure 6.1B). Like RNF168, expression of the LANA (latency-associated nuclear antigen), a chromatin-interacting Kaposi's sarcoma-associated herpes virus (KSHV) peptide in cells or addition of LANA in biochemical peptide inhibition reactions interferes with these Ub reactions resulting in reduced H2A/H2AX ubiquitination by RING1B/BMI1.

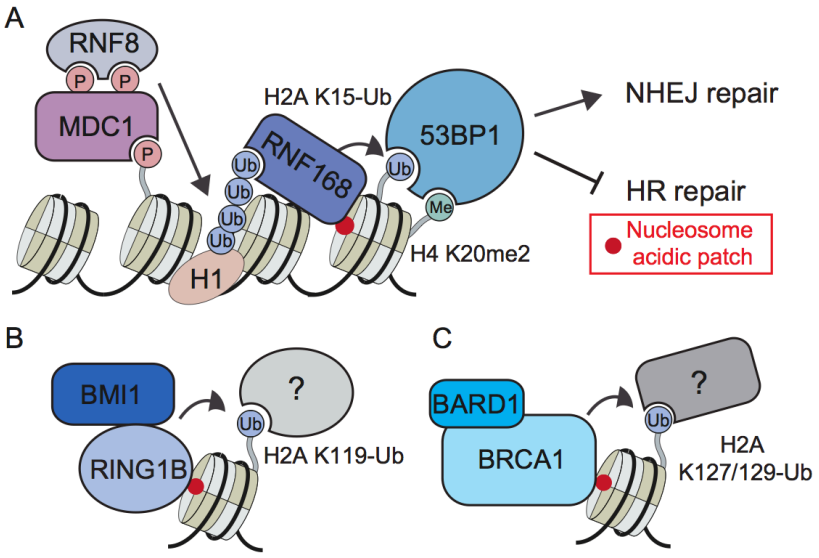

Figure 6.1 The nucleosome acidic patch mediates multiple Ubs on H2A/X

These Ub reactions are catalyzed by different E3 ligases for DDR signaling (A) RNF168 (B) BMI1/RING1B and (C) BRCA1(38).

The use of the acidic patch to mediate DDR-dependent E3 Ub ligase activities does not seem to be limited to RNF168 and RING1B/BMI1. Another E3 Ub ligase involved in the DDR, BRCA1 (251), has recently been shown to ubiquitinate nucleosomal H2A K127/129 in an acidic patch-dependent reaction (252) (Figure 6.1C). The functional significance of H2A ubiquitination in the DDR by BRCA1 is still unclear. Previous work on mouse models of cancer has proposed that the E3 ligase activity of BRCA1 is dispensable for its tumor suppressive activity (253). Similar to RING1B/BMI1 heterodimeric complex, the BRCA1/BARD1 forms a heterodimer to form a RING-type E3 ligase (254). Structural analysis and sequence alignment shows that the nucleosome-interacting region of RING1B (including the lysine-arginine motif) and the corresponding region in BRCA1 are evolutionarily conserved. Furthermore, mutational disruption of this motif on BRCA1 or the nucleosome acidic patch eliminates H2A ubiquitylation by BRCA1 *in vitro* (142). Thus, like RNF168 and RING1B, BRCA1 appears to utilize the acidic patch on the nucleosome to promote its activity. Despite the large number of lysine

residues in the nucleosome, only a select few are ubiquitinated by RNF168, RING1B/BMI1, and BRCA1 E3 ubiquitin ligases and function within DSB signaling and repair.

It is remarkable that all of these ubiquitination sites and their targeting enzymes require the nucleosome acidic patch. This raises an important question of how these enzymes are regulated at the level of the nucleosome to organize and promote the requisite activity at any given chromatin location without interference from a competing pathway. The nucleosome acidic patch on H2A/H2AX must therefore serve as a signaling hub that is able to accommodate and integrate a host of signals from different pathways that coordinate the chromatin activities that are essential for DSB signaling and repair (50, 52, 53, 255). Although structural and biochemical studies have provided key insights into enzyme-nucleosome interactions, additional experiments in cells are necessary to better understand mechanistically how the nucleosome acidic patch interacting network is set-up and regulated. For example, many of these pathways are implicated in diseases, including cancer (256-259). It will be interesting to know whether an imbalance of these, or other acidic patch interacting proteins, could negatively impact the function of other pathways reliant on this nucleosome surface motif. For example, cells infected with viruses or cancer cells that express high levels of acidic patch interacting proteins might impede the interactions of other factors that use the same interaction platform resulting in perturbation of these pathways. As more and more acidic patch interacting factors are identified, answers to these questions will be important to rationalize how chromatin functions to integrate these signals to promote genome stability and cellular homeostasis.

NUCLEOSOME ACIDIC PATCH INTERACTING FACTORS

In contrast to the prominent negatively charged surfaces of the NCP, the histone tails contain many arginine and lysine residues and carry a strong net positive charge. As

discussed earlier, the acidic patch domain is involved in nucleosome–nucleosome interactions via the basic histone H4 tail, a critical step for chromatin folding and compaction (57). In addition, the acidic patch is implicated as a crucial interaction platform for many nucleosome–protein complexes, some of which have been structurally demonstrated. For instance, the first complex structure of a nucleosome–peptide that was resolved and biochemically described was the viral peptide LANA from KSHV bound with the nucleosome (67, 118, 140). This pioneering work established how a viral protein interacted with the nucleosome through the acidic patch. Structural, computational modeling, and experimental analyses of other nucleosome binding proteins including HMGN2, RCC1, CENP-C, Sir3, IL-33, H4-tail, and the viral protein IE1 have revealed that these proteins interact with the acidic patch, which serves as the principal protein-docking region for these proteins with the nucleosome (57, 149, 260-263) (Figure 6.2).

It is intriguing that most of these proteins use a basic residue, generally an arginine or lysine, to make contact with one or more of the 8 negatively charged residues that constitute the nucleosomal acidic patch (66, 67, 149, 260, 262, 264) (Table 2)(38). Song Tan and colleagues published the co-crystal structure of the nucleosome-PRC1 ubiquitylation module, which has provided a detailed mechanistic view of how the enzyme RING1B/BMI1 interacts with the acidic patch to facilitate its substrate recognition on the nucleosome (142). All 6 PCGF E3s of the PRC1 and PRC2 complexes including RING1B/BMI1, recognize the H2A/H2B acidic patch (142, 247, 265). Based on the identification of a host of nucleosome acidic patch interacting it seems highly likely that additional proteins will be identified that rely on interactions with the nucleosome acidic patch for their function, including those involved in the DDR, on chromatin.

A key question to address in the future is how do chromatin features, including the nucleosome acidic patch, regulate specific interactions with DDR and chromatin factors in the presence of other nucleosome binding proteins that target the same acidic

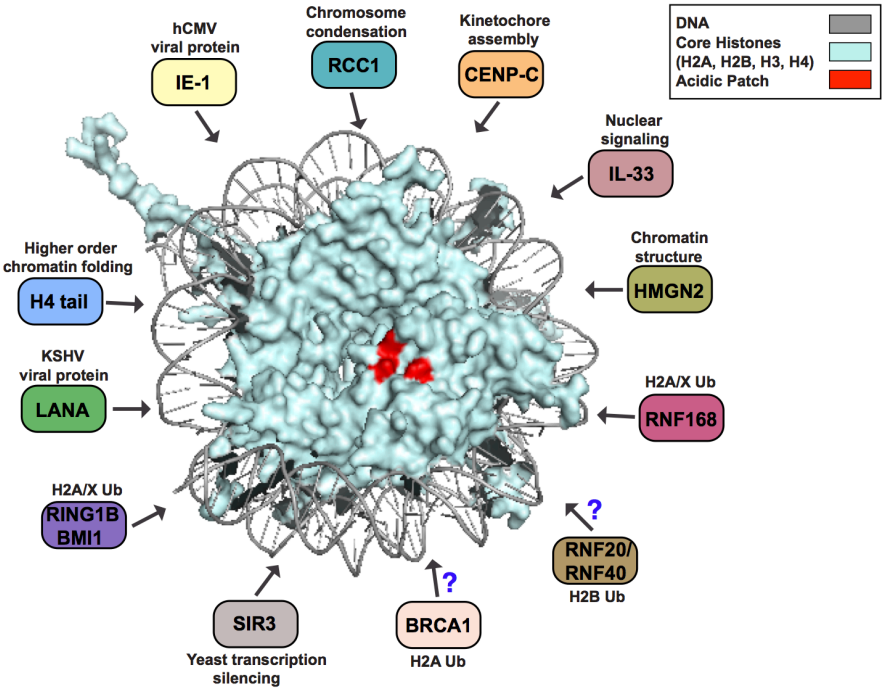

Figure 6.2 Nucleosome acidic patch interacting proteins

The acidic patch is a central hub for nucleosome interactions for multiple proteins involved in diverse biological processes. The crystal structure of NCP was retrieved from protein data bank (PDB code 1AOI) and modeled in Pymol. Color coding is as follows: DNA, grey; histones, pale cyan; acidic patch, red (38).

pocket on the nucleosome. Chromatin is also highly modified, and an understanding of how additional modifications regulate interactions with chromatin factors and the nucleosome acidic patch are unknown. Another level of complexity is offered by the fact that in addition to the interactions between proteins and the nucleosome surface, negatively charged DNA also interacts electrostatically with specific basic regions of the histones and non-histone proteins in various chromatin templated processes, including DNA damage signaling. For example, the RING1B/BMI1-UbcH5c E3-E2 complex, forming the ubiquitin signaling module that is activated upon DSB induction, is known to interact with both the nucleosomal DNA and the acidic patch of the nucleosome (142). Given the weak interactions of many proteins with the nucleosome acidic patch, including DDR factors, these additional interactions between nucleosomal DNA and the

Acidic patch interacting proteins	Co-structures with nucleosome	Histone PTMs involved	Involvement in pathways	References
LANA	Yes	No	Viral infection	(Barbera et al., 2006)
IL-33	Yes	No	Nuclear signaling	(Roussel et al., 2008)
RCC1	Yes	No	Chromosome condensation	(Makde et al., 2010)
HMGN2	Yes	No	Chromatin structure	(Kato et al., 2011)
SIR3	Yes	No	Transcription silencing	(Armache et al., 2011)
CENP-C	Yes	No	Kinetochore assembly	(Kato et al., 2013)
RING1B/BMI1 (PRC1)	Yes	H2A/X K118/119 Ub	DDR signaling	(Chen et al., 2013; Leung et al., 2014; McGinty et al., 2014)
RNF168	Not shown	H2A/X K13/15 Ub, H2AZ	DDR signaling	(Chen et al., 2013; Leung et al., 2014; Mattiroli et al., 2014).
BRCA1	Predicted	H2A K127 /129 Ub	DDR signaling	(Kalb et al., 2014; McGinty et al., 2014)
IE-1	Yes	No	hCMV infection	(Fang et al., 2016)
H4 N'-tail	Yes	No	Chromatin structure	(Luger et al., 1997)

Table 6.1 Nucleosome acidic patch interacting factors

protein could also contribute to their productive interactions with the nucleosome. Writing the histone-code involved in DSB signaling and repair thereby utilizes complex signaling events, including those occurring on the surface of the nucleosome that aid in recognizing, sensing, and repairing DSBs throughout the various chromatin environments that exist across the genome of mammalian cells.

NUCLEOSOME ACIDIC PATCH AS A THERAPEUTIC TARGET

Combining the above observations with the emerging paradigm that many proteins involved in DSB repair physically associate with the acidic patch to modulate chromatin dynamics, this unique chromatin interaction domain on the nucleosomal surface acts a central hub for DNA repair factor interactions with chromatin. Although cancer treatments have been "drugging" the DNA component of chromatin for over a half-century (i.e., cisplatin, ionizing radiation (2), or modifications of DNA or histones (i.e., FDA-approved inhibitors of DNA methylation or histone deacetylases) (98, 266, 267), no therapy currently targets the unmodified histone protein component of chromatin within the nucleosome (95). Given the tremendous success of DNA targeting drugs as

therapeutic agents in cancer, the nucleosome surface represents a potentially attractive drug target (140, 266). Although both RING1B/BMI1 and RNF168 E3 ubiquitin ligases are involved in DDR signaling, overexpression and hyperactivation of these enzymes have been implicated in cancer initiation and development (158, 256-259). Supporting the potential for these pathways as therapeutic targets, small molecule inhibitors degrading or inhibiting RING1B/BMI1 ubiquitin ligase complex have been developed and show promise in anti-tumor activity in colorectal cancer models (268-270).

The wealth of available structural and biochemical information on nucleosome and nucleosome acid patch-interacting proteins can be leveraged to design, synthesize, and test small molecule or peptide-derived inhibitors of nucleosome acidic patch interaction factors including RING1B/BMI1 and RNF168. The combination of genetic screens and *in vitro* structural and biochemical analyses is providing additional novel insights into how diverse chromatin-associated machineries interact with the nucleosome, in addition to the nucleosome acidic patch, to promote chromatin-based DDR activities. Several topological features beyond the charged acidic pocket exist on the nucleosomal surface that control and regulate nuclear processes, which could include DNA damage signaling and repair. Future work is required to understand whether these factors are mutually exclusive or act combinatorially on the nucleosome surface to write the requisite code for the DDR within a specific chromatin context. Studies furthering our mechanistic understanding of how chromatin proteins interact with the nucleosome to promote the DDR are warranted to have a better understanding of chromatin-based DDR pathways can be used to improve the development and application of DNA damaging agents and epigenetic drugs for the improved treatment of human diseases.

CHROMATIN AND GENOME TARGETING CHEMOTHERAPEUTICS

Chromatin targeting drugs constitute a major treatment for human cancer. The emerging roles of HDACs in DNA repair provide new opportunities for improving

traditional genotoxic drugs. Co-administration of HDAC inhibitors (HDACi) has been shown to enhance anticancer potency of drugs including cisplatin (110). The dynamic nature of genomes and epigenomes makes it challenging to predict and control chromatin-targeting drug responses. However, emerging evidence suggests that functional interactions between these drugs and the genome are non-stochastic and are influenced by a dynamic interplay between DNA sequences and chromatin states. Therefore, in the second part of my thesis project we screened a select few chromatin regulators or modulators of the chromatin states to assess how these influence targeting of anticancer Pt drugs used commonly as anticancer therapeutics. We developed a click-chemistry based technique to visualize DNA-lesions in the cells and found that combination of an anticancer drug, cisplatin derivative, APPA that acts on the genome with an HDACi cotreatment with SAHA regulates its genome targeting capabilities to provide a unique drug response that induces hyper loading of platinum onto specific genomic loci promoting TLS dependent apoptosis and cell death. Our previous studies have shown that APPA preferentially targets the early S-phase cells. Damage induction in S-phase cells is known to activate translesion synthesis (TLS) pathway as a means to bypass the DNA lesion at stalled replication forks by recruitment of error-prone DNA polymerases including Polη and Polζ mediated by monoubiquitination of PCNA. Translesion synthesis assays using human Polη has the ability to bypass cisplatin-GG adducts. Analyzing the changes in PCNA localization and RAD18 foci upon combined treatment of APPA with HDACi SAHA provided insights on the functional effects of chromatin reprogramming by these combination treatments. Our technique allows labeling of drugs with a tag while maintaining superior functionality of these small molecules that can be used for downstream applications including localization studies and genome-wide deep sequencing or proteomics to identify biologically relevant genomic target sites and drug-protein interactors (Figure 6.3). We believe knowledge gained from this study will have a transformative influence on our understanding, use and

development of combination therapies. These innovative approaches for identifying genomic target sites, responses and properties of genome and epigenome drugs could transform drug discovery by providing powerful methodologies to identify unanticipated and complex drug mechanisms.

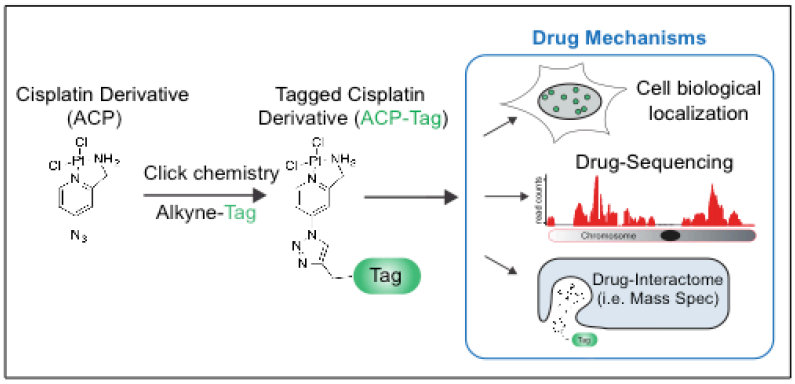

Figure 6.3 Click-chemistry based chemical labeling of DNA lesions in cells

Visualizing DNA-Pt in cells enables to localize and identify genomic target sites of chromatin drugs. *(This figure was provided by K.M.M.)*

Mechanistic details of the DDR and chromatin will provide insights into novel therapeutic targets and therapies because these pathways are currently targeted by anti-cancer chemotherapeutic treatments in the clinic. Given the potential of combination therapies, a systematic analysis of cell populations from patient samples to study drug-genome interactions could provide the basis to evaluate whether these patients would respond to treatment. For instance, using high throughput next generation sequencing, comparison of DNA-drug interactome between different cell lines could provide information about qualitative and quantitative differences in DNA targeting that could be exploited for therapeutic benefits. This technology could be extended to further study resistance mechanisms and to identify other small molecule modulators of cisplatin targeting by means of high throughput small molecule screening in an unbiased manner. For example, additional DNA damaging (Taxol) and chromatin regulating drugs including methylation inhibitors (5-azacytidine) that are relevant for biomedicine can be

combined with the Pt drugs. A key question to be addressed in the future is how orchestration of drug targeting by chromatin influences the intrinsic resistance or sensitivity of cancer cells to drug treatments and acquired drug resistance, which represent serious obstacles for therapeutic applications. Many chemotherapeutic compounds used as cancer therapies such as platinum drugs including cisplatin, oxaloplatin etc. readily result in chemoresistance through different mechanisms (108). Importantly, cisplatin resistant cancer cells can be resensitized to cisplatin by combined treatment with HDAC inhibitor treatments (109). Two FDA approved chromatin modulators; histone deacetylase inhibitors (HDACi) and DNA methylation inhibitor 5-azacytidine are tested in phase trials for combinatorial use with other DNA damage for cancer treatments (110). Similar to genome-drug interactions, another key aspect that can be significantly informative is characterization of RNA targets of these platinum drugs including APPA, which could also contribute to the APPA-mediated alteration of gene expression. Furthermore, recent advancements in quantitative mass spectrometry along with our pull-down protocol may be employed to isolate and characterize proteins involved in the detection and processing of platinated DNA lesions in specific combinatorial treatment studies. Collectively, these studies will provide innovative tools and strategies for interrogating drug mechanisms and acquired drug resistance to better predict and control these responses in cancer and its treatments.

BRD CONTAINING TRIM PROTEINS IN THE DDR

Bromodomain (BRD) containing proteins are key mediators of chromatin based DDR mechanisms in eukaryotic cells via their potential to recognize and transmit signals that reside within acetylated chromatin. A host of BRD chromatin reader proteins have been unraveled that interact with damage associated acetylation to promote the DDR and thus maintain genome integrity. Some of the BRD containing proteins accumulate at sites of DNA lesions where they participate in the DDR whereas a few of them do not

accumulate at damage sites (82). A comprehensive analysis of all the human BRD proteins in the Miller Lab identified TRIM24 as a new DDR factor that recognizes DNA damage and recruits to damaged chromatin. Two other TRIM family proteins, TRIM28 and TRIM33, which also contain the BRD, were identified to be recruited to DNA damage lesions. Another member of the TRIM-BRD protein family, TRIM66 is not studied here due to its tissue specific abundance and no recruitment to damage sites. However, TRIM24 is not well characterized in the context of DDR signaling and repair. How these three TRIM-BRD proteins collectively orchestrate the DDR in response to DNA breaks remains unclear.

TRIM24 has previously been studied in specific cancer types where its elevated expression promotes progression of cancer including breast ((210, 213), head and neck (271), non-small cell lung (272), glioblastoma (273), cervical cancer (274) and HCC (275). Some studies highlight TRIM24 as a tumor suppressor in hepatocellular carcinoma (276, 277). It is known to serve as an E3 Ub ligase to regulate p53 levels resulting in p53 degradation thereby affecting cell cycle arrest and apoptosis (211). It is also known as a transcriptional intermediary factor or transcriptional activator for various genes (278, 279) and its interaction with several nuclear receptors (280).

We showed that TRIM24 recruitment is affected upon down regulating the HAT KAT6B to facilitate DNA repair revealing the importance of acetylation signaling in this pathway. Cells depleted in TRIM24 showed defective NHEJ repair and had lower levels of the master regulator protein MDC1. Our proteomic and genetic analyses indicate that these three proteins, TRIM24, TRIM28 and TRIM33 functionally interact to orchestrate DDR signaling and repair. We found that both TRIM24 and TRIM33 interact with components of the histone chaperone complex, FACT. In addition, TRIM24 interacts with the replicative helicase MCM complex. Previous studies have established that the individual FACT and MCM subunits form at least two different and sequential subassemblies to coordinate origin establishment and progression of replication initiation

and S-phase (242). The physical association of the DDR factor TRIM24 with this complex hints towards a distinct function of this BRD protein in resolving damage at active replication regions such as the replication forks. Therefore, further mechanistic details of involvement of this protein complex in replication-associated DNA damage repair will illuminate critical pathways in which these are involved. Moreover, our data revealed that the recruitment of three BRD-TRIM proteins, TRIM24, TRIM28 and TRIM33 is regulated by the methyltransferase SUV39H1 that catalyzes the repressive histone mark, H3K9me3. It is therefore, plausible that these three factors display synergistic or redundant functions in the regulation of repair activities at specific chromatin states containing DNA-damage sites.

A new cardiac role of TRIM24 was recently reported where it was shown to interact with cardiac Dysbindin and TRIM32 in cardiomyocytes. In this study, the differential expression of the two TRIM proteins, TRIM24 and TRIM32, was found to have opposing roles in regulating their common interactor Dysbindin protein levels and thereby cardiomyocyte hypertrophy. TRIM24 expression levels are higher than TRIM32 levels in the heart and it protects Dysbindin from degradation by TRIM32 to promote cardiomyotrophy (281). It is conceivable that a similar mechanism exists in DDR involving the three BRD-TRIM proteins where they function and interact in a synergistic or antagonistic way to regulate specific steps and pathways involved in DNA repair based on their total levels in the complex formation. ATM mediated phosphorylation of TRIM24 at S768 has been shown to play an auto inhibitory role to promote TRIM24 degradation during DNA damage (282). However, other PTMs on TRIM24 might have a role in the DDR that needs to be explored. Emerging evidence from our studies suggest that TRIM24 is an important component of the DDR pathway, however, it remains to be identified which pathway other than the gene silencing machinery is activated by TRIM24 to mount DDR signaling upon DNA damage. Collectively, the data provided here defines TRIM24 as a new player in cellular response to genotoxic insults. Further

work elucidating DDR functions for TRIM24 along with its chromatin associated interactors, MCM and FACT complex is warranted and essential for cancer research given that drugs targeting chromatin remodelers are currently being extensively explored for cancer therapies either alone or in conjunction with other DNA-damaging therapeutic agents. We anticipate that additional studies will have the potential to shed light on the various chromatin associated mechanisms of the DNA damage response, including those mediated by nucleosome interactions and BRD proteins, knowledge gained from which can be utilized to develop new or optimized existing therapeutic strategies and drugs to treat cancer.

APPENDIX

Poonam Agarwal's publications during her graduate study at UT:

- Zacharioudakis, E.*, Agarwal, P.*, Bartoli, A., Abell, N., Bergoglio, V., Xhemalce, B., Kunalingam, L., Miller, K.M., and Rodriguez, R. (2017). Chromatin regulates genome targeting with cisplatin. Angewandte Chemie, 56(23):6483-6487 * Co-first author.
- Leung, J.W., Makharashvili, N., Agarwal, P., Chiu L-Y, Poupre, R., Cammarata, M.B., Cannon, J.R., Sherker, A., Durocher, D., Brodbelt, J.S., Paull, T.T., and Miller, K.M. (2017) ZMYM3 regulates BRCA1 localization at damaged chromatin to promote DNA repair. Genes & Development 31(3):260-274.
- Agarwal, P. and Miller, K.M. (2016). Book Chapter: Chromatin Dynamics and DNA Repair. In: Chromatin Regulation and Dynamics Book. Elsevier.
- Agarwal, P. and Miller, K.M. (2016). The Nucleosome: Orchestrating DNA Damage Signaling and Repair within Chromatin. Biochemistry and Cell Biology. 94: 381-395.
- O'Connor, H., Lyon, N., Leung, J.W., Agarwal, P., Swaim, C., Miller, K.M., and Huibregtse, J. (2015). Ubiquitin-Activated Interaction Traps (UBAITs) identify E3 ligase binding partners. EMBO Reports. 16(12): 1699-712.
- Gong, F., Chiu, L., Cox, B., Aymard, F., Clouaire, T., Leung, J.W., Cammarata, M., Perez, M., Agarwal, P., Brodbelt, J.S., Legube, G. & Miller, K.M. (2015). Screen identifies bromodomain protein ZMYND8 in chromatin recognition of transcription-associated DNA damage that promotes homologous recombination. Genes & Development 29:197-211.
- Leung, J.W.*, Agarwal, P.*, Canny, M.D., Gong, F., Robison, A.D., Finkelstein, I.J., Durocher, D. and Miller, K.M. (2014). Nucleosome Acidic Patch Promotes

RNF168- and RING1B/BMI1-Dependent H2AX and H2A Ubiquitination and DNA Damage Signaling. PLOS Genetics 10(3): e1004178. *Co-first author

REFERENCES

1. Ciccia A & Elledge SJ (2010) The DNA damage response: making it safe to play with knives. *Mol Cell* 40(2):179-204.
2. Jackson SP & Bartek J (2009) The DNA-damage response in human biology and disease. *Nature* 461(7267):1071-1078.
3. Agarwal P & Miller KM (2017) Chromatin Dynamics and DNA repair. *Chromatin Regulation and Dynamics,* Translational Epigenetics Series, (Elsevier).
4. Miller KM & Jackson SP (2012) Histone marks: repairing DNA breaks within the context of chromatin. *Biochemical Society transactions* 40(2):370-376.
5. Polo SE & Jackson SP (2011) Dynamics of DNA damage response proteins at DNA breaks: a focus on protein modifications. *Genes & development* 25(5):409-433.
6. Smeenk G & van Attikum H (2013) The chromatin response to DNA breaks: leaving a mark on genome integrity. *Annual review of biochemistry* 82:55-80.
7. Soria G, Polo SE, & Almouzni G (2012) Prime, repair, restore: the active role of chromatin in the DNA damage response. *Mol Cell* 46(6):722-734.
8. Huertas P (2010) DNA resection in eukaryotes: deciding how to fix the break. *Nature structural & molecular biology* 17(1):11-16.
9. Beucher A, *et al*. (2009) ATM and Artemis promote homologous recombination of radiation-induced DNA double-strand breaks in G2. *The EMBO journal* 28(21):3413-3427.
10. Lieber MR (2010) The mechanism of double-strand DNA break repair by the nonhomologous DNA end-joining pathway. *Annual review of biochemistry* 79:181-211.
11. San Filippo J, Sung P, & Klein H (2008) Mechanism of eukaryotic homologous recombination. *Annual review of biochemistry* 77:229-257.
12. Kouzarides T (2007) Chromatin modifications and their function. *Cell* 128(4):693-705.
13. Luijsterburg MS & van Attikum H (2011) Chromatin and the DNA damage response: the cancer connection. *Molecular oncology* 5(4):349-367.
14. Misteli T & Soutoglou E (2009) The emerging role of nuclear architecture in DNA repair and genome maintenance. *Nature reviews. Molecular cell biology* 10(4):243-254.
15. Price BD & D'andrea AD (2013) Chromatin Remodeling at DNA Double-Strand Breaks. *Cell* 152(6):1344-1354.
16. Seeber A, Hauer M, & Gasser SM (2013) Nucleosome remodelers in double-strand break repair. *Current opinion in genetics & development* 23(2):174-184.
17. Fradet-Turcotte A, *et al*. (2013) 53BP1 is a reader of the DNA-damage-induced H2A Lys 15 ubiquitin mark. *Nature* 499(7456):50-54.
18. Sobhian B, *et al*. (2007) RAP80 targets BRCA1 to specific ubiquitin structures at DNA damage sites. *Science* 316(5828):1198-1202.

19. Musselman CA, Lalonde ME, Cote J, & Kutateladze TG (2012) Perceiving the epigenetic landscape through histone readers. *Nature structural & molecular biology* 19(12):1218-1227.
20. Ruthenburg AJ, Li H, Patel DJ, & Allis CD (2007) Multivalent engagement of chromatin modifications by linked binding modules. *Nature reviews. Molecular cell biology* 8(12):983-994.
21. van Attikum H & Gasser SM (2005) The histone code at DNA breaks: A guide to repair? *Nat Rev Mol Cell Bio* 6(10):757-765.
22. Rogakou EP, Pilch DR, Orr AH, Ivanova VS, & Bonner WM (1998) DNA double-stranded breaks induce histone H2AX phosphorylation on serine 139. *The Journal of biological chemistry* 273(10):5858-5868.
23. Burma S, Chen BP, Murphy M, Kurimasa A, & Chen DJ (2001) ATM phosphorylates histone H2AX in response to DNA double-strand breaks. *Journal of Biological Chemistry* 276(45):42462-42467.
24. Chapman JR & Jackson SP (2008) Phospho-dependent interactions between NBS1 and MDC1 mediate chromatin retention of the MRN complex at sites of DNA damage. *Embo Rep* 9(8):795-801.
25. Lukas C, *et al*. (2004) Mdc1 couples DNA double-strand break recognition by Nbs1 with its H2AX-dependent chromatin retention. *The EMBO journal* 23(13):2674-2683.
26. Rogakou EP, Boon C, Redon C, & Bonner WM (1999) Megabase chromatin domains involved in DNA double-strand breaks in vivo. *The Journal of cell biology* 146(5):905-916.
27. Savic V, *et al*. (2009) Formation of Dynamic gamma-H2AX Domains along Broken DNA Strands Is Distinctly Regulated by ATM and MDC1 and Dependent upon H2AX Densities in Chromatin. *Mol Cell* 34(3):298-310.
28. Scully R & Xie A (2013) Double strand break repair functions of histone H2AX. *Mutation research* 750(1-2):5-14.
29. Sedelnikova OA, Rogakou EP, Panyutin IG, & Bonner WM (2002) Quantitative detection of (125)IdU-induced DNA double-strand breaks with gamma-H2AX antibody. *Radiation research* 158(4):486-492.
30. Stucki M, *et al*. (2005) MDC1 directly binds phosphorylated histone H2AX to regulate cellular responses to DNA double-strand breaks. *Cell* 123(7):1213-1226.
31. Celeste A, *et al*. (2002) Genomic instability in mice lacking histone H2AX. *Science* 296(5569):922-927.
32. Fernandez-Capetillo O, Celeste A, & Nussenzweig A (2003) Focusing on foci: H2AX and the recruitment of DNA-damage response factors. *Cell Cycle* 2(5):426-427.
33. Furuta T, *et al*. (2003) Phosphorylation of histone H2AX and activation of Mre11, Rad50, and Nbs1 in response to replication-dependent DNA double-strand breaks induced by mammalian DNA topoisomerase I cleavage complexes. *The Journal of biological chemistry* 278(22):20303-20312.
34. Paull TT, *et al*. (2000) A critical role for histone H2AX in recruitment of repair factors to nuclear foci after DNA damage. *Current biology : CB* 10(15):886-895.

35. Pilch DR, *et al*. (2003) Characteristics of gamma-H2AX foci at DNA double strand breaks sites. *Biochemistry and Cell Biology-Biochimie Et Biologie Cellulaire* 81(3):123-129.
36. Jackson SP & Durocher D (2013) Regulation of DNA damage responses by ubiquitin and SUMO. *Mol Cell* 49(5):795-807.
37. Panier S & Durocher D (2009) Regulatory ubiquitylation in response to DNA double-strand breaks. *DNA repair* 8(4):436-443.
38. Agarwal P & Miller KM (2016) The nucleosome: orchestrating DNA damage signaling and repair within chromatin. *Biochemistry and Cell Biology* 94(5):381-395.
39. Thorslund T, *et al*. (2015) Histone H1 couples initiation and amplification of ubiquitin signalling after DNA damage. *Nature* 527(7578):389-393.
40. Doil C, *et al*. (2009) RNF168 binds and amplifies ubiquitin conjugates on damaged chromosomes to allow accumulation of repair proteins. *Cell* 136(3):435-446.
41. Stewart GS, *et al*. (2009) The RIDDLE Syndrome Protein Mediates a Ubiquitin-Dependent Signaling Cascade at Sites of DNA Damage. *Cell* 136(3):420-434.
42. Botuyan MV, *et al*. (2006) Structural basis for the methylation state-specific recognition of histone H4-K20 by 53BP1 and Crb2 in DNA repair. *Cell* 127(7):1361-1373.
43. Gong FD & Miller KM (2013) Mammalian DNA repair: HATs and HDACs make their mark through histone acetylation. *Mutat Res-Fund Mol M* 750(1-2):23-30.
44. Hsiao KY & Mizzen CA (2013) Histone H4 deacetylation facilitates 53BP1 DNA damage signaling and double-strand break repair. *J Mol Cell Biol* 5(3):157-165.
45. Tang JB, *et al*. (2013) Acetylation limits 53BP1 association with damaged chromatin to promote homologous recombination. *Nature structural & molecular biology* 20(3):317-325.
46. Shahbazian MD & Grunstein M (2007) Functions of site-specific histone acetylation and deacetylation. *Annu Rev Biochem* 76:75-100.
47. Aymard F, *et al*. (2014) Transcriptionally active chromatin recruits homologous recombination at DNA double-strand breaks. *Nature structural & molecular biology* 21(4):366-U172.
48. Carvalho S, *et al*. (2014) SETD2 is required for DNA double-strand break repair and activation of the p53-mediated checkpoint. *Elife* 3.
49. Pfister SX, *et al*. (2014) SETD2-Dependent Histone H3K36 Trimethylation Is Required for Homologous Recombination Repair and Genome Stability. *Cell Rep* 7(6):2006-2018.
50. Chen WT, *et al*. (2013) Systematic identification of functional residues in mammalian histone H2AX. *Molecular and cellular biology* 33(1):111-126.
51. Gursoy-Yuzugullu O, Ayrapetov MK, & Price BD (2015) Histone chaperone Anp32e removes H2A.Z from DNA double-strand breaks and promotes nucleosome reorganization and DNA repair. *Proceedings of the National Academy of Sciences of the United States of America* 112(24):7507-7512.
52. Leung JW, *et al*. (2014) Nucleosome acidic patch promotes RNF168- and RING1B/BMI1-dependent H2AX and H2A ubiquitination and DNA damage signaling. *PLoS genetics* 10(3):e1004178.

53. Mattiroli F, Uckelmann M, Sahtoe DD, van Dijk WJ, & Sixma TK (2014) The nucleosome acidic patch plays a critical role in RNF168-dependent ubiquitination of histone H2A. *Nature communications* 5:3291.
54. Wyrick JJ, Kyriss MN, & Davis WB (2012) Ascending the nucleosome face: recognition and function of structured domains in the histone H2A-H2B dimer. *Biochimica et biophysica acta* 1819(8):892-901.
55. Campos EI & Reinberg D (2009) Histones: annotating chromatin. *Annual review of genetics* 43:559-599.
56. Davey CA, Sargent DF, Luger K, Maeder AW, & Richmond TJ (2002) Solvent mediated interactions in the structure of the nucleosome core particle at 1.9 angstrom resolution. *Journal of molecular biology* 319(5):1097-1113.
57. Luger K, Mader AW, Richmond RK, Sargent DF, & Richmond TJ (1997) Crystal structure of the nucleosome core particle at 2.8 angstrom resolution. *Nature* 389(6648):251-260.
58. Chakravarthy S, Park YJ, Chodaparambil J, Edayathumangalam RS, & Luger K (2005) Structure and dynamic properties of nucleosome core particles. *FEBS letters* 579(4):895-898.
59. Gatti M, *et al*. (2012) A novel ubiquitin mark at the N-terminal tail of histone H2As targeted by RNF168 ubiquitin ligase. *Cell Cycle* 11(13):2538-2544.
60. Ginjala V, *et al*. (2011) BMI1 is recruited to DNA breaks and contributes to DNA damage-induced H2A ubiquitination and repair. *Mol Cell Biol* 31(10):1972-1982.
61. Ismail IH, Andrin C, McDonald D, & Hendzel MJ (2010) BMI1-mediated histone ubiquitylation promotes DNA double-strand break repair. *Journal of Cell Biology* 191(1):45-60.
62. Mattiroli F, *et al*. (2012) RNF168 ubiquitinates K13-15 on H2A/H2AX to drive DNA damage signaling. *Cell* 150(6):1182-1195.
63. Moyal L, *et al*. (2011) Requirement of ATM-dependent monoubiquitylation of histone H2B for timely repair of DNA double-strand breaks. *Mol Cell* 41(5):529-542.
64. Nakamura K, *et al*. (2011) Regulation of homologous recombination by RNF20-dependent H2B ubiquitination. *Mol Cell* 41(5):515-528.
65. Yan QS, *et al*. (2009) BBAP Monoubiquitylates Histone H4 at Lysine 91 and Selectively Modulates the DNA Damage Response. *Mol Cell* 36(1):110-120.
66. Chodaparambil JV, *et al*. (2007) A charged and contoured surface on the nucleosome regulates chromatin compaction. *Nature structural & molecular biology* 14(11):1105-1107.
67. Kalashnikova AA, Porter-Goff ME, Muthurajan UM, Luger K, & Hansen JC (2013) The role of the nucleosome acidic patch in modulating higher order chromatin structure. *Journal of the Royal Society, Interface / the Royal Society* 10(82):20121022.
68. McGinty RK & Tan S (2015) Nucleosome structure and function. *Chemical reviews* 115(6):2255-2273.
69. Tremethick DJ (2007) Higher-order structures of chromatin: the elusive 30 nm fiber. *Cell* 128(4):651-654.
70. Glatt S, Alfieri C, & Muller CW (2011) Recognizing and remodeling the nucleosome. *Current opinion in structural biology* 21(3):335-341.

71. Bonisch C & Hake SB (2012) Histone H2A variants in nucleosomes and chromatin: more or less stable? *Nucleic acids research* 40(21):10719-10741.
72. Fan JY, Gordon F, Luger K, Hansen JC, & Tremethick DJ (2002) The essential histone variant H2A.Z regulates the equilibrium between different chromatin conformational states. *Nature structural biology* 9(3):172-176.
73. Suto RK, Clarkson MJ, Tremethick DJ, & Luger K (2000) Crystal structure of a nucleosome core particle containing the variant histone H2A.Z. *Nature structural biology* 7(12):1121-1124.
74. Chakravarthy S, Bao Y, Roberts VA, Tremethick D, & Luger K (2004) Structural characterization of histone H2A variants. *Cold Spring Harbor symposia on quantitative biology* 69:227-234.
75. Brondello JM, *et al*. (2008) Novel evidences for a tumor suppressor role of Rev3, the catalytic subunit of Pol zeta. *Oncogene* 27(47):6093-6101.
76. Pankotai T, Bonhomme C, Chen D, & Soutoglou E (2012) DNAPKcs-dependent arrest of RNA polymerase II transcription in the presence of DNA breaks. *Nature structural & molecular biology* 19(3):276-282.
77. Miller KM, *et al*. (2010) Human HDAC1 and HDAC2 function in the DNA-damage response to promote DNA nonhomologous end-joining. *Nature structural & molecular biology* 17(9):1144-1151.
78. Tang J, *et al*. (2013) Acetylation limits 53BP1 association with damaged chromatin to promote homologous recombination. *Nature structural & molecular biology* 20(3):317-325.
79. Filippakopoulos P, *et al*. (2012) Histone recognition and large-scale structural analysis of the human bromodomain family. *Cell* 149(1):214-231.
80. Filippakopoulos P & Knapp S (2012) The bromodomain interaction module. *FEBS letters* 586(17):2692-2704.
81. Gong F, Chiu LY, & Miller KM (2016) Acetylation Reader Proteins: Linking Acetylation Signaling to Genome Maintenance and Cancer. *PLoS genetics* 12(9):e1006272.
82. Gong FD, *et al*. (2015) Screen identifies bromodomain protein ZMYND8 in chromatin recognition of transcription-associated DNA damage that promotes homologous recombination. *Genes & development* 29(2):197-211.
83. Marmorstein R & Zhou MM (2014) Writers and readers of histone acetylation: structure, mechanism, and inhibition. *Cold Spring Harbor perspectives in biology* 6(7):a018762.
84. Muller S, Filippakopoulos P, & Knapp S (2011) Bromodomains as therapeutic targets. *Expert Rev Mol Med* 13:1-21.
85. Barbieri I, Cannizzaro E, & Dawson MA (2013) Bromodomains as therapeutic targets in cancer. *Briefings in functional genomics* 12(3):219-230.
86. Dawson MA, *et al*. (2011) Inhibition of BET Recruitment to Chromatin As An Effective Treatment for MLL-Fusion Leukaemia. *Blood* 118(21):27-28.
87. Filippakopoulos P, *et al*. (2010) Selective inhibition of BET bromodomains. *Nature* 468(7327):1067-1073.
88. Barnett C & Krebs JE (2011) WSTF does it all: a multifunctional protein in transcription, repair, and replication. *Biochemistry and Cell Biology-Biochimie Et Biologie Cellulaire* 89(1):12-23.

89. Floyd SR, *et al*. (2013) The bromodomain protein Brd4 insulates chromatin from DNA damage signalling. *Nature* 498(7453):246-250.
90. Iyengar S & Farnham PJ (2011) KAP1 protein: an enigmatic master regulator of the genome. *The Journal of biological chemistry* 286(30):26267-26276.
91. Ogiwara H, *et al*. (2011) Histone acetylation by CBP and p300 at double-strand break sites facilitates SWI/SNF chromatin remodeling and the recruitment of non-homologous end joining factors. *Oncogene* 30(18):2135-2146.
92. Goodarzi AA, Kurka T, & Jeggo PA (2011) KAP-1 phosphorylation regulates CHD3 nucleosome remodeling during the DNA double-strand break response. *Nature structural & molecular biology* 18(7):831-839.
93. Goodarzi AA, *et al*. (2008) ATM signaling facilitates repair of DNA double-strand breaks associated with heterochromatin. *Mol Cell* 31(2):167-177.
94. Ziv Y, *et al*. (2006) Chromatin relaxation in response to DNA double-strand breaks is modulated by a novel ATM and KAP-1 dependent pathway. *Nature cell biology* 8(8):870-U142.
95. Cheung-Ong K, Giaever G, & Nislow C (2013) DNA-damaging agents in cancer chemotherapy: serendipity and chemical biology. *Chemistry & biology* 20(5):648-659.
96. Lord CJ & Ashworth A (2012) The DNA damage response and cancer therapy. *Nature* 481(7381):287-294.
97. Dawson MA, Kouzarides T, & Huntly BJ (2012) Targeting epigenetic readers in cancer. *The New England journal of medicine* 367(7):647-657.
98. Baylin SB & Jones PA (2011) A decade of exploring the cancer epigenome - biological and translational implications. *Nat Rev Cancer* 11(10):726-734.
99. Arrowsmith CH, Bountra C, Fish PV, Lee K, & Schapira M (2012) Epigenetic protein families: a new frontier for drug discovery. *Nature reviews. Drug discovery* 11(5):384-400.
100. Yoo CB & Jones PA (2006) Epigenetic therapy of cancer: past, present and future. *Nature reviews. Drug discovery* 5(1):37-50.
101. Rodriguez R & Miller KM (2014) Unravelling the genomic targets of small molecules using high-throughput sequencing. *Nature reviews. Genetics*.
102. Helin K & Dhanak D (2013) Chromatin proteins and modifications as drug targets. *Nature* 502(7472):480-488.
103. Plass C, *et al*. (2013) Mutations in regulators of the epigenome and their connections to global chromatin patterns in cancer. *Nature reviews. Genetics* 14(11):765-780.
104. Rodriguez R & Miller KM (2014) Unravelling the genomic targets of small molecules using high-throughput sequencing. *Nature reviews. Genetics* 15(12):783-796.
105. Rodriguez R, *et al*. (2012) Small-molecule-induced DNA damage identifies alternative DNA structures in human genes. *Nature chemical biology* 8(3):301-310.
106. Anders L, *et al*. (2014) Genome-wide localization of small molecules. *Nature biotechnology* 32(1):92-96.
107. Jin C, *et al*. (2014) Chem-seq permits identification of genomic targets of drugs against androgen receptor regulation selected by functional phenotypic screens.

Proceedings of the National Academy of Sciences of the United States of America 111(25):9235-9240.
108. Galluzzi L, *et al*. (2012) Molecular mechanisms of cisplatin resistance. *Oncogene* 31(15):1869-1883.
109. Sharma SV, *et al*. (2010) A chromatin-mediated reversible drug-tolerant state in cancer cell subpopulations. *Cell* 141(1):69-80.
110. Kim MS, *et al*. (2003) Inhibition of histone deacetylase increases cytotoxicity to anticancer drugs targeting DNA. *Cancer research* 63(21):7291-7300.
111. Zacharioudakis E, *et al*. (2017) Chromatin Regulates Genome Targeting with Cisplatin. *Angew Chem Int Edit* 56(23):6483-6487.
112. Abell NS, Mercado M, Caneque T, Rodriguez R, & Xhemalce B (2017) Click Quantitative Mass Spectrometry Identifies PIWIL3 as a Mechanistic Target of RNA Interference Activator Enoxacin in Cancer Cells. *J Am Chem Soc* 139(4):1400-1403.
113. Shee C, *et al*. (2013) Engineered proteins detect spontaneous DNA breakage in human and bacterial cells. *Elife* 2:e01222.
114. Bartke T, *et al*. (2010) Nucleosome-interacting proteins regulated by DNA and histone methylation. *Cell* 143(3):470-484.
115. Dyer PN, *et al*. (2004) Reconstitution of nucleosome core particles from recombinant histones and DNA. *Methods Enzymol* 375:23-44.
116. Lee JY & Greene EC (2011) Assembly of recombinant nucleosomes on nanofabricated DNA curtains for single-molecule imaging. *Methods Mol Biol* 778:243-258.
117. Bentley ML, *et al*. (2011) Recognition of UbcH5c and the nucleosome by the Bmi1/Ring1b ubiquitin ligase complex. *The EMBO journal* 30(16):3285-3297.
118. Barbera AJ, *et al*. (2006) The nucleosomal surface as a docking station for Kaposi's sarcoma herpesvirus LANA. *Science* 311(5762):856-861.
119. Leung JW, *et al*. (2012) Fanconi anemia (FA) binding protein FAAP20 stabilizes FA complementation group A (FANCA) and participates in interstrand cross-link repair. *Proc Natl Acad Sci U S A* 109(12):4491-4496.
120. Ran FA, *et al*. (2013) Genome engineering using the CRISPR-Cas9 system. *Nat Protoc* 8(11):2281-2308.
121. Jackson SP & Durocher D (2013) Regulation of DNA damage responses by ubiquitin and SUMO. *Mol Cell* 49(5):795-807.
122. Panier S & Durocher D (2013) Push back to respond better: regulatory inhibition of the DNA double-strand break response. *Nat Rev Mol Cell Biol*.
123. Chagraoui J, Hebert J, Girard S, & Sauvageau G (2011) An anticlastogenic function for the Polycomb Group gene Bmi1. *Proceedings of the National Academy of Sciences of the United States of America* 108(13):5284-5289.
124. Facchino S, Abdouh M, Chatoo W, & Bernier G (2010) BMI1 confers radioresistance to normal and cancerous neural stem cells through recruitment of the DNA damage response machinery. *The Journal of neuroscience : the official journal of the Society for Neuroscience* 30(30):10096-10111.
125. Ismail IH, Andrin C, McDonald D, & Hendzel MJ (2010) BMI1-mediated histone ubiquitylation promotes DNA double-strand break repair. *J Cell Biol* 191(1):45-60.

126. Fradet-Turcotte A, *et al*. (2013) 53BP1 is a reader of the DNA-damage-induced H2A Lys 15 ubiquitin mark. *Nature*.
127. Sobhian B, *et al*. (2007) RAP80 targets BRCA1 to specific ubiquitin structures at DNA damage sites. *Science* 316(5828):1198-1202.
128. Lukas J, Lukas C, & Bartek J (2011) More than just a focus: The chromatin response to DNA damage and its role in genome integrity maintenance. *Nature cell biology* 13(10):1161-1169.
129. Wang H, *et al*. (2004) Role of histone H2A ubiquitination in Polycomb silencing. *Nature* 431(7010):873-878.
130. Gudjonsson T, *et al*. (2012) TRIP12 and UBR5 suppress spreading of chromatin ubiquitylation at damaged chromosomes. *Cell* 150(4):697-709.
131. Huen MS, *et al*. (2007) RNF8 transduces the DNA-damage signal via histone ubiquitylation and checkpoint protein assembly. *Cell* 131(5):901-914.
132. Kolas NK, *et al*. (2007) Orchestration of the DNA-damage response by the RNF8 ubiquitin ligase. *Science* 318(5856):1637-1640.
133. Mailand N, *et al*. (2007) RNF8 ubiquitylates histones at DNA double-strand breaks and promotes assembly of repair proteins. *Cell* 131(5):887-900.
134. Fang J, *et al*. (2002) Purification and functional characterization of SET8, a nucleosomal histone H4-lysine 20-specific methyltransferase. *Curr Biol* 12(13):1086-1099.
135. Fan JY, Rangasamy D, Luger K, & Tremethick DJ (2004) H2A.Z alters the nucleosome surface to promote HP1 alpha-mediated chromatin fiber folding. *Mol Cell* 16(4):655-661.
136. Robinson PJJ, *et al*. (2008) 30 nm chromatin fibre decompaction requires both H4-K16 acetylation and linker histone eviction. *Journal of molecular biology* 381(4):816-825.
137. Shogren-Knaak M, *et al*. (2006) Histone H4-K16 acetylation controls chromatin structure and protein interactions. *Science* 311(5762):844-847.
138. Xu Y, *et al*. (2012) Histone H2A.Z Controls a Critical Chromatin Remodeling Step Required for DNA Double-Strand Break Repair. *Mol Cell* 48(5):723-733.
139. O'Connor HF, *et al*. (2015) Ubiquitin-Activated Interaction Traps (UBAITs) identify E3 ligase binding partners. *Embo Rep* 16(12):1699-1712.
140. da Silva ITG, de Oliveira PSL, & Santos GM (2015) Featuring the nucleosome surface as a therapeutic target. *Trends Pharmacol Sci* 36(5):263-269.
141. Panier S, *et al*. (2012) Tandem protein interaction modules organize the ubiquitin-dependent response to DNA double-strand breaks. *Molecular cell* 47(3):383-395.
142. McGinty RK, Henrici RC, & Tan S (2014) Crystal structure of the PRC1 ubiquitylation module bound to the nucleosome. *Nature* 514(7524):591-596.
143. Bentley ML, *et al*. (2011) Recognition of UbcH5c and the nucleosome by the Bmi1/Ring1b ubiquitin ligase complex. *Embo Journal* 30(16):3285-3297.
144. Ismail IH, McDonald D, Strickfaden H, Xu Z, & Hendzel MJ (2013) A small molecule inhibitor of Polycomb repressive complex 1 inhibits ubiquitin signaling at DNA double-strand breaks. *J Biol Chem*.
145. Pan MR, Peng G, Hung WC, & Lin SY (2011) Monoubiquitination of H2AX protein regulates DNA damage response signaling. *J Biol Chem* 286(32):28599-28607.

146. Wu CY, *et al*. (2011) Critical role of monoubiquitination of histone H2AX protein in histone H2AX phosphorylation and DNA damage response. *J Biol Chem* 286(35):30806-30815.
147. Kato H, *et al*. (2011) Architecture of the high mobility group nucleosomal protein 2-nucleosome complex as revealed by methyl-based NMR. *Proceedings of the National Academy of Sciences of the United States of America* 108(30):12283-12288.
148. Luger K, Mader AW, Richmond RK, Sargent DF, & Richmond TJ (1997) Crystal structure of the nucleosome core particle at 2.8 A resolution. *Nature* 389(6648):251-260.
149. Makde RD, England JR, Yennawar HP, & Tan S (2010) Structure of RCC1 chromatin factor bound to the nucleosome core particle. *Nature* 467(7315):562-566.
150. Roussel L, Erard M, Cayrol C, & Girard JP (2008) Molecular mimicry between IL-33 and KSHV for attachment to chromatin through the H2A-H2B acidic pocket. *Embo Rep* 9(10):1006-1012.
151. Stewart GS, *et al*. (2009) The RIDDLE syndrome protein mediates a ubiquitin-dependent signaling cascade at sites of DNA damage. *Cell* 136(3):420-434.
152. Zimmermann M & de Lange T (2013) 53BP1: pro choice in DNA repair. *Trends Cell Biol*.
153. Chapman JR, *et al*. (2013) RIF1 is essential for 53BP1-dependent nonhomologous end joining and suppression of DNA double-strand break resection. *Mol Cell* 49(5):858-871.
154. Di Virgilio M, *et al*. (2013) Rif1 prevents resection of DNA breaks and promotes immunoglobulin class switching. *Science* 339(6120):711-715.
155. Escribano-Diaz C, *et al*. (2013) A cell cycle-dependent regulatory circuit composed of 53BP1-RIF1 and BRCA1-CtIP controls DNA repair pathway choice. *Mol Cell* 49(5):872-883.
156. Feng L, Fong KW, Wang J, Wang W, & Chen J (2013) RIF1 counteracts BRCA1-mediated end resection during DNA repair. *J Biol Chem* 288(16):11135-11143.
157. Zimmermann M, Lottersberger F, Buonomo SB, Sfeir A, & de Lange T (2013) 53BP1 Regulates DSB Repair Using Rif1 to Control 5 ' End Resection. *Science* 339(6120):700-704.
158. Bunting SF, *et al*. (2010) 53BP1 inhibits homologous recombination in Brca1-deficient cells by blocking resection of DNA breaks. *Cell* 141(2):243-254.
159. Chaurushiya MS, *et al*. (2012) Viral E3 ubiquitin ligase-mediated degradation of a cellular E3: viral mimicry of a cellular phosphorylation mark targets the RNF8 FHA domain. *Mol Cell* 46(1):79-90.
160. Lilley CE, *et al*. (2010) A viral E3 ligase targets RNF8 and RNF168 to control histone ubiquitination and DNA damage responses. *EMBO J* 29(5):943-955.
161. Weitzman MD, Lilley CE, & Chaurushiya MS (2010) Genomes in conflict: maintaining genome integrity during virus infection. *Annu Rev Microbiol* 64:61-81.
162. Wang D & Lippard SJ (2005) Cellular processing of platinum anticancer drugs. *Nature reviews. Drug discovery* 4(4):307-320.

163. Danford AJ, Wang D, Wang Q, Tullius TD, & Lippard SJ (2005) Platinum anticancer drug damage enforces a particular rotational setting of DNA in nucleosomes. *Proceedings of the National Academy of Sciences of the United States of America* 102(35):12311-12316.
164. Alt A, *et al*. (2007) Bypass of DNA lesions generated during anticancer treatment with cisplatin by DNA polymerase eta. *Science* 318(5852):967-970.
165. Damsma GE, Alt A, Brueckner F, Carell T, & Cramer P (2007) Mechanism of transcriptional stalling at cisplatin-damaged DNA. *Nature structural & molecular biology* 14(12):1127-1133.
166. Sale JE (2012) Competition, collaboration and coordination--determining how cells bypass DNA damage. *Journal of cell science* 125(Pt 7):1633-1643.
167. Mailand N, Gibbs-Seymour I, & Bekker-Jensen S (2013) Regulation of PCNA-protein interactions for genome stability. *Nature reviews. Molecular cell biology* 14(5):269-282.
168. Sale JE (2013) Translesion DNA synthesis and mutagenesis in eukaryotes. *Cold Spring Harb Perspect Biol* 5(3):a012708.
169. Larrieu D, Britton S, Demir M, Rodriguez R, & Jackson SP (2014) Chemical inhibition of NAT10 corrects defects of laminopathic cells. *Science* 344(6183):527-532.
170. Ding S, *et al*. (2013) Using fluorescent post-labeling to probe the subcellular localization of DNA-targeted platinum anticancer agents. *Angew Chem Int Ed Engl* 52(12):3350-3354.
171. Wirth R, *et al*. (2015) Azide vs Alkyne Functionalization in Pt(II) Complexes for Post-treatment Click Modification: Solid-State Structure, Fluorescent Labeling, and Cellular Fate. *J Am Chem Soc* 137(48):15169-15175.
172. Vaisman A, *et al*. (1999) Effect of DNA polymerases and high mobility group protein 1 on the carrier ligand specificity for translesion synthesis past platinum-DNA adducts. *Biochemistry* 38(34):11026-11039.
173. Baskin JM, *et al*. (2007) Copper-free click chemistry for dynamic in vivo imaging. *Proceedings of the National Academy of Sciences of the United States of America* 104(43):16793-16797.
174. Jewett JC & Bertozzi CR (2010) Cu-free click cycloaddition reactions in chemical biology. *Chem Soc Rev* 39(4):1272-1279.
175. Liang XJ, *et al*. (2005) Trafficking and localization of platinum complexes in cisplatin-resistant cell lines monitored by fluorescence-labeled platinum. *J Cell Physiol* 202(3):635-641.
176. Qiao X, Ding S, Liu F, Kucera GL, & Bierbach U (2014) Investigating the cellular fate of a DNA-targeted platinum-based anticancer agent by orthogonal double-click chemistry. *Journal of biological inorganic chemistry : JBIC : a publication of the Society of Biological Inorganic Chemistry* 19(3):415-426.
177. Christman JK (2002) 5-Azacytidine and 5-aza-2'-deoxycytidine as inhibitors of DNA methylation: mechanistic studies and their implications for cancer therapy. *Oncogene* 21(35):5483-5495.
178. Taunton J, Hassig CA, & Schreiber SL (1996) A mammalian histone deacetylase related to the yeast transcriptional regulator Rpd3p. *Science* 272(5260):408-411.

179. Marks PA (2007) Discovery and development of SAHA as an anticancer agent. *Oncogene* 26(9):1351-1356.
180. Rosato RR, Almenara JA, & Grant S (2003) The histone deacetylase inhibitor MS-275 promotes differentiation or apoptosis in human leukemia cells through a process regulated by generation of reactive oxygen species and induction of p21CIP1/WAF1 1. *Cancer research* 63(13):3637-3645.
181. Todd RC & Lippard SJ (2009) Inhibition of transcription by platinum antitumor compounds. *Metallomics* 1(4):280-291.
182. Muller S, Kumari S, Rodriguez R, & Balasubramanian S (2010) Small-molecule-mediated G-quadruplex isolation from human cells. *Nature chemistry* 2(12):1095-1098.
183. Hendel A, *et al*. (2011) PCNA ubiquitination is important, but not essential for translesion DNA synthesis in mammalian cells. *PLoS genetics* 7(9):e1002262.
184. Hicks JK, *et al*. (2010) Differential Roles for DNA Polymerases Eta, Zeta, and REV1 in Lesion Bypass of Intrastrand versus Interstrand DNA Cross-Links. *Mol Cell Biol* 30(5):1217-1230.
185. Reissner T, Schneider S, Schorr S, & Carell T (2010) Crystal Structure of a Cisplatin-(1,3-GTG) Cross-Link within DNA Polymerase eta. *Angew Chem Int Edit* 49(17):3077-3080.
186. Schneider S, Reissner T, Ziv O, Livneh Z, & Carell T (2010) Translesion synthesis of 1,3-GTG cisplatin DNA lesions. *Chembiochem : a European journal of chemical biology* 11(11):1521-1524.
187. Koch SC, *et al*. (2015) Structural insights into the recognition of cisplatin and AAF-dG lesion by Rad14 (XPA). *Proceedings of the National Academy of Sciences of the United States of America* 112(27):8272-8277.
188. Ghosal G & Chen J (2013) DNA damage tolerance: a double-edged sword guarding the genome. *Translational cancer research* 2(3):107-129.
189. Vaisman A, Masutani C, Hanaoka F, & Chaney SG (2000) Efficient translesion replication past oxaliplatin and cisplatin GpG adducts by human DNA polymerase eta. *Biochemistry* 39(16):4575-4580.
190. Bassett E, *et al*. (2004) The role of DNA polymerase eta in translesion synthesis past platinum-DNA adducts in human fibroblasts. *Cancer research* 64(18):6469-6475.
191. Doles J, *et al*. (2010) Suppression of Rev3, the catalytic subunit of Pol{zeta}, sensitizes drug-resistant lung tumors to chemotherapy. *Proceedings of the National Academy of Sciences of the United States of America* 107(48):20786-20791.
192. Xie K, Doles J, Hemann MT, & Walker GC (2010) Error-prone translesion synthesis mediates acquired chemoresistance. *Proceedings of the National Academy of Sciences of the United States of America* 107(48):20792-20797.
193. Zhao Y, *et al*. (2012) Structural basis of human DNA polymerase eta-mediated chemoresistance to cisplatin. *Proceedings of the National Academy of Sciences of the United States of America* 109(19):7269-7274.
194. Dasari S & Tchounwou PB (2014) Cisplatin in cancer therapy: molecular mechanisms of action. *European journal of pharmacology* 740:364-378.

195. Waters LS, *et al*. (2009) Eukaryotic Translesion Polymerases and Their Roles and Regulation in DNA Damage Tolerance. *Microbiol Mol Biol R* 73(1):134-+.
196. Yuan BF, Jiang Y, Wang YS, & Wang YS (2010) Efficient Formation of the Tandem Thymine Glycol/8-Oxo-7,8-dihydroguanine Lesion in Isolated DNA and the Mutagenic and Cytotoxic Properties of the Tandem Lesions in Escherichia coli Cells. *Chem Res Toxicol* 23(1):11-19.
197. Sage E & Harrison L (2011) Clustered DNA lesion repair in eukaryotes: Relevance to mutagenesis and cell survival. *Mutat Res-Fund Mol M* 711(1-2):123-133.
198. Asangani IA, *et al*. (2014) Therapeutic targeting of BET bromodomain proteins in castration-resistant prostate cancer. *Nature* 510(7504):278-+.
199. Blattmann C, *et al*. (2010) Enhancement of radiation response in osteosarcoma and rhabdomyosarcoma cell lines by histone deacetylase inhibition. *Int J Radiat Oncol Biol Phys* 78(1):237-245.
200. Chaidos A, *et al*. (2014) Potent antimyeloma activity of the novel bromodomain inhibitors I-BET151 and I-BET762. *Blood* 123(5):697-705.
201. Nicodeme E, *et al*. (2010) Suppression of inflammation by a synthetic histone mimic. *Nature* 468(7327):1119-1123.
202. Ogiwara H, *et al*. (2013) Curcumin suppresses multiple DNA damage response pathways and has potency as a sensitizer to PARP inhibitor. *Carcinogenesis* 34(11):2486-2497.
203. Lee HS, Park JH, Kim SJ, Kwon SJ, & Kwon J (2010) A cooperative activation loop among SWI/SNF, gamma-H2AX and H3 acetylation for DNA double-strand break repair. *Embo Journal* 29(8):1434-1445.
204. Ziv Y, *et al*. (2006) Chromatin relaxation in response to DNA double-strand breaks is modulated by a novel ATM- and KAP-1 dependent pathway. *Nature cell biology* 8(8):870-876.
205. Kulkarni A, *et al*. (2013) Tripartite Motif-containing 33 (TRIM33) protein functions in the poly(ADP-ribose) polymerase (PARP)-dependent DNA damage response through interaction with Amplified in Liver Cancer 1 (ALC1) protein. *The Journal of biological chemistry* 288(45):32357-32369.
206. Haynes SR, *et al*. (1992) The bromodomain: a conserved sequence found in human, Drosophila and yeast proteins. *Nucleic acids research* 20(10):2603.
207. Reddy BA, Etkin LD, & Freemont PS (1992) A novel zinc finger coiled-coil domain in a family of nuclear proteins. *Trends in biochemical sciences* 17(9):344-345.
208. Zeng L, *et al*. (2008) Structural insights into human KAP1 PHD finger-bromodomain and its role in gene silencing. *Nature structural & molecular biology* 15(6):626-633.
209. Agricola E, Randall RA, Gaarenstroom T, Dupont S, & Hill CS (2011) Recruitment of TIF1 gamma to Chromatin via Its PHD Finger-Bromodomain Activates Its Ubiquitin Ligase and Transcriptional Repressor Activities. *Mol Cell* 43(1):85-96.
210. Tsai WW, *et al*. (2010) TRIM24 links a non-canonical histone signature to breast cancer. *Nature* 468(7326):927-932.

211. Allton K, *et al*. (2009) Trim24 targets endogenous p53 for degradation. *Proceedings of the National Academy of Sciences of the United States of America* 106(28):11612-11616.
212. Ayrapetov MK, Gursoy-Yuzugullu O, Xu C, Xu Y, & Price BD (2014) DNA double-strand breaks promote methylation of histone H3 on lysine 9 and transient formation of repressive chromatin. *Proceedings of the National Academy of Sciences of the United States of America* 111(25):9169-9174.
213. Chambon M, *et al*. (2011) Prognostic significance of TRIM24/TIF-1alpha gene expression in breast cancer. *Am J Pathol* 178(4):1461-1469.
214. Remboutsika E, *et al*. (1999) The putative nuclear receptor mediator TIF1alpha is tightly associated with euchromatin. *Journal of cell science* 112 (Pt 11):1671-1683.
215. Klugbauer S & Rabes HM (1999) The transcription coactivator HTIF1 and a related protein are fused to the RET receptor tyrosine kinase in childhood papillary thyroid carcinomas. *Oncogene* 18(30):4388-4393.
216. Le Douarin B, *et al*. (1995) The N-terminal part of TIF1, a putative mediator of the ligand-dependent activation function (AF-2) of nuclear receptors, is fused to B-raf in the oncogenic protein T18. *The EMBO journal* 14(9):2020-2033.
217. Zhong S, *et al*. (1999) A RA-dependent, tumour-growth suppressive transcription complex is the target of the PML-RARalpha and T18 oncoproteins. *Nat Genet* 23(3):287-295.
218. Stewart GS, Wang B, Bignell CR, Taylor AM, & Elledge SJ (2003) MDC1 is a mediator of the mammalian DNA damage checkpoint. *Nature* 421(6926):961-966.
219. Dantuma NP, Groothuis TA, Salomons FA, & Neefjes J (2006) A dynamic ubiquitin equilibrium couples proteasomal activity to chromatin remodeling. *The Journal of cell biology* 173(1):19-26.
220. Cammas F, *et al*. (2002) Cell differentiation induces TIF1beta association with centromeric heterochromatin via an HP1 interaction. *Journal of cell science* 115(Pt 17):3439-3448.
221. Matsuoka S, *et al*. (2007) ATM and ATR substrate analysis reveals extensive protein networks responsive to DNA damage. *Science* 316(5828):1160-1166.
222. Shiloh Y & Ziv Y (2013) The ATM protein kinase: regulating the cellular response to genotoxic stress, and more. *Nature reviews. Molecular cell biology* 14(4):197-210.
223. White DE, *et al*. (2006) KAP1, a novel substrate for PIKK family members, colocalizes with numerous damage response factors at DNA lesions. *Cancer research* 66(24):11594-11599.
224. Lemaitre C & Soutoglou E (2014) Double strand break (DSB) repair in heterochromatin and heterochromatin proteins in DSB repair. *DNA repair* 19:163-168.
225. Bannister AJ, *et al*. (2001) Selective recognition of methylated lysine 9 on histone H3 by the HP1 chromo domain. *Nature* 410(6824):120-124.
226. Grewal SI & Jia S (2007) Heterochromatin revisited. *Nat Rev Genet* 8(1):35-46.

227. Sun YL, *et al*. (2009) Histone H3 methylation links DNA damage detection to activation of the tumour suppressor Tip60. *Nature cell biology* 11(11):1376-U1273.
228. Eberl HC, Spruijt CG, Kelstrup CD, Vermeulen M, & Mann M (2013) A Map of General and Specialized Chromatin Readers in Mouse Tissues Generated by Label-free Interaction Proteomics. *Mol Cell* 49(2):368-378.
229. Ma L, *et al*. (2016) Histone H3 lysine 23 acetylation is associated with oncogene TRIM24 expression and a poor prognosis in breast cancer. *Tumor Biol* 37(11):14803-14812.
230. Simo-Riudalbas L, *et al*. (2015) KAT6B Is a Tumor Suppressor Histone H3 Lysine 23 Acetyltransferase Undergoing Genomic Loss in Small Cell Lung Cancer. *Cancer research* 75(18):3936-3945.
231. Blow JJ & Gillespie PJ (2008) Replication licensing and cancer - a fatal entanglement? *Nature Reviews Cancer* 8(10):799-806.
232. Bochman ML & Schwacha A (2009) The Mcm Complex: Unwinding the Mechanism of a Replicative Helicase. *Microbiol Mol Biol R* 73(4):652-683.
233. Sclafani RA, Fletcher RJ, & Chen XJS (2004) Two heads are better than one: regulation of DNA replication by hexameric helicases. *Genes & development* 18(17):2039-2045.
234. Bailis JM & Forsburg SL (2004) MCM proteins: DNA damage, mutagenesis and repair. *Current opinion in genetics & development* 14(1):17-21.
235. Drissi R, Dubois ML, Douziech M, & Boisvert FM (2015) Quantitative Proteomics Reveals Dynamic Interactions of the Minichromosome Maintenance Complex (MCM) in the Cellular Response to Etoposide Induced DNA Damage. *Molecular & cellular proteomics : MCP* 14(7):2002-2013.
236. Forsburg SL (2004) Eukaryotic MCM proteins: beyond replication initiation. *Microbiol Mol Biol Rev* 68(1):109-131.
237. Orr SJ, *et al*. (2010) Reducing MCM levels in human primary T cells during the G(0)-->G(1) transition causes genomic instability during the first cell cycle. *Oncogene* 29(26):3803-3814.
238. Cortez D, Glick G, & Elledge SJ (2004) Minichromosome maintenance proteins are direct targets of the ATM and ATR checkpoint kinases. *Proceedings of the National Academy of Sciences of the United States of America* 101(27):10078-10083.
239. Ibarra A, Schwob E, & Mendez J (2008) Excess MCM proteins protect human cells from replicative stress by licensing backup origins of replication. *Proceedings of the National Academy of Sciences of the United States of America* 105(26):8956-8961.
240. Orphanides G, Wu WH, Lane WS, Hampsey M, & Reinberg D (1999) The chromatin-specific transcription elongation factor FACT comprises human SPT16 and SSRP1 proteins. *Nature* 400(6741):284-288.
241. Tan BCM, Chien CT, Hirose S, & Lee SC (2006) Functional cooperation between FACT and MCM helicase facilitates initiation of chromatin DNA replication. *Embo Journal* 25(17):3975-3985.

242. Tan BCM, Liu HA, Lin CL, & Lee SC (2010) Functional cooperation between FACT and MCM is coordinated with cell cycle and differential complex formation. *J Biomed Sci* 17.
243. Noon AT, *et al*. (2010) 53BP1-dependent robust localized KAP-1 phosphorylation is essential for heterochromatic DNA double-strand break repair. *Nature cell biology* 12(2):177-184.
244. Bennett J, *et al*. (2016) Discovery of a Chemical Tool Inhibitor Targeting the Bromodomains of TRIM24 and BRPF. *J Med Chem* 59(4):1642-1647.
245. Palmer WS (2016) Development of small molecule inhibitors of BRPF1 and TRIM24 bromodomains. *Drug Discov Today Technol* 19:65-71.
246. de Napoles M, *et al*. (2004) Polycomb group proteins Ring1A/B link ubiquitylation of histone H2A to heritable gene silencing and X inactivation. *Dev Cell* 7(5):663-676.
247. Buchwald G, *et al*. (2006) Structure and E3-ligase activity of the Ring-Ring complex of polycomb proteins Bmi1 and Ring1b. *Embo Journal* 25(11):2465-2474.
248. Eskeland R, *et al*. (2010) Ring1B Compacts Chromatin Structure and Represses Gene Expression Independent of Histone Ubiquitination. *Mol Cell* 38(3):452-464.
249. Chou DM, *et al*. (2010) A chromatin localization screen reveals poly (ADP ribose)-regulated recruitment of the repressive polycomb and NuRD complexes to sites of DNA damage. *Proceedings of the National Academy of Sciences of the United States of America* 107(43):18475-18480.
250. Ginjala V, *et al*. (2011) BMI1 Is Recruited to DNA Breaks and Contributes to DNA Damage-Induced H2A Ubiquitination and Repair. *Molecular and cellular biology* 31(10):1972-1982.
251. Li ML & Greenberg RA (2012) Links between genome integrity and BRCA1 tumor suppression. *Trends in biochemical sciences* 37(10):418-424.
252. Kalb R, Mallery DL, Larkin C, Huang JTJ, & Hiom K (2014) BRCA1 Is a Histone-H2A-Specific Ubiquitin Ligase. *Cell Rep* 8(4):999-1005.
253. Shakya R, *et al*. (2011) BRCA1 Tumor Suppression Depends on BRCT Phosphoprotein Binding, But Not Its E3 Ligase Activity. *Science* 334(6055):525-528.
254. Brzovic PS, Rajagopal P, Hoyt DW, King MC, & Klevit RE (2001) Structure of a BRCA1-BARD1 heterodimeric RING-RING complex. *Nature structural biology* 8(10):833-837.
255. Gursoy-Yuzugullu O, House N, & Price BD (2016) Patching Broken DNA: Nucleosome Dynamics and the Repair of DNA Breaks. *Journal of molecular biology* 428(9 Pt B):1846-1860.
256. Becker M, *et al*. (2009) Polycomb Group Protein Bmi1 Is Required for Growth of RAF Driven Non-Small-Cell Lung Cancer. *PloS one* 4(1).
257. Berezovska OP, *et al*. (2006) Essential role for activation of the Polycomb group (PcG) protein chromatin silencing pathway in metastatic prostate cancer. *Cell Cycle* 5(16):1886-1901.
258. Lessard J & Sauvageau G (2003) Bmi-1 determines the proliferative capacity of normal and leukaemic stem cells. *Nature* 423(6937):255-260.

259. Li X, *et al*. (2013) Overexpression of Bmi-1 contributes to the invasion and metastasis of hepatocellular carcinoma by increasing the expression of matrix metalloproteinase (MMP)2, MMP-9 and vascular endothelial growth factor via the PTEN/PI3K/Akt pathway. *International journal of oncology* 43(3):793-802.
260. Armache KJ, Garlick JD, Canzio D, Narlikar GJ, & Kingston RE (2011) Structural basis of silencing: Sir3 BAH domain in complex with a nucleosome at 3.0 A resolution. *Science* 334(6058):977-982.
261. Fang Q, *et al*. (2016) Human cytomegalovirus IE1 protein alters the higher-order chromatin structure by targeting the acidic patch of the nucleosome. *Elife* 5.
262. Kato H, *et al*. (2013) A conserved mechanism for centromeric nucleosome recognition by centromere protein CENP-C. *Science* 340(6136):1110-1113.
263. Mucke K, *et al*. (2014) Human cytomegalovirus major immediate early 1 protein targets host chromosomes by docking to the acidic pocket on the nucleosome surface. *Journal of virology* 88(2):1228-1248.
264. Roussel L, Erard M, Cayrol C, & Girard JP (2008) Molecular mimicry between IL-33 and KSHV for attachment to chromatin through the H2A-H2B acidic pocket. *Embo Rep* 9(10):1006-1012.
265. Taherbhoy AM, Huang OW, & Cochran AG (2015) BMI1-RING1B is an autoinhibited RING E3 ubiquitin ligase. *Nature communications* 6.
266. Rodriguez R & Miller KM (2014) Unravelling the genomic targets of small molecules using high-throughput sequencing. *Nat Rev Genet* 15(12):783-796.
267. Rodriguez-Paredes M & Esteller M (2011) Cancer epigenetics reaches mainstream oncology. *Nat Med* 17(3):330-339.
268. Cao LX, *et al*. (2011) BMI1 As a Novel Target for Drug Discovery in Cancer. *Journal of cellular biochemistry* 112(10):2729-2741.
269. Ismail IH, McDonald D, Strickfaden H, Xu ZZ, & Hendzel MJ (2013) A Small Molecule Inhibitor of Polycomb Repressive Complex 1 Inhibits Ubiquitin Signaling at DNA Double-strand Breaks. *Journal of Biological Chemistry* 288(37):26944-26954.
270. Kreso A, *et al*. (2014) Self-renewal as a therapeutic target in human colorectal cancer. *Nat Med* 20(1):29-+.
271. Cui ZB, *et al*. (2013) TRIM24 Overexpression Is Common in Locally Advanced Head and Neck Squamous Cell Carcinoma and Correlates with Aggressive Malignant Phenotypes. *PloS one* 8(5).
272. Li HY, *et al*. (2012) Overexpression of TRIM24 Correlates with Tumor Progression in Non-Small Cell Lung Cancer. *PloS one* 7(5).
273. Zhang LH, *et al*. (2015) TRIM24 promotes glioma progression and enhances chemoresistance through activation of the PI3K/Akt signaling pathway. *Oncogene* 34(5):600-610.
274. Lin L, Zhao WH, Sun B, Wang XY, & Liu Q (2017) Overexpression of TRIM24 is correlated with the progression of human cervical cancer. *Am J Transl Res* 9(2):620-628.
275. Liu X, *et al*. (2014) Overexpression of TRIM24 Is Associated with the Onset and Progress of Human Hepatocellular Carcinoma. *PloS one* 9(1).
276. Herquel B, *et al*. (2011) Transcription cofactors TRIM24, TRIM28, and TRIM33 associate to form regulatory complexes that suppress murine hepatocellular

carcinoma. *Proceedings of the National Academy of Sciences of the United States of America* 108(20):8212-8217.
277. Jiang SM, *et al*. (2015) TRIM24 suppresses development of spontaneous hepatic lipid accumulation and hepatocellular carcinoma in mice. *J Hepatol* 62(2):371-379.
278. Groner AC, *et al*. (2016) TRIM24 Is an Oncogenic Transcriptional Activator in Prostate Cancer. *Cancer Cell* 29(6):846-858.
279. Le Douarin B, Nielsen AL, You J, Chambon P, & Losson R (1997) TIF1 alpha: a chromatin-specific mediator for the ligand-dependent activation function AF-2 of nuclear receptors? *Biochemical Society transactions* 25(2):605-612.
280. Thenot S, Henriquet C, Rochefort H, & Cavailles V (1997) Differential interaction of nuclear receptors with the putative human transcriptional coactivator hTIF1. *Journal of Biological Chemistry* 272(18):12062-12068.
281. Borlepawar A, *et al*. (2017) TRIM24 protein promotes and TRIM32 protein inhibits cardiomyocyte hypertrophy via regulation of dysbindin protein levels. *Journal of Biological Chemistry* 292(24):10180-10196.
282. Jain AK, Allton K, Duncan AD, & Barton MC (2014) TRIM24 Is a p53-Induced E3-Ubiquitin Ligase That Undergoes ATM-Mediated Phosphorylation and Autodegradation during DNA Damage. *Molecular and cellular biology* 34(14):2695-2709.

VITA

Poonam Agarwal was born in Barpeta Town, Assam, India. She attended Bangalore University in Bangalore, India in 2001 and received a Bachelor's degree in Microbiology in 2003. She received a Master's degree in Biotechnology from Bangalore University in 2005. After working as a research scientist in agro-based firm Camson Biotechnologies Limited, Bangalore, India and in biopharmaceutical company Biocon Limited, Bangalore, India for over 5 years she started her graduate study in Cell and Molecular Biology program under the supervision of Dr. Kyle Miller in the Department of Molecular Biosciences at the University of Texas at Austin in the fall of 2012.

During her graduate studies at UT Austin, Poonam Agarwal has won several awards from the Department of Molecular Biosciences and Graduate School. Her awards include:

- Graduate School's 2017 Summer Fellowship, UT Austin (2017)
- Stipend support from National Cancer Institute and College of Natural Sciences, UT Austin (2016)
- Joseph F. Short Memorial Endowed Scholarship, UT Austin (2016)
- Lois Sager Foxhall Memorial Fund Travel Fund Award (2015)
- Best graduate student poster 2nd Place, Molecular Biosciences Retreat, UT Austin (2014)

Email: poonam.ag@utexas.edu

This dissertation was typed by Poonam Agarwal.